2007

The role of L-carnitine in preventing mitochondrial dysfunction after neonatal hypoxia-ischemia

Thomas Fredrick Rau
The University of Montana

THE ROLE OF L-CARNITINE IN PREVENTING MITOCHONDRIAL
DYSFUNCTION AFTER NEONATAL HYPOXIA-ISCHEMIA

By

Thomas Fredrick Rau

B.A. Cell and Molecular Biology, University of Montana, Missoula, Montana, 1997

Dissertation

presented in partial fulfillment of the requirements
for the degree of

Doctor of Philosophy
in
Neuroscience

The University of Montana
Missoula, MT

Spring 2007

Approved by:

Dr. David A. Strobel, Dean
Graduate School

Stephen Black, PhD
Cardiovascular Biology, Medical College of Georgia

David Poulsen, PhD
Biomedical and Pharmaceutical Sciences
University of Montana

Diana Lurie, PhD
Biomedical and Pharmaceutical Sciences
University of Montana

Richard Bridges, PhD
Biomedical and Pharmaceutical Sciences
University of Montana

Jesse Hay, PhD
Department of Biology
University of Montana

Rau, Thomas, PhD, May 2007   Neuroscience

The role of L-carnitine in preventing mitochondrial dysfunction after neonatal hypoxia-ischemia.

Chairperson or Co-Chairperson: Stephen Black, PhD

Co-Chairperson: David Poulsen, PhD

  Neonatal hypoxia-ischemia (HI) represents an intractable clinical condition that lacks an effective treatment and results in blindness, cerebral palsy, and cognitive deficits. A primary mechanism of cell death induced by neonatal HI is mitochondrial dysfunction leading to metabolic crisis and apoptosis. L-carnitine (LCAR) is an endogenous compound that transports fatty acids across the mitochondrial membrane for metabolism, buffers endogenous acyl-coA pools and improves the health and efficiency of the mitochondria. In light of the mitochondrial dysfunction observed after HI we hypothesized treatment with LCAR would reduce cell death after HI. Using a novel rat hippocampal slice culture model we observed a decrease in cell death in RHSC treated with 5mM LCAR for 2 hours prior to oxygen glucose deprivation (OGD). Under the same conditions we observed an LCAR induced decrease in both necrosis and mitochondrially-mediated apoptosis. To elucidate the mechanism for these data we studied the effect of LCAR on reactive oxygen species (ROS) before and after OGD. We observed a decrease in superoxide and H_2O_2 in RHSC treated with LCAR and exposed to OGD. In further experiments we observed LCAR treatment increased the expression and activity of superoxide dismutase 1 (SOD1) and catalase prior to OGD and this effect resulted in decreased cell death after OGD. In addition to increased (ROS) scavenging, we observed an LCAR mediated increase in levels of uncoupling protein 2 (UCP-2). In a series of experiments we observed a correlation between UCP-2 expression, the reversible modulation of mitochondrial membrane potential, and a decrease in cell death after OGD. These observations taken together suggest LCAR decreases cell death in RHSC after OGD by increasing ROS scavenging and UCP-2 expression in the mitochondria prior to OGD.

TABLE OF CONTENTS

Chapter 3: Results

Chapter 1

INTRODUCTION

1.1 Neonatal hypoxia ischemia

Neonatal hypoxic-ischemic encephalopathy (HIE) is a pathological condition caused by reduced cerebral blood flow that results in acute brain hypoxia ischemia (HI) [1-3]. Neonatal HIE occurs in approximately 1-6 per 1000 live births and results in significant neurodevelopmental disabilities in affected infants [4]. In the United States, severe (stage 3) HIE results in a mortality rate of 50-75% within the first month of life with up to 80% of survivors developing seizures, blindness, severe cognitive deficits and cerebral palsy characterized by hemiplegia, paraplegia, or quadriplegia [1, 5-9] [10].

While severe HIE results in a high mortality/morbidity rate, the majority of neonates exposed to HI will develop moderate HIE that, while not fatal, will impair the cognitive and physical functioning of the individual throughout their lifespan. Among infants who survive moderate HIE, 30-50% will suffer from serious complications and 10-20% will experience minor neurological abnormalities that result in movement disorders, mild learning deficits and neurobehavioral alterations.[11-13] [1, 2, 10, 14, 15].

In many cases the causative factors that induce HI remain idiopathic and therefore complicate rapid diagnosis and treatment. Currently, HIE has been linked to placental abruptio, cord accidents, traumatic compression lesions, congenital cyanotic heart disease, bacterial endocarditis, encephalitis, and coagulation irregularities due to deficiencies in protein C,S and anti-thrombin III [12]. While the causative agents involved vary, they all induce profound hypoxic-ischemic conditions (asphyxia, acidosis)

1

that result in acute or subacute brain injury leading to HIE in the neonate [12, 14, 15] [2, 15].

In the initial stages of neonatal HI, cerebral blood flow (CBF) is increased (irrespective of blood pressure) in a compensation response to decreased oxygen. If this adaptive response fails, the CBF becomes pressure-passive and is modulated directly by systemic blood pressure (BP). As BP drops, CBF falls below critical levels and glucose and oxygen levels continue to decrease leading to acute metabolic crisis. Simultaneously, brain temperature drops and GABA release increases in an attempt to minimize the initial effects of HI [16-18]. If the impairment of fetal oxygen and glucose persists over time it induces a cascade of molecular events that results in acidosis, inflammation, edema, and neuronal death resulting in lesions in the basal ganglia, hippocampus, cortex and subcortical white matter that are hallmarks of HIE [1, 7] [2, 19].

The course of neonatal HI is characterized by a bi-phasic energy crisis in which the first phase of energy failure occurs during the ischemic event. During the second phase, cerebral metabolism briefly recovers only to deteriorate during reperfusion (6-24 hours after initial injury) [2, 12, 20]. In the primary phase of energy failure oxygen sensitive neurons undergo calcium mediated necrosis. During the secondary phase of energy failure, widespread edema and apoptotic cell death occurs in the hippocampus and cortex lasting up to 72 hours following the initial insult[21, 22] [20, 23].

The neonatal brain is critically dependent on a steady supply of glucose and oxygen. When the brain is rendered ischemic, synaptic transmission ceases within 10-20 seconds followed by an energetic failure of the Na+/K+ pump. Impairment of Na+/K+ pump allows the influx of sodium and water resulting in early stage cytotoxic edema.

Within 5-10 minutes cellular glucose is exhausted and intracellular lactate levels increase fivefold. After several hours the blood brain barrier is disrupted allowing an abnormal diffusion of nutrients leading to acidosis and white blood cell infiltration [1, 2, 9, 24-27]. Release of histamine, arachdonic acid, bradykinin, interleukins, and excitatory amino acids occur as a reactive response to hypoxia-ischemia and collectively induce vasogenic edema [26]. This effect coupled with acute lactic acidosis results in the denaturation of proteins and the inactivation of pH dependent enzymes [22, 26, 28].

At a molecular level HI induces increases in glutamate and aspartate release in the cerebral cortex and basal ganglia. The release of excitatory amino acids activates NMDA, AMPA, and kainate receptors leading to sustained increases in intracellular and subcellular Ca^{++} levels that accumulate in the cytosol. Under basal conditions increased Ca^{++} release is countered by increased mitochondrial uptake to buffer polarization within the matrix. During HI, calcium buffering is rapidly overwhelmed inducing a spontaneous depolarization of the mitochondrial membrane that results in a massive, uncontrolled Ca^{++} efflux into the cytoplasm and the initiation apoptotic cell death [15, 25, 29, 30] [31, 32].

A secondary effect of excessive Ca^{++} buffering in the mitochondria is the activation of the mitochondrial permeability transition pore (MPTP). The MPTP is protein pore composed of adenine nucleotide translocase (ANT), voltage dependent anion channel (VDAC), the mitochondrial inner membrane transporter (Tim) and the mitochondrial outer membrane transporter (Tom). High levels of Ca^{++} or reactive oxygen species (ROS) induce permeability transition through the MPTP that results in an irreversible depolarization of mitochondrial membrane potential (MMP) and a loss of

ATP production through the cytochrome complex V in the electron transport chain (ETC) [31] [25]. The loss of ATP prevents the Na^+/Ca^+ exchanger from clearing excess calcium from the cell and triggers a cycle of Ca^+ accumulation and ATP depletion that leads to necrosis and apoptosis [25] [20].

A direct effect of HI induced mitochondrial dysfunction is the increased production of reactive oxygen species (ROS; superoxide, hydrogen peroxide, peroxynitrite, and hydroxyl radical). HI disrupts cellular respiration and shunts energy from this process into the production of superoxide. Initially, superoxide dismutase (SOD) catalyzes the conversion of superoxide to hydrogen peroxide. As HI progresses the superoxide load increases rapidly, overwhelming basal SOD levels and allowing excess superoxide to scavenge lipid membranes, damage DNA and initiate apoptotic mechanisms [31, 33] [1, 20].

As SOD converts superoxide to hydrogen peroxide, glutathione peroxidase, catalase, and GSH reductase convert hydrogen peroxide to water. During HI the increase in hydrogen peroxide overwhelms enzymatic defenses resulting in an excess of hydrogen peroxide that can combine with Cu or Fe (Fenton reaction) and produce hydroxyl radical [20] [4]. The result of this dysfunction is cycle of damage in which ROS attack mitochondrial membranes destroying lipid integrity and increasing levels of toxic, oxidized fatty acids. As the ROS levels increase they perpetuate a cycle of damage that destroys ATP production, attacks DNA, and eventually scavenges cardiolipin allowing the release and translocation of cytochrome C leading to apoptosis[34, 35] [4] [31, 36] [20].

1.2 The role of L-carnitine in the mitochondria

A consequence of the HI induced mitochondrial dysfunction is the buildup of toxic acyl-CoA units, which, under basal conditions, is maintained in homeostasis by carnitine metabolism. Carnitine, a solubule molecule derived from dietary protein or synthesized in the liver and kidneys, facilitates the transport of long chain fatty acids from the cytosol across the mitochondrial matrix for metabolism via beta-oxidation and utilization in the citric acid cycle [37-39] . Three enzymes (carnitine palmitoyl transferase 1, carnitine acylcarnitine translocase, and carnitine palmitoyl transferase 2) shuttle fatty acids into the mitochondria as long-chain fatty acylcarnitine esters. Once inside the mitochondrial matrix carnitine removes toxic fatty acyl-CoA metabolites and supplements a pool of free CoA that is actively utilized to maintain acyl-CoA/free CoA homeostasis [40] [39].

However, during HI, mitochondrial dysfunction causes an accumulation of acyl-CoA moieties that inhibit enzymes responsible for catalyzing glycolysis, gluconeogenesis, the citric acid and urea cycles, and fatty acid and protein catabolism [41] [27, 42-44]. To counter this effect researchers have added exogenous carnitine to cultured cells and noted a significant decrease in acyl-CoA moieties. Further studies in human trials have found exogenous carnitine treatment reduces acyl-CoA moieties in mitochondrial metabolic disorders and results in reduced mitochondrial dysfunction [9, 38, 41, 42, 45-49].

The possible metabolic benefit of carnitine treatment was elucidated in work performed by Liu et al [50] and Ames et al [39] showing carnitine treatment improved ambulation and cognition in aged rats by increasing mitochondrial efficiency [50] [51]

[38]. Further *in vivo* studies by Al-Majed et al [52, 53] showed carnitine prevents the HI induced decrease in ATP production in neurons [52, 54].

To directly investigate the effect of carnitine during neonatal HI, Wainwright et al 2003 administered carnitine to neonatal rat pups (IP injection; 30min prior to ligation), induced HI (unilateral carotid ligation followed by hypoxia) and observed significant decreases in infarct size at both 7 days and 28 days post HI. Furthermore, he noted L-carnitine decreased neuronal death in both the cortex and hippocampus of animals subjected to HI suggesting the neuroprotective effect was not limited to a specific region of the brain [41].

Based on his findings in the *in vivo* model, Wainwright hypothesized the neuroprotection observed was due to carnitine mediated decreases in toxic acyl-CoA esters. While HI has been shown to increase acyl-CoA levels, it was unclear if carnitine treatment was reducing HI mediated damage by modulating this specific mechanism. In further studies, Wainwright observed a loss of neuroprotection and an increase in infarct size in animals administered carnitine after HI. This observation raised two specific questions about the acyl-CoA buffering hypothesis: 1.) if carnitine mediated acyl-CoA buffering decreased damage, why was this effect lost when treatment was given after HI? 2.) Why does carnitine treatment after oxygen glucose deprivation (OGD) increase the damage from HI? While previous experimental observations do not directly refute the acyl-CoA buffering hypothesis, it does suggest the possibility of multiple neuroprotective mechanisms altered by carnitine treatment.

1.3 Overall Hypothesis and Aims

In light of Dr. Wainwright's previous work and the unanswered questions discussed above, we undertook an *in vitro* study utilizing neonatal rat hippocampal slice cultures. The primary hypothesis we tested in this study was that L-carnitine would prevent cell death after OGD by decreasing mitochondrial dysfunction induced by oxygen glucose deprivation (OGD). To test this hypothesis the aims of this study were as follows:

1.) Determine if carnitine reduces neuronal death in a hippocampal slice culture model of OGD.

        -If observed, measure the effect on OGD-induced necrosis and apoptosis.

        -Determine if carnitine preserves synaptic viability after OGD.

2.) Determine if carnitine prevents mitochondrial dysfunction induced by OGD by utilizing three separate parameters of mitochondrial health.

        -Measurement of mitochondrial metabolic viability after OGD

        -Elucidate the effect of carnitine treatment on ROS levels

        -Measurement of mitochondrial membrane potential (MMP) after OGD

3.) If OGD-induced mitochondrial dysfunction is prevented by carnitine treatment, delineate the mechanism(s) responsible.

Chapter 2

MATERIALS AND METHODS

2.1 Hippocampal Slice Preparation and Induction of Oxygen Glucose Deprivation:

Neonatal rats (Sprague-Dawley) at postnatal Day 7 (P7) were decapitated and the hippocampi dissected out under sterile conditions. The hippocampi were cut into 400μm slices on a McIlwain tissue chopper and individual slices were cultured on Millicell permeable membranes (0.4μM pore size) in six well plates for 6 days at 37° C in 5% CO_2. For the first two days, the slices were maintained in a primary plating media (50% DMEM (+) glucose, 25% HBSS (+) glucose, 25% heat inactivated horse serum, 5 mg/mL D-glucose (Sigma), 1mM Glutamax, 1.5% PenStrep/Fungizone (Gibco), and 5 mL of 50X B27 (Gibco) supplement plus anti-oxidants. On the fourth day in culture slices were placed in serum-free neurobasal medium (10mL Neurobasal-A, 200 μL of 50X B27 supplement, 100 μL of 100X Fungizone, and 100 μL of 100X Glutamax). At 24h prior to experimentation (day 6), the inserts were placed in a serum-free neurobasal A media and B27 supplement without antioxidants. Prior to the oxygen-glucose deprivation (OGD), a glucose free balanced salt solution (BSS) (120 mM NACl, 5mM KCl, 1.25 mM NaH_2PO_4, 2mM $MgSO_4$, 2mM $CaCl_2$, 25 mM $NaHCO_3$, 20 mM HEPES, 25 mM sucrose pH of 7.3) was infused for 1h with 5% CO_2/95% nitrogen at approximately 10L/h. Deoxygenated BSS was placed in a 6 well plate and warmed in a (Pro-Ox) chamber with an oxygen feedback sensor that maintained gas levels at 0.1% O_2 for 15 minutes. The inserts were then transferred into deoxygenated BSS and placed back into the tank at

0.1% oxygen for 90 minutes. After this they were immediately transferred into prewarmed serum-free Neurobasal supplemented with B27 without antioxidants.

2.2 Determination of Neuronal Population:

Representative brain slices were stained with NeuroTracer (Molecular Probes) to determine neuronal populations in hippocampal slices. Brain slices were fixed in 4° C 4% paraformaldehyde for 20 minutes, rinsed three times in PBS, removed from the Millicell inserts with a #5 paintbrush and placed on a glass slide. Slices were washed on the glass slide for 10 minutes in PBS plus 0.1% Triton X-100 to permeabilize membranes. NeuroTrace stain was diluted 1:20 in PBS and 200μl was placed on each individual slice for 20 minutes. After 20 minutes the stain was washed again with the Triton X-100 for 10 minutes. The sections were then washed for 2 hours at room temperature and visualized on a Olympus IX51 fluorescent microscope at 506/529 ex/em using a 4X objective lens. Images were captured on a Hamamatsu camera using Image Pro Plus software.

2.3 Measurement of Neuronal Death:

Propidium iodide (Molecular Probes) uptake was utilized to determine decreases in overall neuronal death associated with L-carnitine (LCAR) treatment prior to neonatal HI. Neonatal hippocampal brain slices were incubated with propidium iodide for 24 hours at 100ng/ml washed 3 times with pre-warmed PBS without calcium or magnesium, and captured on an Olympus IX51 fluorescent microscope at 518/604 ex/em using a 4X objective lens. The fluorescent intensity was quantified in Image Pro Plus using IOD

(average density*area) measurement. All values obtained were normalized to the

untreated control mean and expressed as a percent change.

2.4 Measurement of Necrotic Death:

Lactate dehydrogenase was analyzed to determine if L-CAR treatment prevents

HI-induced necrotic cell death. 24h post-OGD, 100μl of media was removed and assayed

utilizing the CytoTox-ONE (Promega) assay kit to determine LDH release. The assay

buffer and equilibrate substrate mix reagents were prepared according to manufacturers

specified protocols. Maximal LDH release was determined by mechanically lysing

untreated brain slices in 20μl of the manufacturer supplied Triton X-100 (9%) and

measuring LDH release. Untreated hippocampal slices were utilized as a negative control

and a blank well served as a vehicle control. Cell culture media was equilibrated to 22° C

and 100μl of culture media was mixed with 100μl of CytoTox-ONE reagent in a 96 well

plate and incubated at 22° C for 10min. After incubation 50μl of stop solution was added

to each well, the plate was shaken gently for 10min and fluorescence read at 560/590

ex/em. Protein content was determined by Bradford assay and all results were normalized

for total protein.

2.5 Measurement of Caspase Activation:

A caspase activation assay (Promega) was performed to determine if L-CAR

decreased caspase activation after acute HI. 24h post-OGD brain slices were incubated

with at 10uM assay reagent for 20min. Slices were washed 3 times with pre-warmed

PBS without calcium or magnesium, and images captured on an Olympus IX51

fluorescent microscope at 506/529 ex/em using the 4X objective lens. The fluorescent intensity was quantified in Image Pro Plus using IOD (average density*area) function. All values obtained were normalized to the untreated control mean and expressed as a percent change.

2.6 Measurement of Apoptotic Death:

Apoptotic neuronal death was measured by nick labeled DNA utilizing the TUNEL (Promega) assay. Slices were fixed in 4% paraformaldehyde for 20min at room temperature, rinsed in PBS three times and removed from Millicell inserts using a #5 paintbrush. After removal slices were placed on glass slides and processed according to the manufacturer's protocol. Images were captured at 506/529 ex/em and analyzed using ImagePro software. All values obtained were normalized to the untreated control mean and expressed as a percent change.

2.7 Western Blot Analysis of Cleaved Caspase-9:

Rat hippocampal slices were harvested from inserts and pooled (4) in 200μl of SDS lysis buffer with 5% protease inhibitor cocktail (Sigma). Tissue was ground for 30 seconds, sonicated for 5 seconds on ice water, and centerfuged at 14,000g at 4° C for 10min. Protein content was determined by Bradford assay and 30-50μg of protein was prepared with Lamelli sample buffer and loaded into 10 well gels (Gradipore). The gels were transferred to PVDF membranes (Biorad Immun-Blot; 0.2μM pore size) for 90min, blocked in 5% non-fat dry milk and TBST for 1 hour, and incubated overnight on a roller at 4° with a cleaved caspase 9 anti-body at 1:1000 in 5% non-fat milk, (CC-9, Cell

11

Signaling). Blots were developed with a Femto kit (Pierce) and exposed for 10min (15 captures) on a 440CF Kodak image station. Densitometry was performed using Kodak analysis software. Blots were stripped using Restore Western Blot Stripping buffer (Pierce), washed three times in TBST, and blocked for 1 hour in 5% non-fat dry milk and TBST. Blots were incubated overnight at 4° with a monoclonal antibody for β-actin (Sigma) and developed with a Femto kit (Pierce). All samples were normalized to β-actin values as a loading control prior to statistical analysis. All values obtained were normalized to the untreated control mean and expressed as a percent change.

2.8 Measurement of Cytosolic Superoxide levels:

Cytosolic superoxide levels were determined by dihydroethidium DHE staining. Rat hippocampal slices were incubated with 20μM dihydoethidium (DHE) (Molecular Probes) for 20min, washed 3 times with pre-warmed PBS without calcium or magnesium, and captured on an Olympus IX51 fluorescent microscope at 518/604 ex/em using the 4X objective lens. The fluorescent intensity was quantified in Image Pro Plus using the IOD (average density*area) measurement. All values obtained were normalized to the untreated control mean and expressed as a percent change.

2.9 Measurement of Mitochondrial Superoxide levels:

Mitochondrial superoxide levels were determined by MITOSOX staining. Rat hippocampal slices were incubated with 40μM MITOSOX (Molecular Probes) for 30min, washed 3 times with pre-warmed PBS without calcium or magnesium, and captured on an Olympus IX51 fluorescent microscope at 518/604 ex/em using the 4X objective lens. The

fluorescent intensity was quantified in Image Pro Plus using the IOD (average density*area) measurement. All values obtained were normalized to the untreated control mean and expressed as a percent change.

2.10 Measurement of Hydrogen Peroxide levels:

Hydrogen peroxide levels were determined by DCF-DA staining. Rat hippocampal slices were incubated with 30μM DCF-DA (Molecular Probes) for 30min, washed 3 times with pre-warmed PBS without calcium or magnesium, and captured on an Olympus IX51 fluorescent microscope at 506/529 ex/em using the 4X objective lens. After image capture slices were washed 3 times in PBS without calcium and magnesium and re-incubated at 37°. The fluorescent intensity was quantified in Image Pro Plus using the IOD (average density*area) function. All values obtained were normalized to the untreated control mean and expressed as a percent change.

2.11 Measurement of Superoxide Dismutase Activity:

SOD activity was measured using a WST-1 (tetrazolium salt) SOD assay kit (Dojindo Molecular Technologies). Rat hippocampal slices were treated for 2 hours, harvested using a #5 paintbrush and placed into buffer solution provided in the Dojindo kit with 5% protease inhibitor cocktail (Sigma). Samples were ground for 30 seconds, sonicated for 5 seconds on ice water, and centerfuged at 14,000g at 4° C for 10min. Protein content was determined by Bradford assay and used to normalize results. Specimens, controls, and standards were prepared according to the manufacturer's

specified protocols. Absorbance at 450nm was recorded and SOD activity was calculated based on inhibition rate %.

2.12 Measurement of Catalase Activity levels:

Rat hippocampal slices were harvested from inserts and pooled (4) in 200µl of SDS lysis buffer with 5% protease inhibitor cocktail (Sigma). Tissue was ground for 30 seconds, sonicated for 5 seconds on ice water, and centerfuged at 14,000g at 4° C for 10min. Protein content was determined by Bradford assay and 40µg of protein was added to 99µL of 0.05M potassium phosphate buffer (pH 7.0) Spectrophotometer was set at 240nm and 25° C for 5 minutes and blanked in a quartz cuvette with phosphate solution and hydrogen peroxide. After blanking, 1µl of 3% H_2O_2 was added to phosphate sample buffer and absorbance at 240nm was recorded at 10 second intervals for 60 seconds. The change in absorbance at 240nm was calculated and enzymatic activity determined according to methodology developed by Aebi, 1967.

2.13 Estimation of Mitochondrial Metabolic Viability:

Viability of intracellular esterases was validated by Calcein Am staining. Rat hippocampal slices were incubated with 30µM Calcein AM (Molecular Probes) for 30min, washed 3 times with pre-warmed PBS without calcium or magnesium, and captured on an Olympus IX51 fluorescent microscope at 506/529 ex/em using the 4X objective lens. After image capture slices were washed 3 times in PBS without calcium and magnesium and re-incubated at 37°. The fluorescent intensity of captured images was quantified in Image Pro Plus using the IOD (average density*area) function. All values

obtained were normalized to the untreated control mean and expressed as a percent change.

2.14 Measurement of Mitochondrial Membrane Potential:

Measurement of mitochondrial membrane potential (MMP) over time was performed using Rhodamine 123 (Molecular Probes). Rhodamine 123 at 10μM was pre-loaded 20min prior to image capture. Slices were washed 3 times with pre-warmed PBS without calcium or magnesium and visualized at an excitation/emission of 518/604. After image capture slices were washed 3 times in PBS without calcium and magnesium and re-incubated at 37°. The fluorescent intensity of images was quantified in Image Pro Plus using the IOD (average density*area) function. All values obtained were normalized to the untreated control mean and expressed as a percent change.

2.15 Western Blot Analysis of SOD1, SOD2, Catalase, and UCP-2:

Rat hippocampal slices were harvested from inserts and pooled (4) in 200μl of SDS lysis buffer with 5% protease inhibitor cocktail (Sigma). Tissue was ground for 30 seconds, sonicated for 5 seconds on ice water, and centerfuged at 14,000g at 4° C for 10min. Protein content was determined by Bradford assay and 30-50μg of protein was prepared with Lamelli sample buffer and loaded into 10 well gels (Gradipore). The gels were transferred to PVDF membranes (Biorad Immun-Blot; 0.2μM pore size) for 90min, blocked in 5% non-fat dry milk and TBST for 1 hour, and incubated overnight on a roller at 4° with the primary anti-body (1:1000 5% non-fat milk, UCP-2, Sigma; SOD1, SOD2, Catalase, AbCam). Blots were developed with a Femto kit (Pierce) and exposed for

10min (15 captures) on a 440CF Kodak image station. Densitometry was performed using Kodak analysis software. Blots were stripped using Restore Western Blot Stripping buffer (Pierce), washed three times in TBST, and blocked for 1 hour in 5% non-fat dry milk and TBST. Blots were incubated overnight at 4° with a monoclonal antibody for β-actin (Sigma) and developed with a Femto kit (Pierce). All samples were normalized to β-actin values as a loading control prior to statistical analysis. All values obtained were normalized to the untreated control mean and expressed as a percent change.

2.16 Electrophysiology/ field recording:

Cultured slices on membrane were separated and placed in artificial cerebral spinal fluid (ACSF) containing (in mM): 126 NaCl, 2.5 KCl, 1.2 $MgCl_2$, 2.4 $CaCl_2$, 1.2 NaH_2Po_4, 11.4 glucose, and 21.4 $NaHCO_3$, saturated with 95% O_2 and 5% CO_2 (pH 7.3), and maintained at 30° C. For recording, slices were transferred to a submersion type recording chamber constantly perfused (1.9 ml/min) with saturated ACSF at 30°C. Field excitatory post synaptic potentials (fEPSPs) were recorded using glass electrodes filled with HEPES buffered ACSF (pH 7.3) and induced by stimulating S. radiatum of CA1. Electrodes were placed in the area of CA1 with the most defined cell body layer. If a response was not immediately achieved the electrodes were repositioned several times within CA1. fEPSPs were monitored at 0.05 Hz and were recorded using a Geneclamp 500 amplifier (Axon Instruments) and AxographX (Version 1.0 release candidate 3.0, John Clements) or pClamp9 (Axon Instruments) recording software. All field recording experiments were performed by Dr. Matt Beckman and Greg Leary in the laboratory of Dr. Mike Kavanaugh at the University of Montana.

2.17 Statistical Analysis:

All data was analyzed utilizing Prizm software. One-way ANOVA with Tukey's post-hoc was used to determine statistical significance between groups. Two-tailed, unpaired t-test was used to determine specific differences between single groups. A $p < 0.05$ was considered significant and slices that were greater than +/- 4 standard deviations from the mean were considered outliers and omitted from statistical analyses.

Chapter 3

RESULTS

3.1 Effect of L-CAR on Cell Death after OGD

In previous studies by Wainwright et al [7], carnitine exerted a neuroprotective effect when administered prior to hypoxia-ischemia (HI). *In vivo* studies showed a significant decrease in infarct size in neonatal rats treated with carnitine prior to HI and an increased infarct size when administered after HI [41]. In an effort to elucidate the mechanism(s) responsible for Wainwright's observations, we developed a reproducible oxygen glucose deprivation (OGD) model in neonatal rat hippocampal slice cultures (RHSC's). Utilizing this model system we pre-treated cultures with carnitine, exposed them to OGD, and measured neuronal death. Our initial experiments in RHSC's recapitulated Wainwright's *in vivo* findings; pre-treatment with 5mM L-carnitine 2 hours prior to OGD significantly decreased neuronal death (as determined by propidium iodide staining), and administration of the same dose after OGD significantly increased neuronal death [fig.1a,b]. Furthermore, the pre-treatment effect was nullified when the carnitine was removed 12 hours prior to OGD suggesting treatment must occur within a short time frame prior to OGD to exert a neuroprotective effect [fig. 1].

Our observations at 24 hours showed carnitine treatment prevented neuronal death after OGD. This finding, however, did not rule out the possibility that carnitine treatment merely delayed the onset of apoptotic cell death occurring after 24 hours. To determine if this effect was occurring we repeated carnitine treatments and measured PI uptake at 48 hours post-OGD. At 48 hours neuronal death did not significantly increase
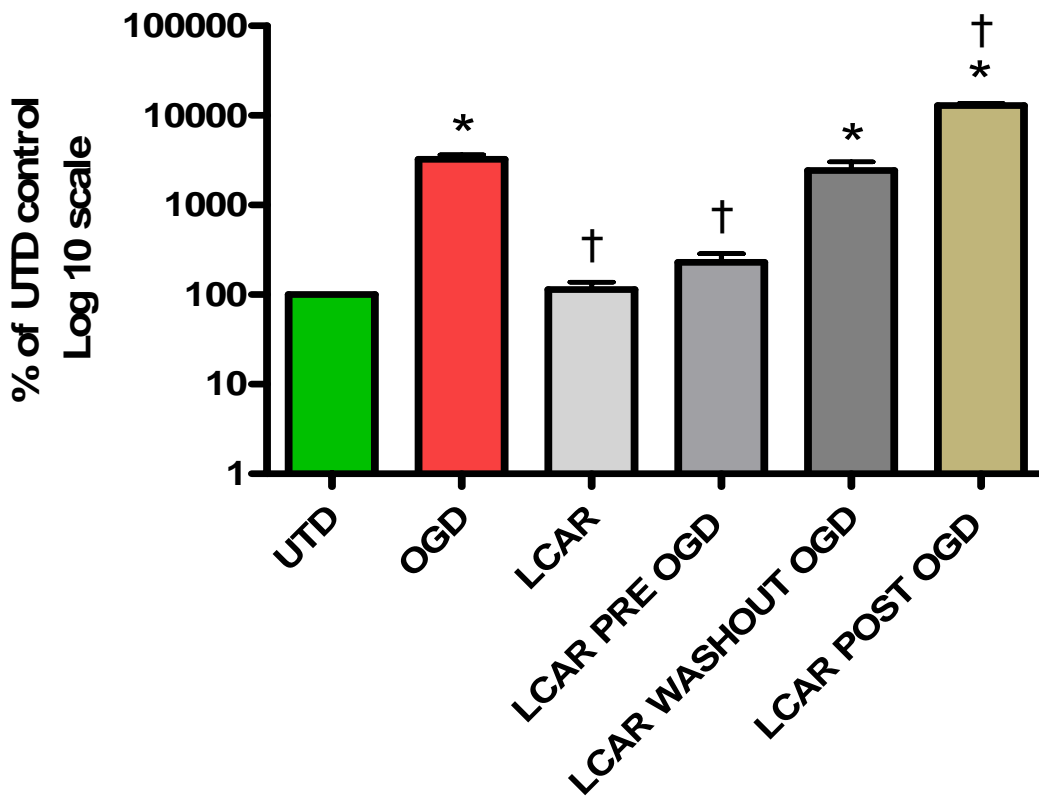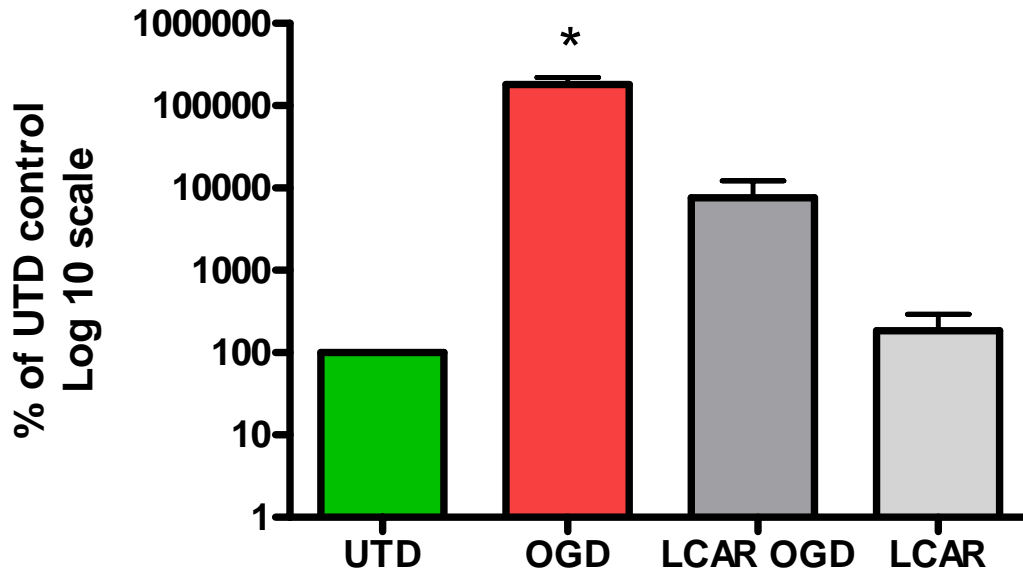
Fig.1a Cell death measured by PI uptake 24 hours post OGD. RHSC treated with carntine and exposed to 90 minutes of OGD showed significantly less neuronal death when compared to untreated OGD. Carnitine treatment after OGD resulted in significantly increased neuronal death. Removing carnitine 12 hours prior to OGD resulted in a loss of neuroprotective effect. UTD= untreated control group. *=p<0.05 all groups vs. UTD control; †=p<0.05 groups vs. OGD.One-way ANOVA, Tukey's post-hoc. Bars represent 6 or more samples.
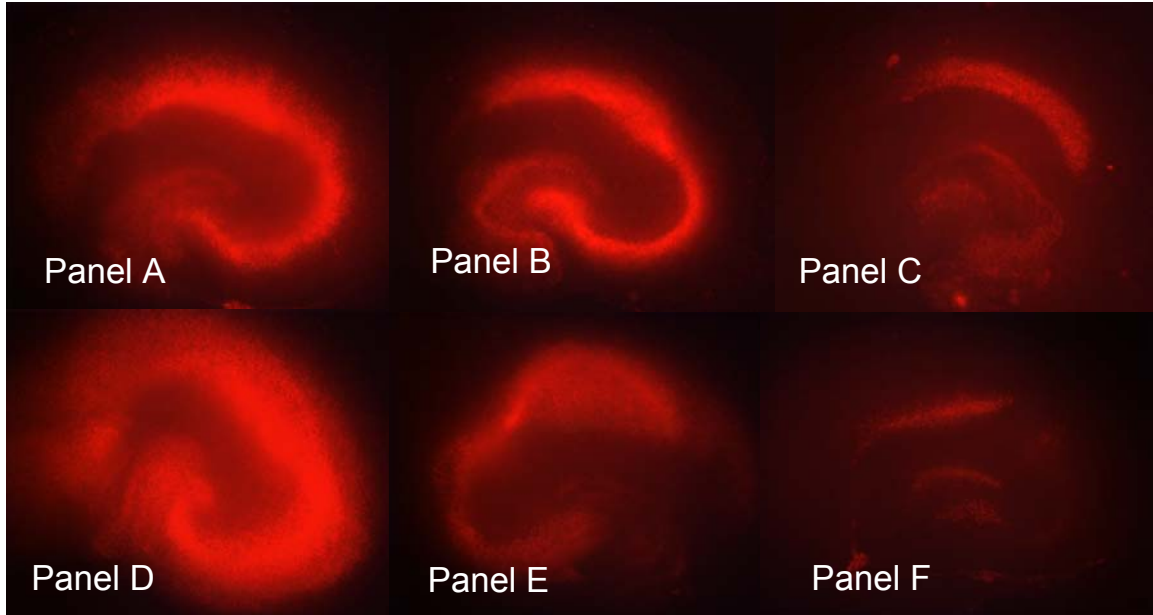
Fig. 1b Representative images of RHSC showing propidium iodide staining 24 h post-OGD. Panel A is untreated OGD, panel B LCAR treatment for 2 hours washed out for 12 hours and exposed to 90 minutes of OGD, panel C is LCAR treated non-OGD, panel D is LCAR treatment after OGD, panel E is LCAR treatment prior to OGD, panel F is untreated non-OGD. Untreated OGD slices show a significant increase in cell death when compared to untreated non-OGD slices. The administration of L-CAR prior to OGD prevents cell death while administration after OGD increases cell death. All slices treated with L-CAR were treated at a concentration of 5mM for 2 hours; OGD exposures were 90 minutes in duration. Images captured at 4x magnification.

Fig. 2a Neuronal death measured by PI uptake at 48 hours post OGD. RHSC treated with carnitine showed decreased neuronal death at 48 hours when compared to untreated OGD. This observation suggests LCAR prevents rather than delays the onset of cell death after OGD. UTD=untreated control. OGD is untreated RHSC exposed to oxygen glucose deprivation. *=p<0.05 UTD vs all groups, One-way ANOVA, Tukey's post hoc. Each bar represents a minimum of 4 samples.

in the carnitine treated groups suggesting carnitine prevents rather than delays neuronal death from OGD [fig.2] From this observation we hypothesized carnitine would prevent the activation of at least one of the two primary mechanisms of neuronal death (necrosis and apoptosis) after OGD. [34]

Based on the carnitine-mediated decrease in cell death, we studied the effect of carnitine on necrosis induced by OGD. Utilizing a lactate dehydrogenase (LDH) release assay we observed a significant decrease in necrotic death in carnitine treated RHSC's. Furthermore this effect was observed at 2, 12, and 24 hours post-OGD indicating carnitine reduces necrosis throughout reperfusion [fig 3]. At 24 hours post-OGD carnitine groups showed a significant increase in LDH release when compared to untreated controls but remained significantly less ($p<0.05$) than the untreated OGD group.

**3.2 The Effect of LCAR on Apoptosis after OGD**

To begin studying the effect carnitine treatment on apoptotic death in RHSC we utilized a fluorescent assay for non-specific caspase activation. At 24 hours post-OGD we observed a carnitine mediated decrease in caspase activation when compared to untreated OGD groups [fig.4]. To further elucidate this effect we performed western blot analysis to measure levels of mitochondrial cleaved (activated) caspase 9 (CC-9) [fig. 5]. We observed a statistically significant, carnitine-mediated decrease in CC-9 levels, suggesting carnitine is reducing neuronal death by decreasing mitochondrially-mediated apoptosis. To ensure carnitine mediated decreases in caspase activation correlated with decreased
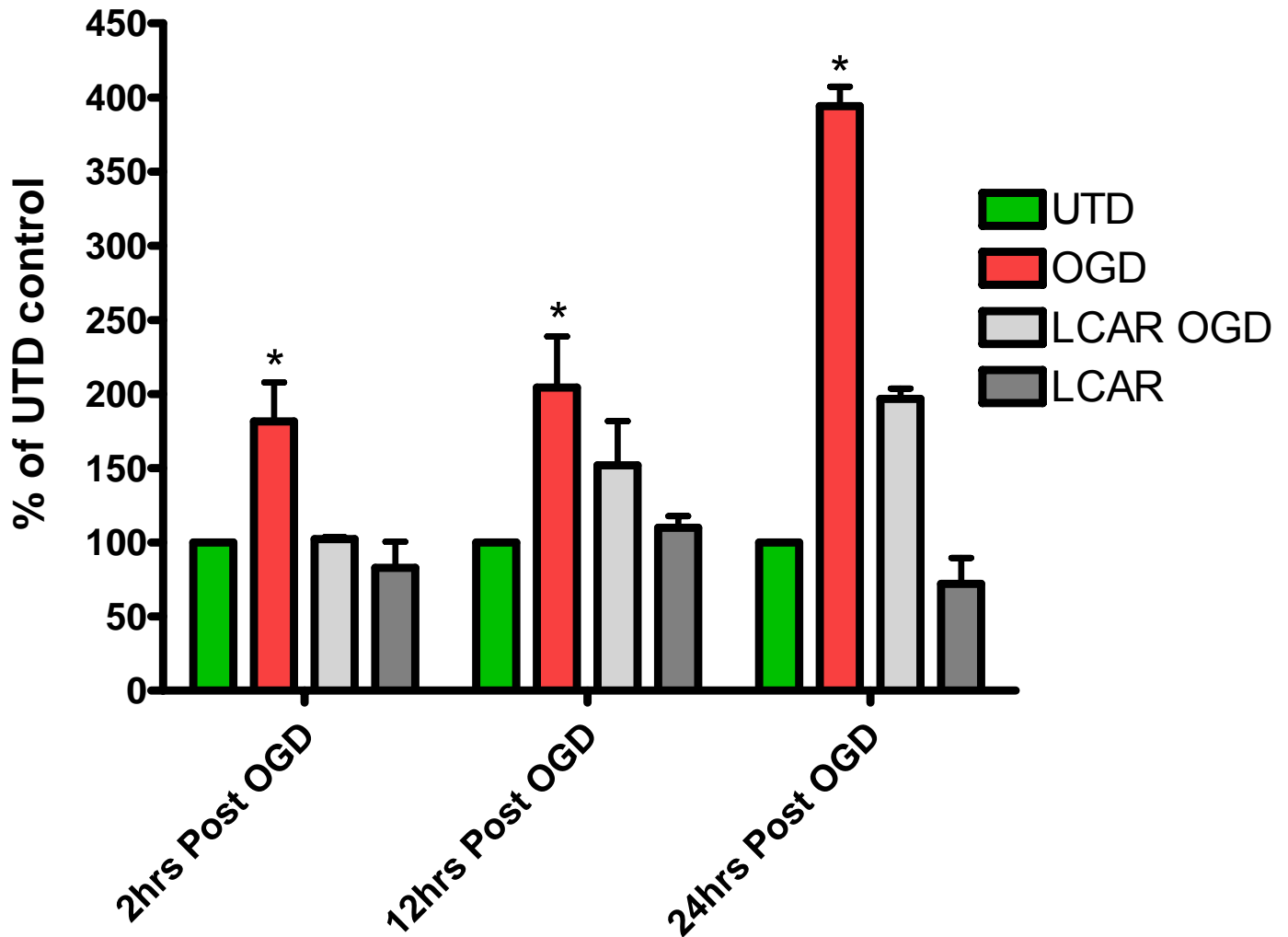
Fig. 3 Necrotic death in RHSC measured by LDH release.
At 2, 12, and 24 hours post-OGD untreated slices exposed
to OGD showed a significant increase in necrotic death.
Carntitine treated slices showed a significant decrease in necrotic
death at 2, 12, and 24 hours post-OGD. UTD=untreated control.
OGD is untreated RHSC exposed to oxygen glucose
deprivation.*=p<0.05 all groups compared to UTD control; One
way ANOVA, Tukey's post-hoc.
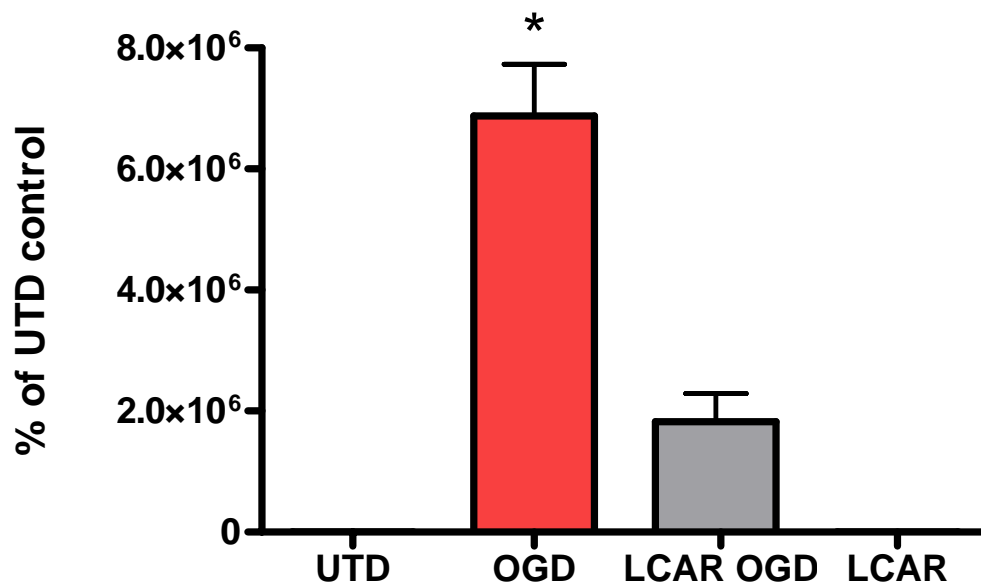
Fig. 4a Caspase activation in RHSC after 24 hours of OGD. Caspase activation was significantly increased in both carnitine treated and untreated RHSC exposed to OGD when compared to untreated non-OGD cultures. Statistical analysis of untreated OGD and carnitine treated OGD showed carnitine significantly decreased caspase activation. *=p<0.05 all groups compared to UTD control; One way ANOVA, Tukey's post-hoc. Bars represent 6 or more samples.
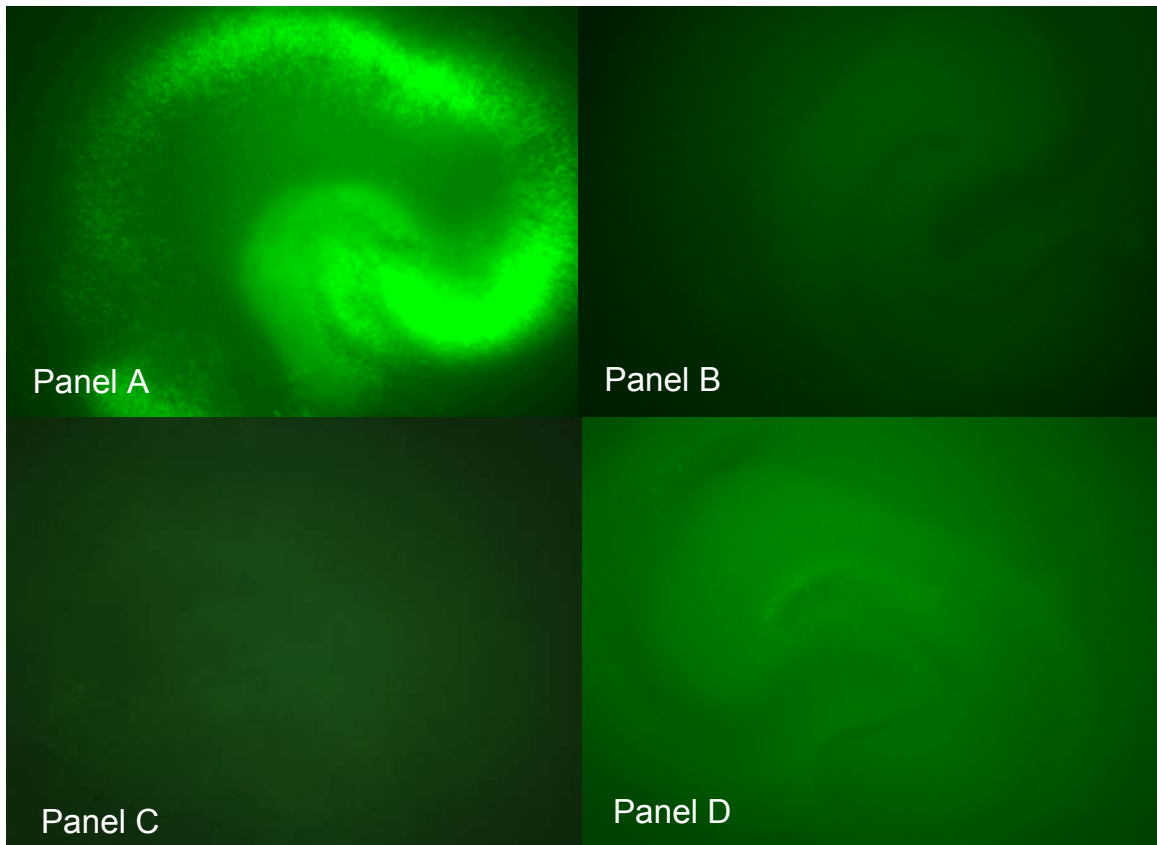
Fig. 4b Representative images of RHSC showing caspase activation at 24h post-OGD. Untreated RHSC exposed to OGD show a significant increase in non-specific caspase activation when compared to untreated, LCAR treated, and LCAR treated OGD exposed RHSC. Panel A is untreated OGD, panel B is untreated control, panel C is LCAR non-OGD, panel D is LCAR OGD. OGD for 90min. LCAR at 5mM present for 2 hours prior to OGD. UTD is untreated control. OGD is untreated RHSC exposed to oxygen glucose deprivation. Images captured at 4x magnification.
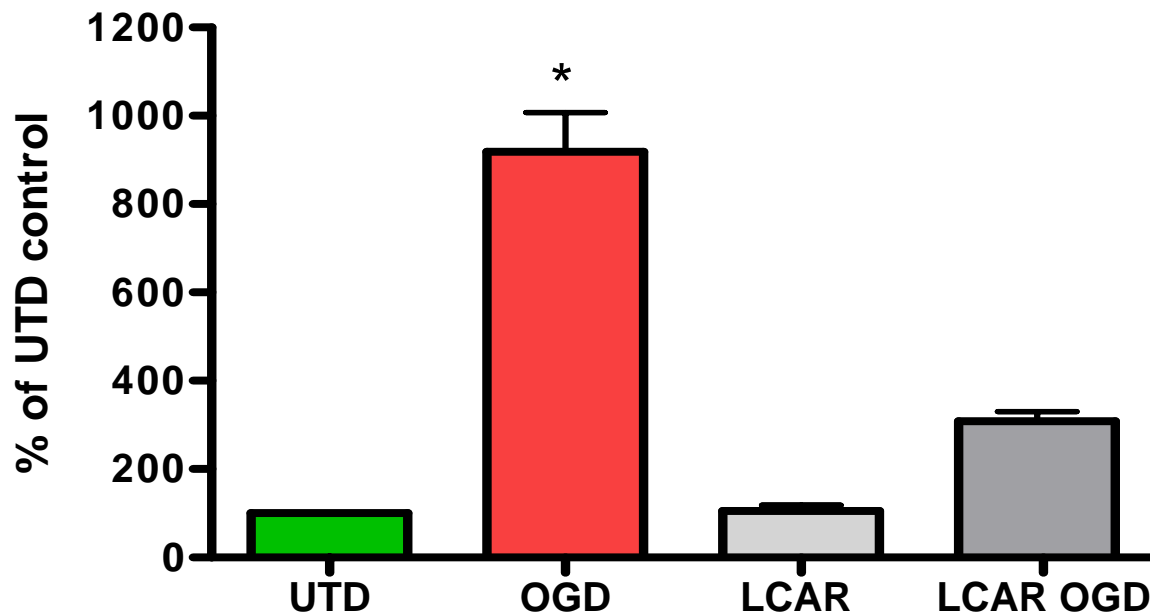
Fig. 5a Western blot analysis data showing LCAR treatment prior to OGD signifcantly reduced levels of cleaved (activated) caspase-9 after OGD. *=p<0.05 all groups compared to UTD control. One way ANOVA, Tukey's post-hoc. Each bar represents a 3 or more samples; each sample composed of 4 pooled slices. (Data square root transformed prior to analysis)
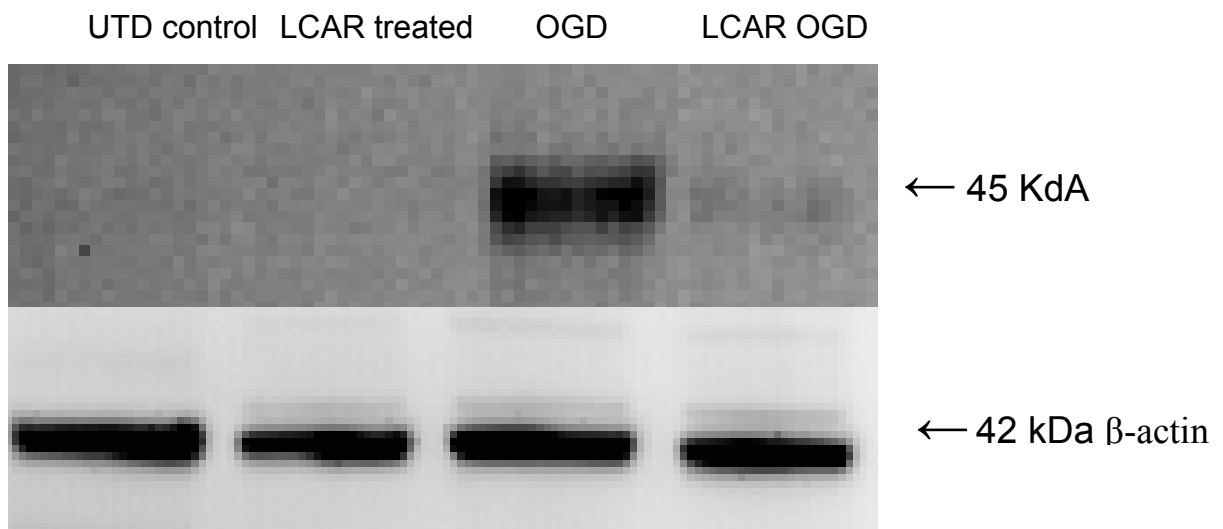
Fig. 5b Representative images of Western blot analysis for cleaved caspase 9 expression at 24hrs post-OGD. Images indicate LCAR treatment decreases the amount of cleaved caspase 9 protein after OGD. Also shown β-actin loading control.

apoptosis we performed the TUNEL assay on fixed hippocampal slices at 1, 6 and 24 hours post-OGD. We observed a carnitine-mediated decrease in TUNEL positive neurons at 24 hours indicating carnitine pre-treatment reduces mitochondrially mediated apoptosis after OGD [fig. 6]. Based on our observation that carnitine pre-treatment reduced both necrosis and apoptosis we hypothesized the prevention of cell death would result in preservation of viable synaptic pathways within the hippocampus. To test this hypothesis we treated hippocampal slices with carnitine, exposed them to OGD, and then utilized field recording techniques to measure synaptic transmission.

3.3 Synaptic Transmission in LCAR Treated Neurons after OGD

Measurement of synaptic transmission in RHSC's following OGD (performed by the Kavanaugh laboratory) showed a significant decrease in EPSP amplitudes (<75uV; p<0.0001). In contrast, carnitine treated slices generated considerably more robust amplitudes (~300µV) after OGD and did not significantly differ from the untreated control at 48 hours [fig. 7]. These data suggest carnitine not only decreases neuronal death, but also prevents the OGD-induced loss of synaptic transmission.

During acute HI, synaptic transmission ceases within 10-20 seconds and ATP reserves are depleted within 2-3 minutes [2]. After reperfusion synaptic transmission returns briefly only to decrease as the secondary phase of energy depletion occurs [20]. Previous studies by Kim et al (2006) showed a percentage of neurons exposed to mild HI will not undergo cell death, but are unable to generate functional EPSP's due to acute mitochondrial dysfunction and ATP depletion [55] [34]. Based on these studies we
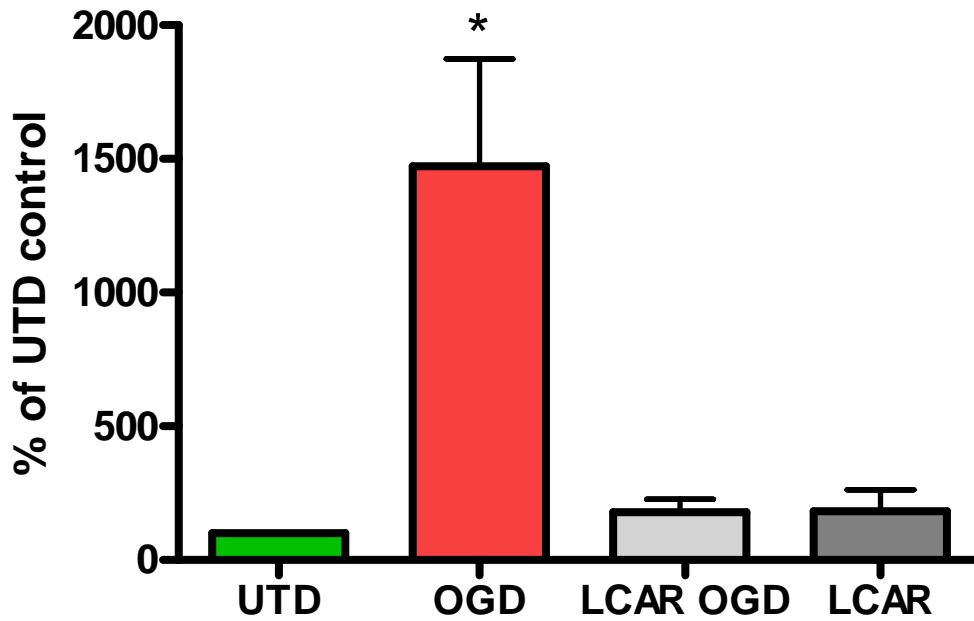
Fig. 6a Tunel staining in apoptotic cells after 24hrs of OGD. LCAR treatment prior to OGD signficantly decreased the percentage of apoptotic cells after OGD. *=p<0.05 all groups vs UTD control; One way ANOVA, Tukey's post-hoc. Bars represent a minimum of 4 samples.
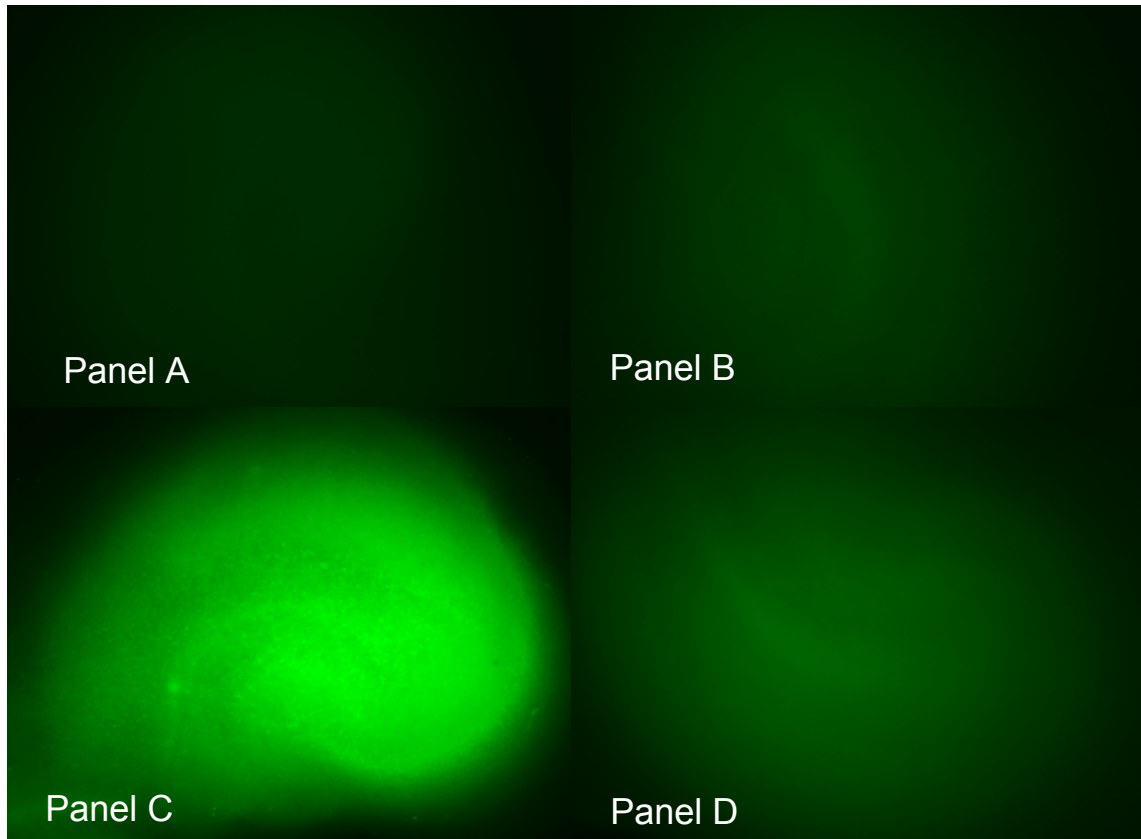
Fig. 6b Representative images of TUNEL stained RHSC at 24 hours post-OGD. Images show OGD increases the amount and intensity of TUNEL staining and LCAR treatment significantly decreases TUNEL staining suggesting LCAR reduces apoptotic cells. Panel A is untreated control, Panel B is LCAR treated, Panel C is OGD, and Panel D is LCAR treated OGD exposed. Images captured at 4x magnification.
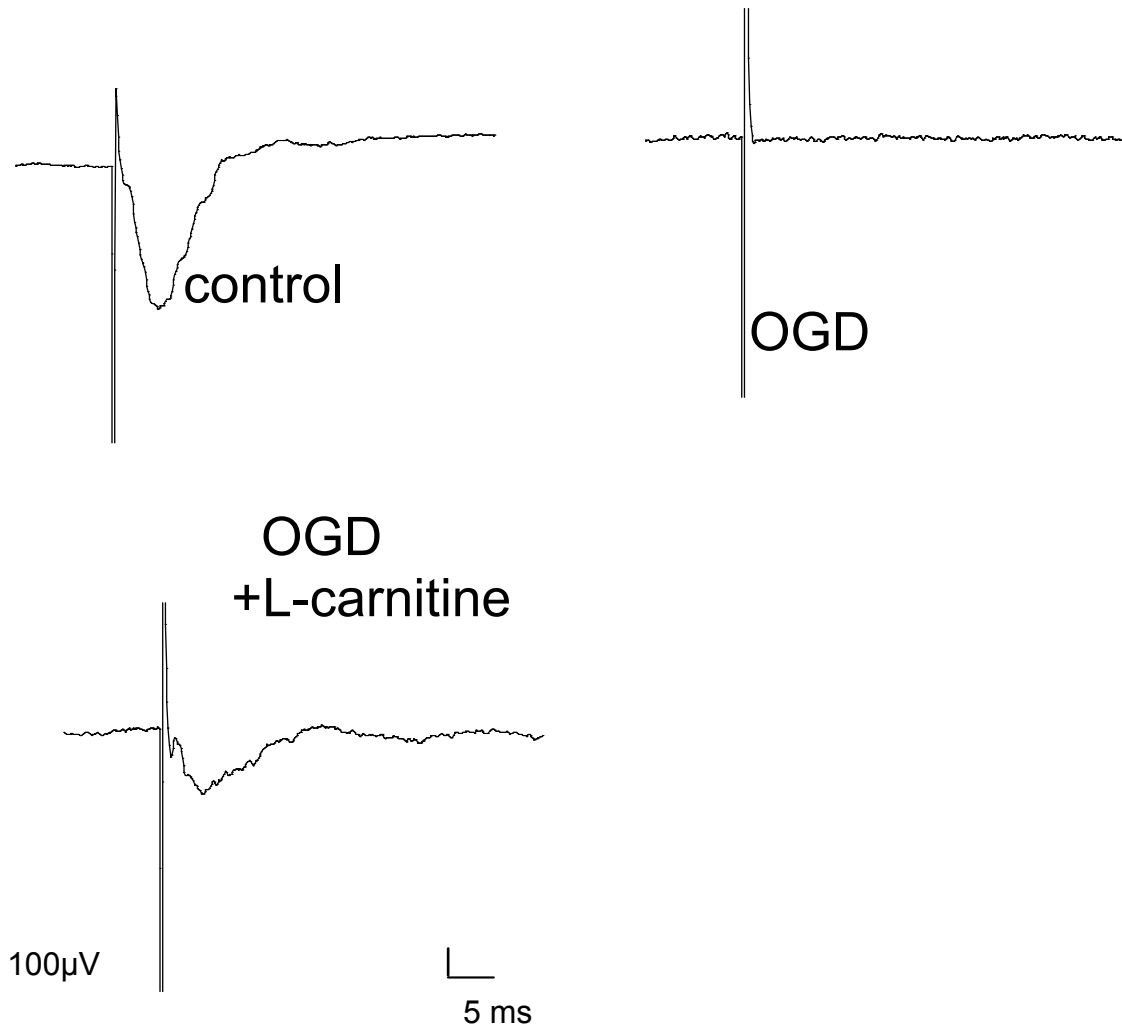
Fig. 7a Representative traces of evoked EPSP's in RHSC 48 hours after OGD. LCAR treated cultures exposed to OGD show a significantly larger EPSP when compared to untreated OGD cultures. This observation suggests LCAR prevents the OGD induced loss of synaptic transmission.
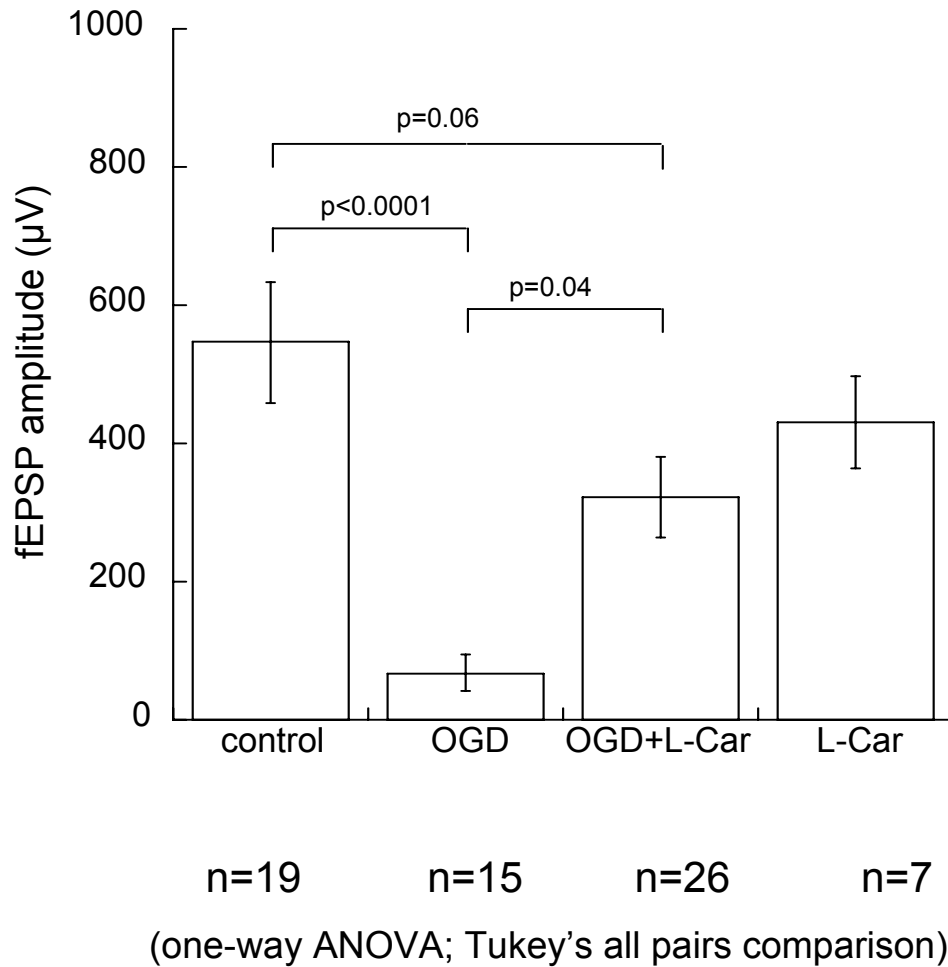
Fig. 7b Evoked EPSP's in RHSC treated with carnitine and exposed to OGD.

At 48 hours post-OGD carnitine treated cultures showed significantly greater

evoked EPSP's when compared to untreated OGD cultures. One way

ANOVA, Tukey's post hoc.

hypothesized the possibility of a link between carnitine treatment, preservation of synaptic viability, and the prevention of OGD-induced mitochondrial dysfunction leading to ATP depletion. This hypothesis was further reinforced by our finding that carnitine decreased mitochondrially mediated apoptosis which is directly linked to mitochondrial health. Based on these observations we elected to study the effect of carnitine on mitochondrial dysfunction induced by OGD.

**3.4 Metabolic Viability in LCAR treated RHSC exposed to OGD**

To begin measuring the effect of carnitine on mitochondrial health after OGD we stained RHSC with Calcein AM, a fluorogenic esterase substrate that is retained in neurons that are metabolically active. Utilizing this dye we measured the effect of mitochondrial metabolic viability in RHSC's at 2, 6, 12, 24, and 48 hours after OGD. In untreated slices exposed to OGD we observed a rapid, irreversible decrease in metabolic activity (decreased fluorescence) that did not occur in the carnitine treated slices. At 6 hours post-OGD carnitine treated slices showed a significant decrease in metabolic viability, but this effect reversed at 12, 24, and 48 hours with metabolic viability returning to basal levels at 48 hours post OGD [fig. 9]. Carnitine treatment alone resulted in an increase in calcein fluorescence suggesting carnitine not only prevents mitochondrial dysfunction but also increases metabolic viability prior to OGD.

In light of this finding we elected to examine the effect of carnitine pre-treatment on reactive oxygen species (ROS) which have been shown to disrupt membrane integrity after OGD leading to reduced metabolic viability and increased apoptosis.
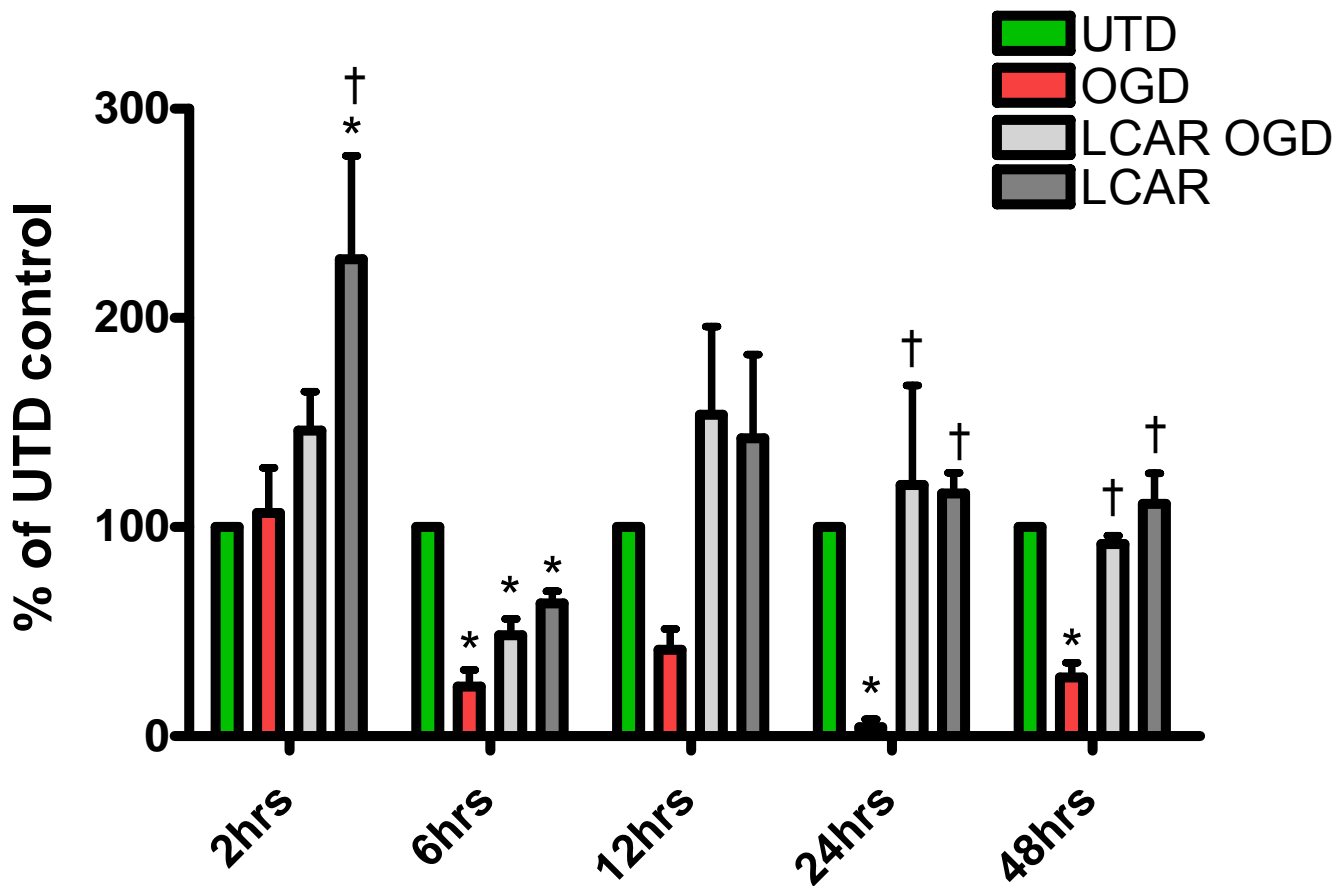
Fig. 8a Metabolic viability in RHSC measured by calcein AM fluorescence. Untreated RHSC exposed to OGD showed a loss of metabolic activity at 6 hours post-OGD that remained consistent through 48 hours post OGD. Carnitine treated RHSC exposed to OGD showed a significant decrease in metabolic viability at 6 hours, but this effect was reversed at 12 hours post-OGD. At 24 and 48 hours carnitine treated slices exposed to OGD showed basal levels of metabolic activity. *=p<0.05 all groups vs. UTD control; †=p<0.05 all groups vs OGD; One-way ANOVA, Tukey's post hoc. Each bar represents a minimum of 4 samples.
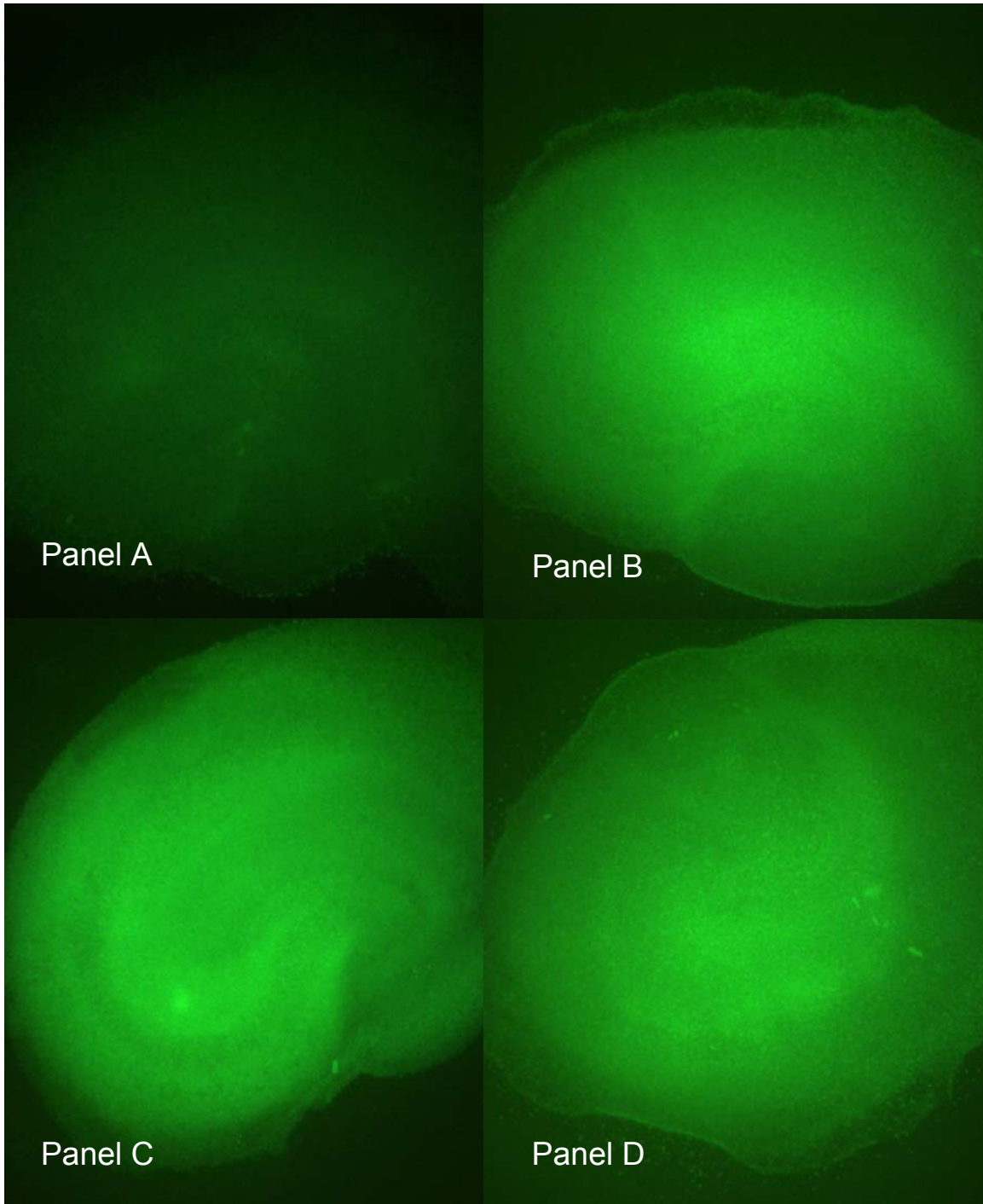
Fig. 8b Representative images of RHSC stained with Calcein AM at 48 hours post OGD. Panel A is untreated OGD, panel B is LCAR non-OGD, panel C is LCAR OGD, panel D is UTD non-OGD. Images captured at 4x magnification.

**3.5 Reactive oxygen species in LCAR treated RHSC exposed to OGD**

During OGD the majority of cellular ROS is produced within the mitochondrial matrix through complexes I-IV of the electron transport chain. The increase in ROS production creates a pathological cycle of membrane damage that depletes ATP. The loss of membrane integrity and ATP depletion further increases ROS eventually damaging DNA and resulting in the translocation of cytochrome c leading to mitochondrially mediated apoptosis. [20] [10, 31]. Based on our observation that carnitine prevents metabolic dysfunction and mitochondrially mediated apoptosis, we hypothesized carnitine treatment would achieve these effects by modulating superoxide produced by OGD exposure.

In previous studies performed by Ames et al (2004) carnitine treatment resulted in increased cellular respiration, and, as a byproduct, increased superoxide production. Utilizing RHSC treated with dihydroethidium (DHE) we also observed a significant, carnitine mediated increase in cytosolic superoxide that remained elevated at 4.5 hours of treatment. After 8 hours of treatment however, superoxide levels had significantly decreased and did not differ from the untreated controls. In RHSC's pre-treated with carnitine and exposed to OGD, superoxide levels were significantly elevated at 1 and 6 hours post-OGD. However, at 12 and 24 hours superoxide levels decreased and did not significantly differ from untreated controls [fig. 10, 11].

The carnitine-mediated decrease in superoxide levels at 12 and 24 hours was not observed when carnitine was administered after OGD suggesting it must be present prior to OGD to activate the mechanism(s) that modulate superoxide increases [fig. 12]. This
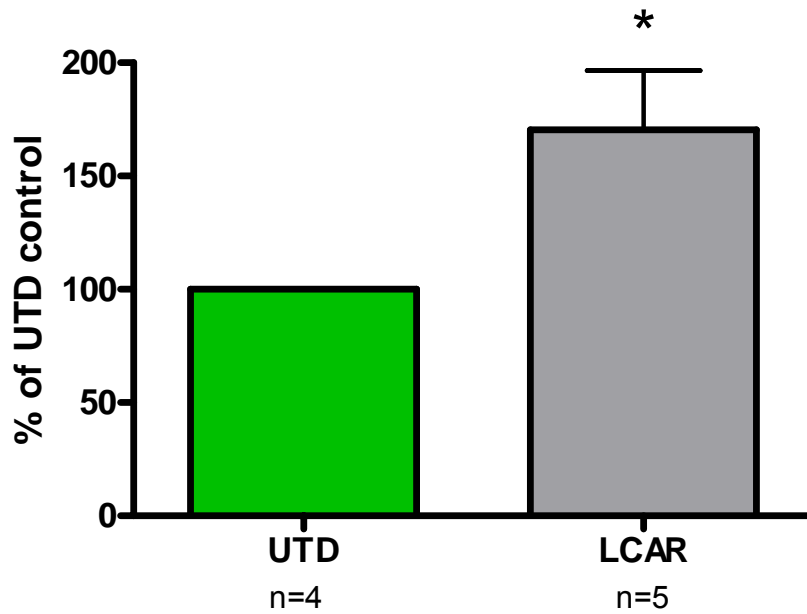
Fig. 9a Cytosolic superoxide in RHSC after 2 hours of carnitine treatment. Carnitine treatment significantly increased superoxide levels. *=p<0.05, Unpaired two-tailed T-test. Each bar represents a minimum of 4 samples (each sample is composed of 4 pooled slices).
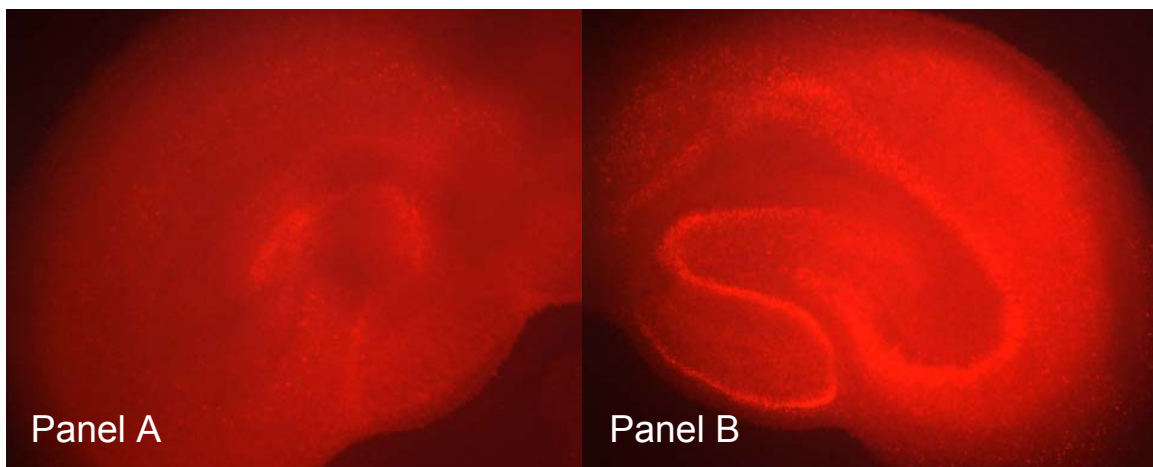

Fig. 9b Representative images of RHSC stained with DHE after 2h of LCAR treatment.

Images indicate LCAR increases superoxide levels prior to OGD. Panel A UTD, panel B

is LCAR treated.
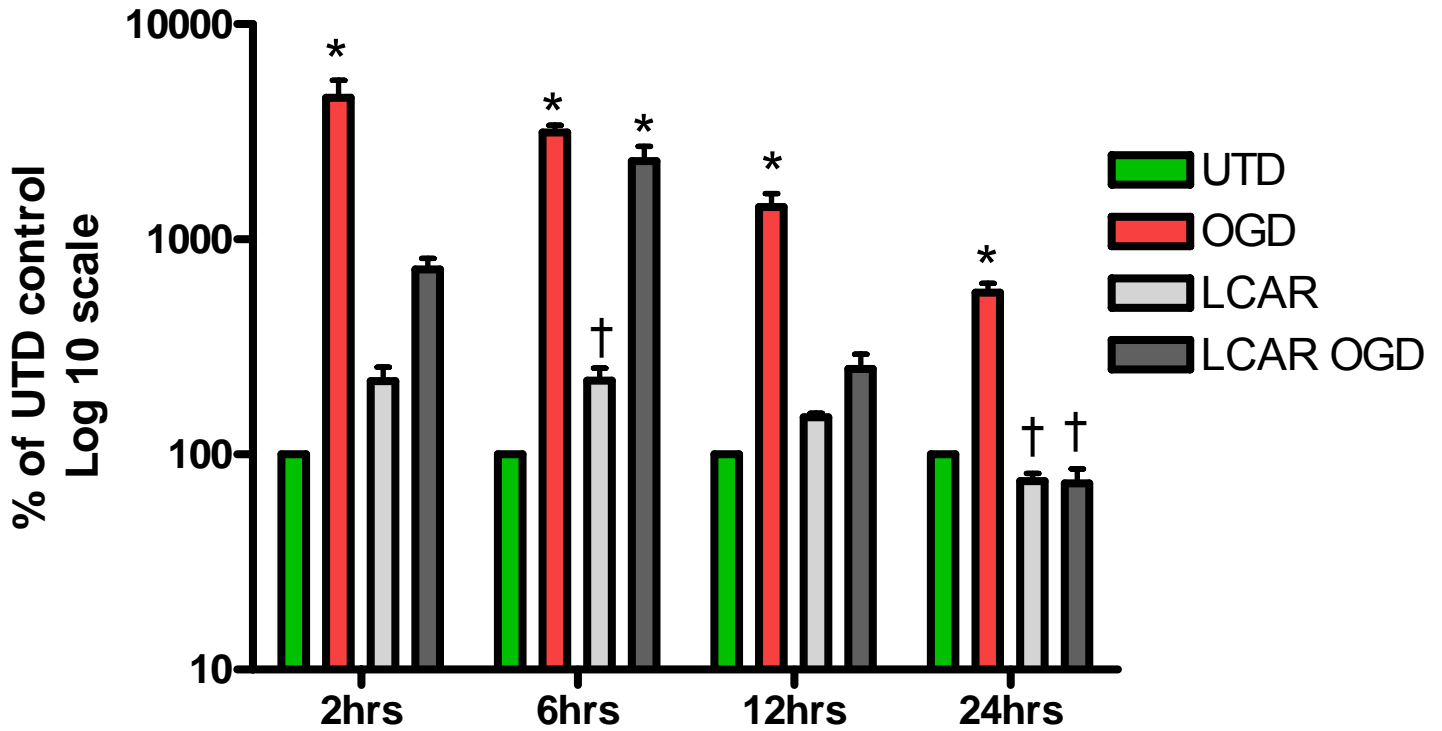
Fig. 10a Cytosolic superoxide levels in RHSC exposed to OGD. Carnitine treated slices exposed to OGD showed superoxide levels at 6 and 12 hours that did not differ from untreated OGD slices. At 12 and 24 hours post OGD carnitine treated slices showed a significant decrease in cytosolic superoxide. *=p<0.05 all groups vs. UTD control; †=p<0.05 groups vs. OGD, One way ANOVA, Tukey's post-hoc. Each bar represents a minimum of 4 samples.
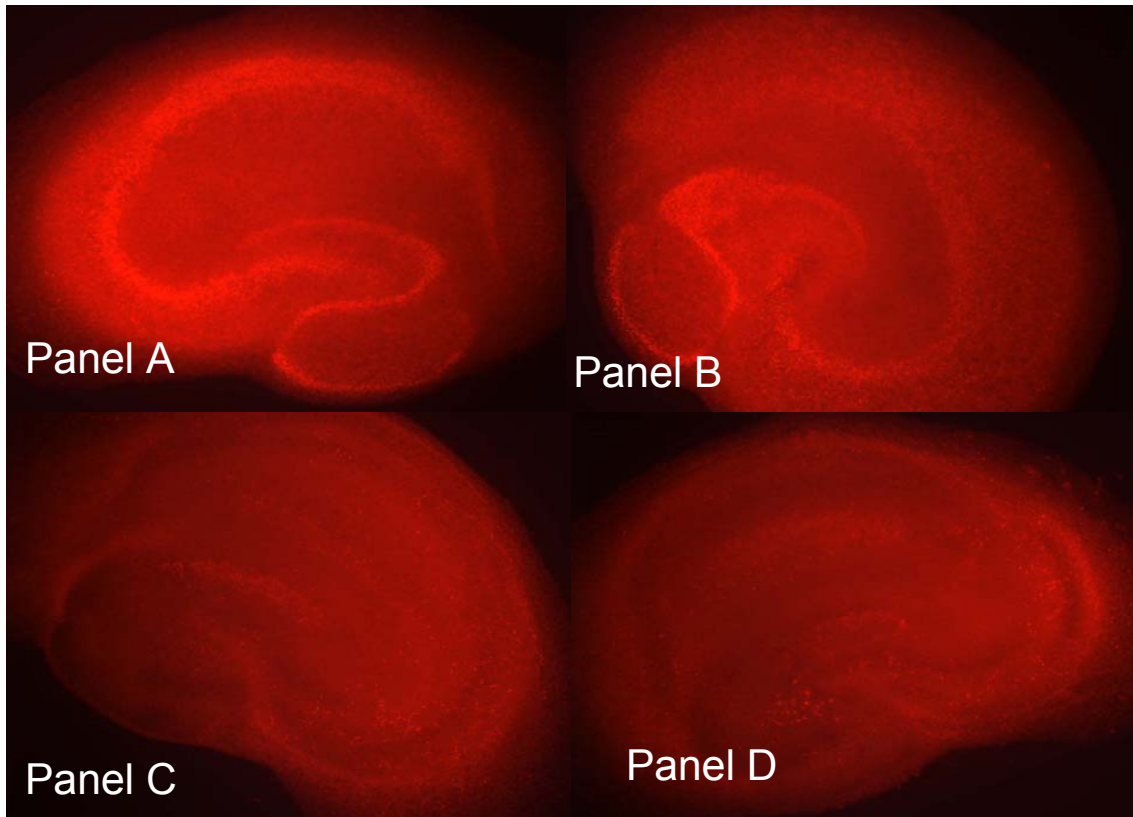
Fig. 10b Representative images of RHSC stained with DHE at 12h post OGD. Images show decreased superoxide staining after OGD in LCAR treated cultures when compared to OGD untreated groups. Panel A is untreated OGD, panel B is LCAR OGD, panel C is LCAR non-OGD, panel D is UTD control. Images captured at 4x magnification.
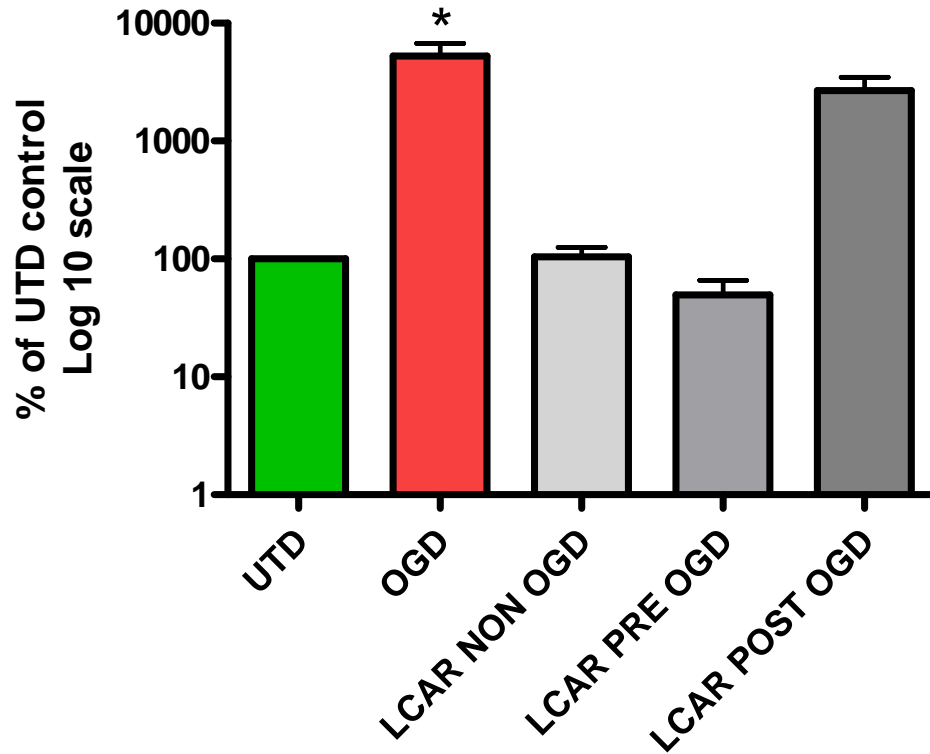
Fig. 11a Cytosolic superoxide levels in RHSC at 24 hours post-OGD. Carnitine treatment prior to OGD resulted in slices with significantly decreased levels of superoxide. Addition of carnitine after OGD resulted in superoxide levels that did not differ from untreated OGD exposed slices. *=p<0.05 all groups vs. UTD control One-way ANOVA, Tukey's post-hoc. Each bar represents a minimum of 4 samples.
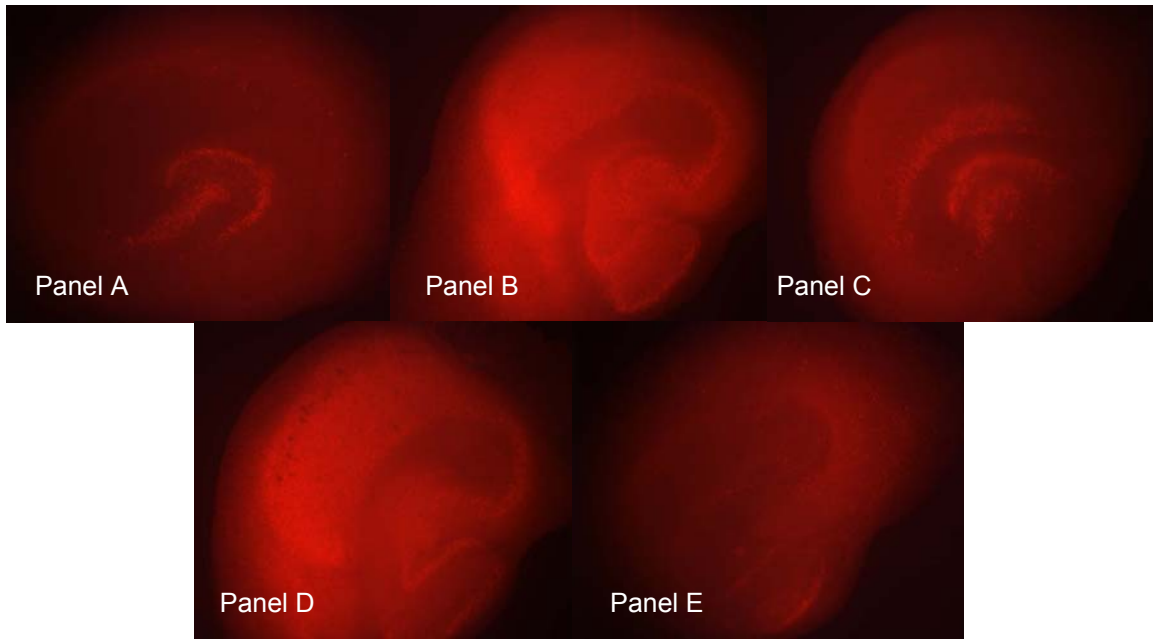
Fig. 11b Representative images of RHSC stained with DHE at 24h post OGD. Panel A UTD non-OGD, panel B is untreated OGD, panel C is LCAR non-OGD, panel D is LCAR post-OGD, panel E is LCAR pre-OGD. At 24 hours post-OGD, LCAR treatment decreased superoxide levels. Images captured at 4x magnification.

hypothesis is further supported by our finding that carnitine administration after OGD failed to protect neurons [fig. 1].

Mitochondrial superoxide levels measured by Mitosox assay correlated with cytosolic superoxide levels measured with DHE; carnitine treatment increasing mitochondrial superoxide prior to OGD and reducing mitochondrial superoxide at 24 hours after OGD [fig. 13, 14]. Based on our observation that carnitine treatment post-OGD failed to reduce superoxide levels and carnitine treatment prior to OGD increases superoxide, we hypothesized carnitine treatment was modulating superoxide levels after OGD by upregulating the expression of CuZn (cytosolic) superoxide dismutase (SOD1) and MnSOD (mitochondrial; SOD2) prior to OGD. This effect would increase superoxide scavenging capability and may account for the temporal decrease in superoxide observed in the carnitine treated groups.

3.6 SOD protein levels and activity in LCAR treated RHSC exposed to OGD

To test this hypothesis we treated RHSC's with carnitine and performed Western blot analysis to evaluate expression levels of SOD1 and SOD2. After 2 hours of carnitine treatment SOD1 showed a significant increase in expression, while SOD2 expression significantly decreased [fig. 15, 16]. Analysis of SOD1 expression at 2 hours post-OGD showed a significant increase in expression in carnitine-treated OGD slices, but at 24 hours post-OGD all experimental groups showed similar levels of SOD1 expression. This finding, taken with our superoxide measurements, suggests RHSC's exposed to OGD have increased amounts of superoxide present at 24 hours but do not
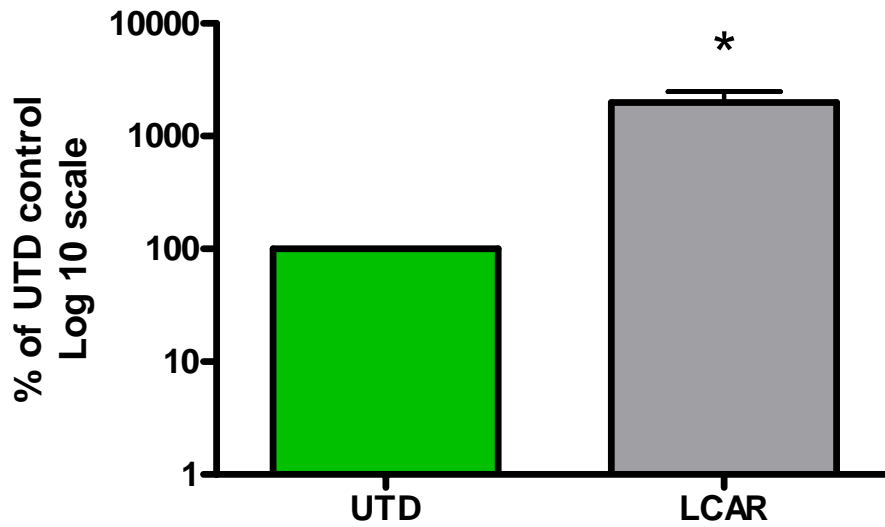
Fig. 12a Mitochondrial superoxide in RHSC after two hours of carnitine treatment. Carnitine treatment significantly increased mitochondrial superoxide prior to OGD. *=p<0.05, unpaired two tailed T-test. Each bar represents a minimum of 4 samples; each sample is composed of 4 pooled slices.
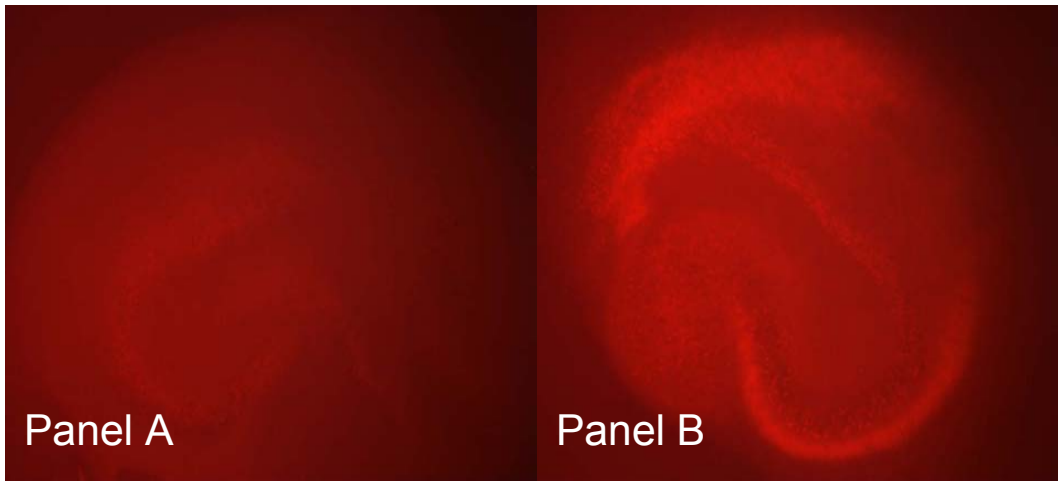
Fig. 12b Representative images of RHSC stained with MITOSOX after 2 hours of LCAR treatment. Panel A is untreated control, panel B is LCAR treated. LCAR treatment increases mitochondrial superoxide. Images captured at 4x magnification.
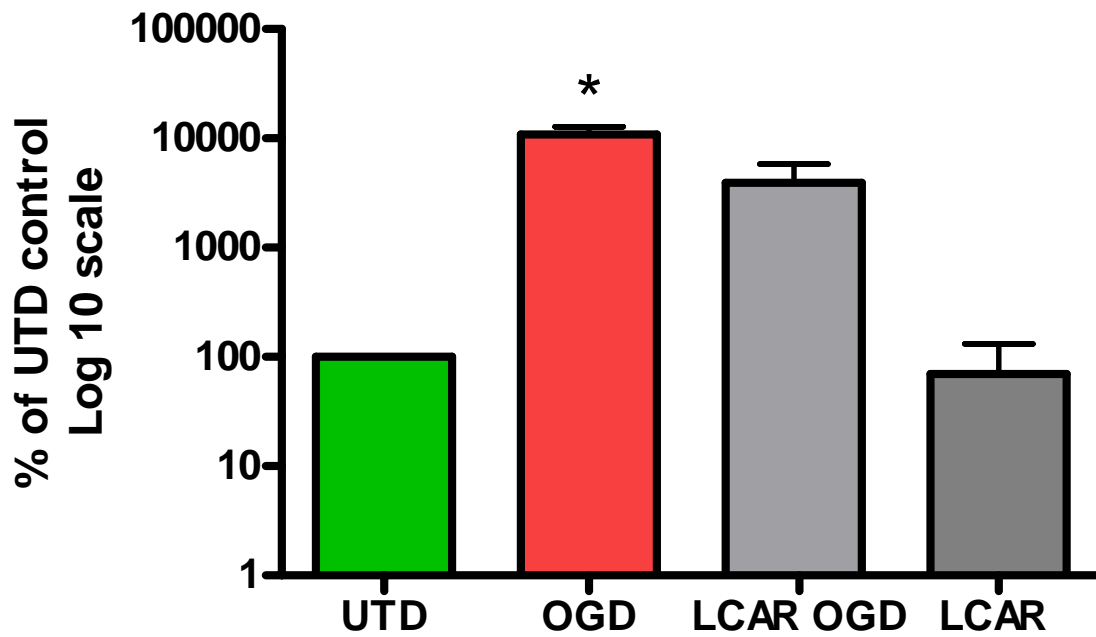
Fig. 13a Mitochondrial superoxide in RHSC 24 hours after OGD. Carnitine treated RHSC showed a significant decrease in mitochondrial superoxide 24 hours after OGD. *=p<0.05, One way ANOVA, Tukey's post-hoc. Each bar represents a minimum of 3 samples.
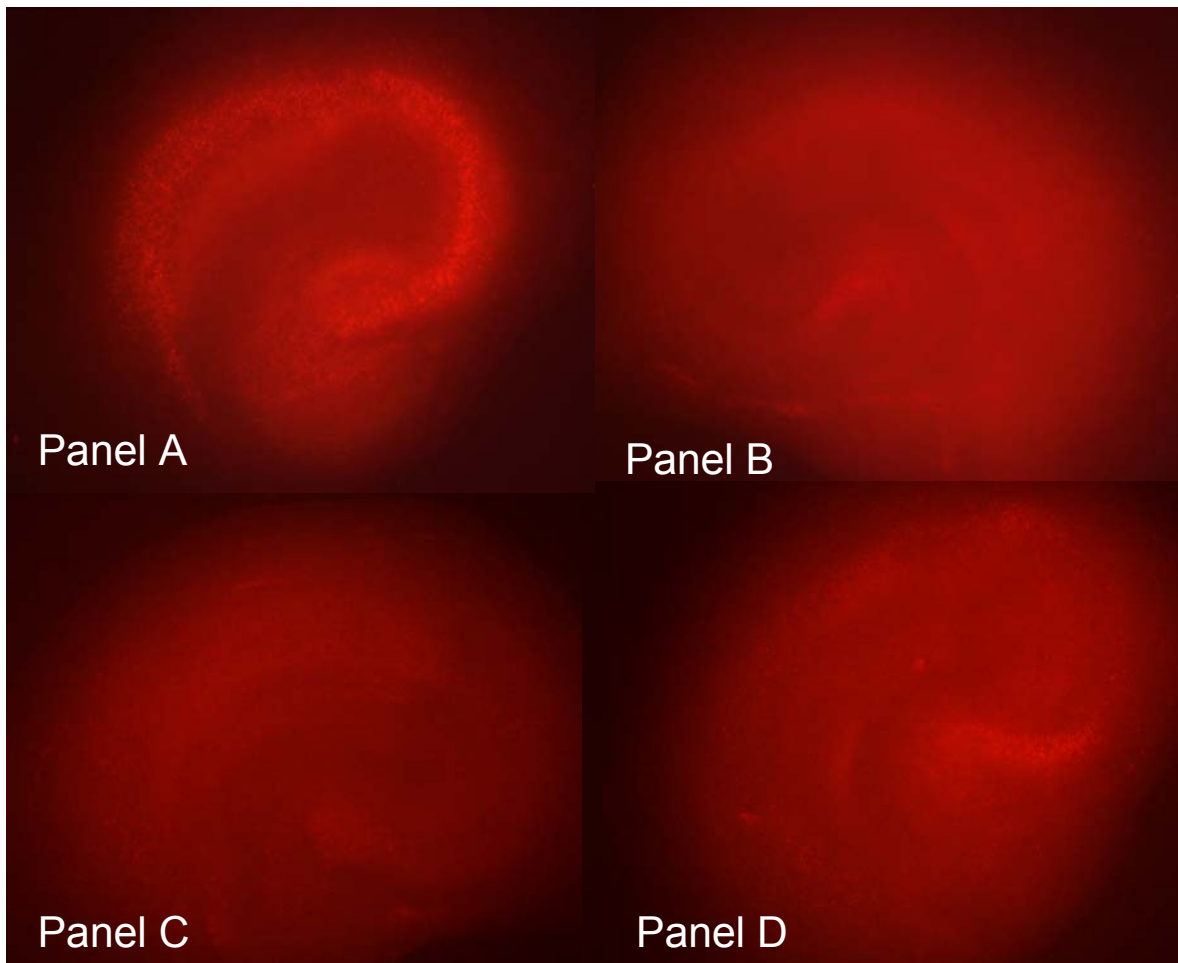
Fig. 13b Representative images of RHSC stained with MITOSOX at 24h post OGD. LCAR treatment significantly reduces mitochondrial superoxide levels 24 hours after OGD. Panel A UTD OGD, panel B is LCAR non-OGD, panel C is untreated control, panel D is LCAR pre-OGD. Images captured at 4x magnification.

Fig. 14a Western blot analysis of SOD2 expression in RHSC after 2 hours of carnitine treatment. Carnitine treatment resulted in a significant decrease in SOD2 expression. *=p<0.05, unpaired two tailed T-test. Each bar represents a minimum of 5 samples; each sample is composed of 4 pooled slices.

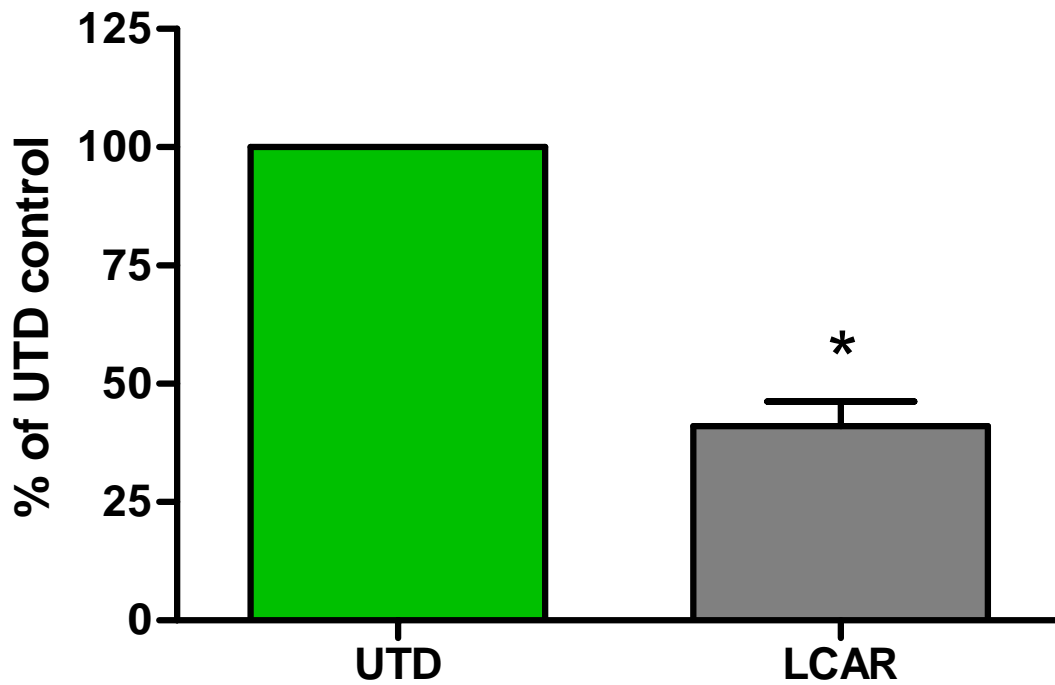UTD control LCAR treated LCAR treated UTD Control

← 26 kDA

← 42 Kda β-actin
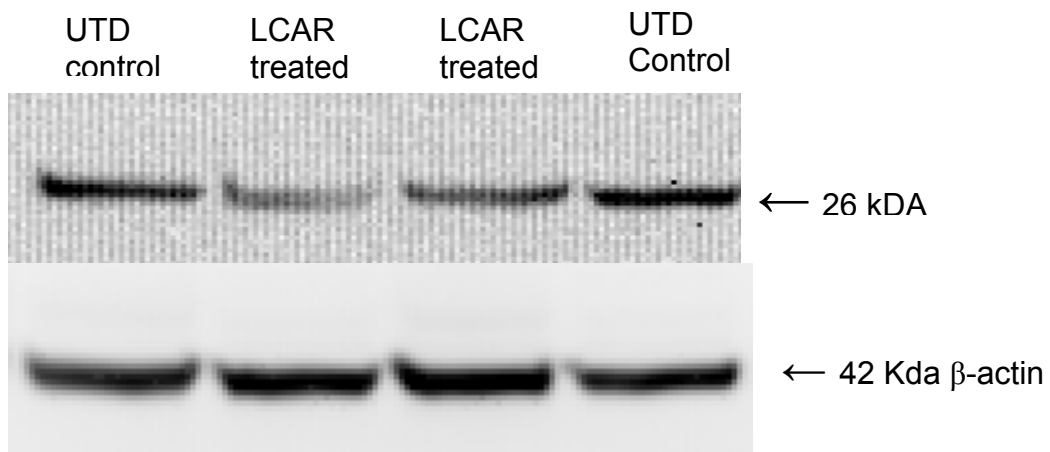
Fig. 14b Representative images of Western blot analysis showing SOD2 expression after two hours of LCAR treatment. Representative images show LCAR decreases SOD2 protein levels. Also shown β-actin loading control.
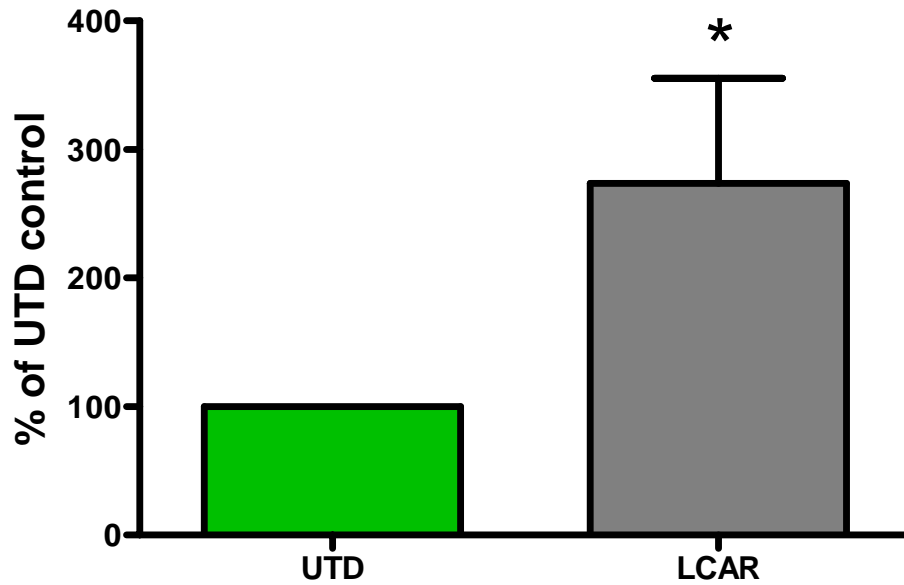
Fig. 15a Western blot analysis of SOD1 in RHSC
treated with carnitine for 2 hours. Carnitine treatment
resulted in a significant increase in SOD1
expression. *=p<0.05, unpaired two tailed T-test.
Each bar represents a minimum of 7 samples; each
sample is composed of 4 pooled slices.
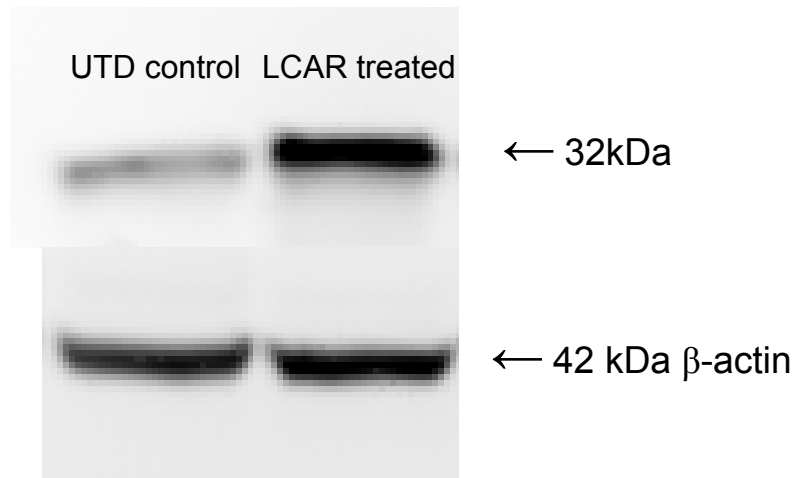
Fig. 15b Representative images of Western blot
analysis showing SOD1 expression after two
hours of LCAR treatment. LCAR treatment increases
SOD2 protein levels. Also shown β-actin loading control.

posses adequate levels of SOD1 protein to effectively convert it to H_2O_2. In contrast, carnitine pre-treatment causes an increase superoxide which induces a corresponding increase in SOD1 expression, and this effect may 'prime' neurons for an acute oxidative stress similar to the insult OGD induces [fig. 17, 18].

Based on this finding we elected to compare the effect of carntitine treatment on the enzymatic activity of SOD1 and determine if increased SOD1 expression correlated with increased enzymatic activity. RHSC treated with carnitine for 2 hours were harvested and assayed for SOD activity. We observed a carnitine-mediated increase in SOD1 activity but did not observe a significant alteration in SOD2 activity, irrespective of the decreases in SOD2 expression [fig. 19]. This observation may be due to decreased enzymatic activity in untreated controls, increased activity in the LCAR treated cultures, or a combination of the two. The increase in mitochondrial superoxide and SOD1 expression and activity prior to OGD also suggests carnitine pretreatment may be generating superoxide in the mitochondria that is leading to increased SOD1 expression and activity.

To test this hypothesis we administered carnitine in the presence of a mitochondrially preferential anti-oxidant, lipoic acid (LA; antioxidant), and measured the effect on both mitochondrial and cytosolic superoxide levels. After determining LA treatment significantly reduces superoxide levels in hippocampal slices [fig. 20, 21], we repeated the pre-treatments, exposed them to OGD, and measured cell death with propidium iodide uptake.

The addition of lipoic acid in conjunction with carnitine treatment resulted in a significant loss of neuroprotection ($p<0.05$) [fig. 22] This observation suggests

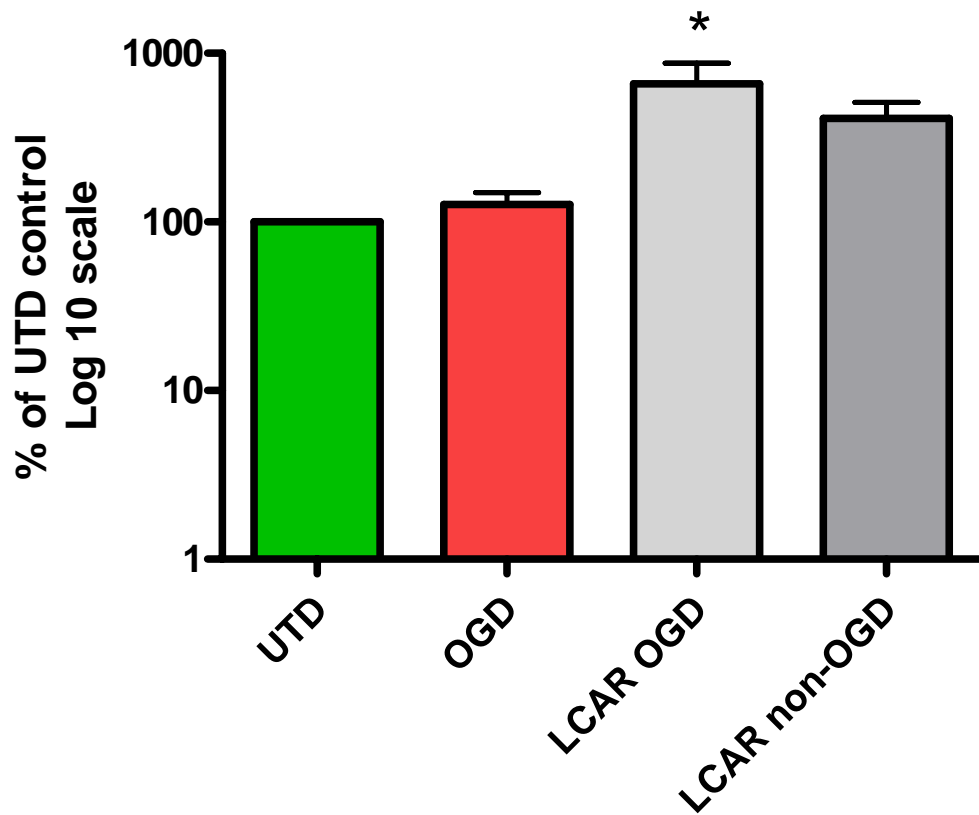**Fig. 16a** Western blot analysis of SOD1 in RHSC 2 hours post-OGD. Carntine treated RHSC showed a significant increase in SOD1 expression 2 hours post-OGD. Untreated slices exposed to OGD showed levels of SOD1 expression that did not significantly differ from untreated non-OGD controls. One way ANOVA, Tukey's post-hoc, each bar represents a minimum of 3 samples; each sample is composed of 4 pooled slices
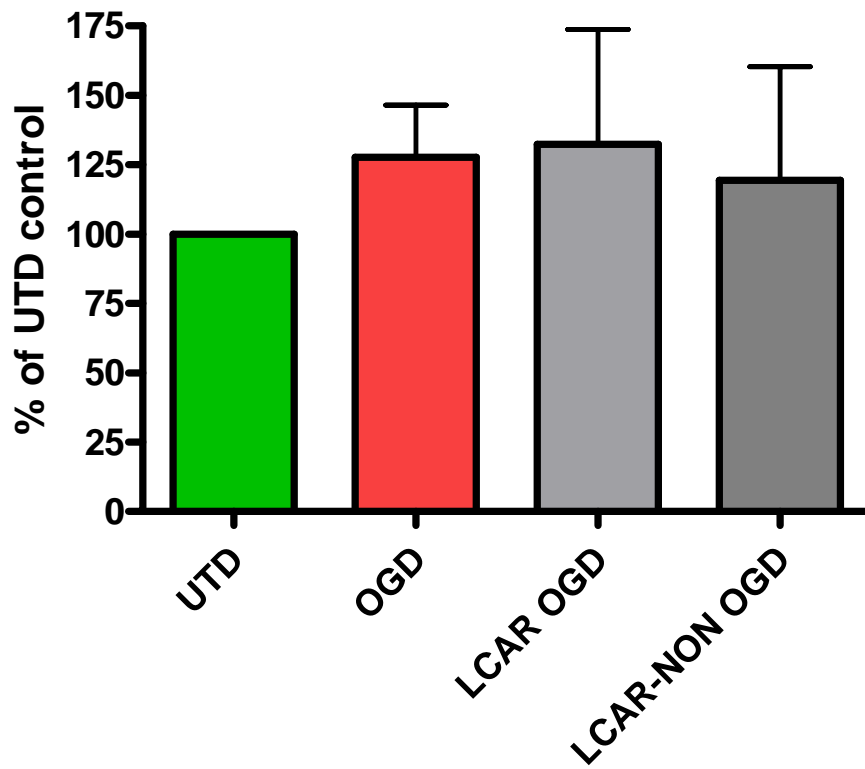
Fig. 17 Western blot analysis of SOD1 expression in RHSC 24 hours post-OGD. No significant changes were observed in slices at 24 hours. One way ANOVA, each bar represents a minimum of 3 samples; each sample represents 4 pooled slices.
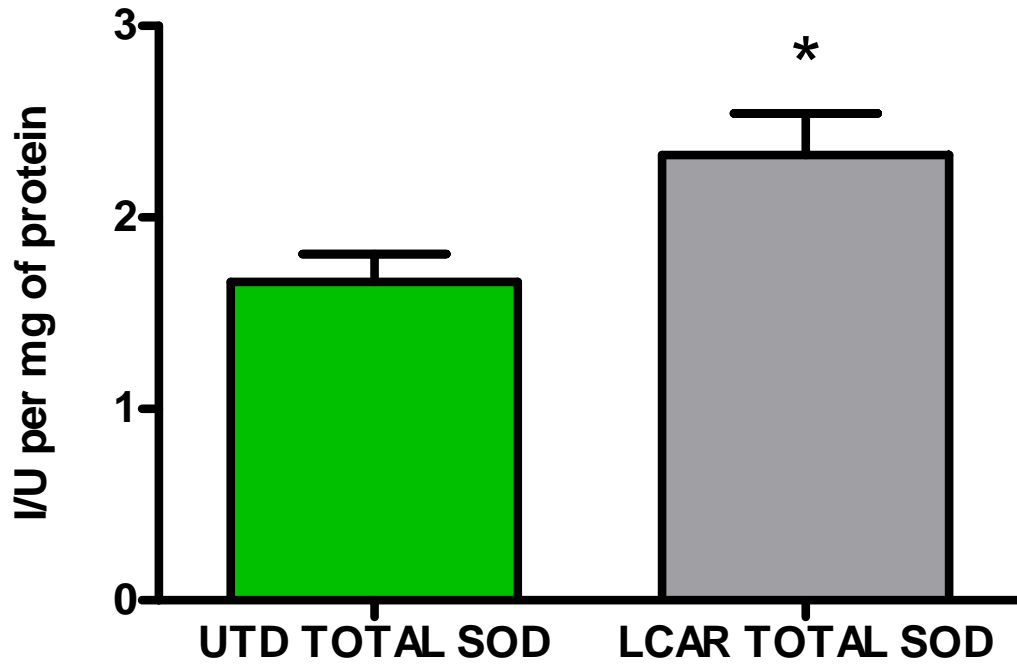
Fig. 18a Total SOD activity in RHSC after 2 hours of carnitine treatment. Carnitine treated cultures showed a significant increase in SOD1 activity. Carnitine treatment did not significantly alter SOD2 activity. Unpaired, two tailed T-test. Each bar represents a minimum of 8 samples; each sample is composed of 4 pooled slices.
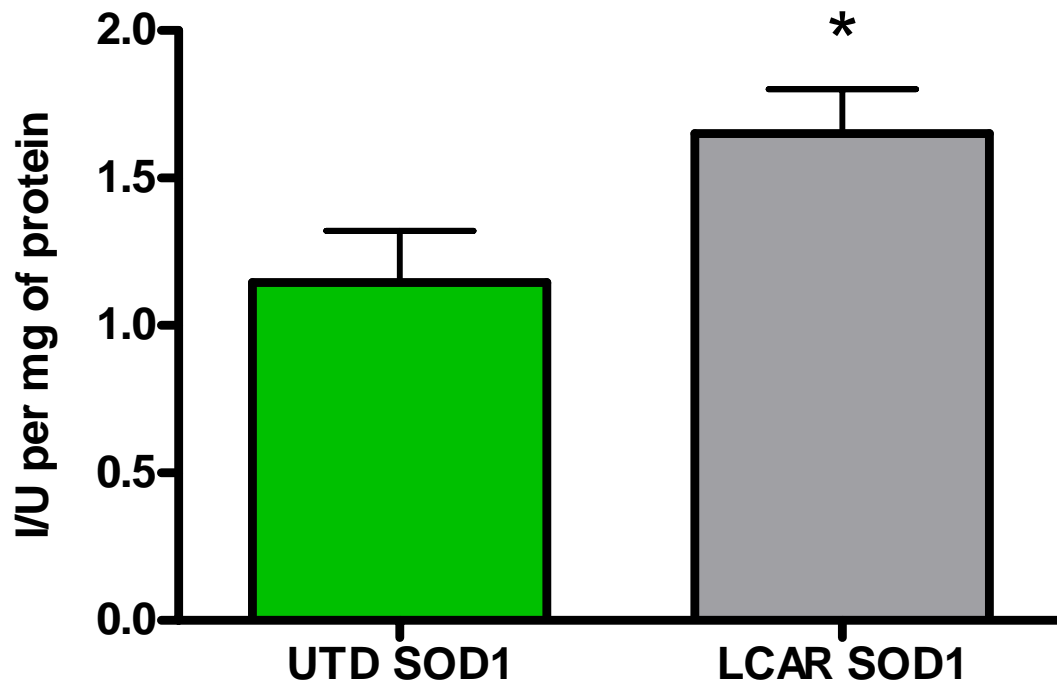
Fig. 18b Cytosolic SOD (SOD1) activity in RHSC after 2 hours of carnitine treatment. Carnitine treated cultures showed a significant increase in SOD1 activity. Unpaired, two tailed T-test. Each bar represents a minimum of 8 samples; each sample is composed of 4 pooled slices.
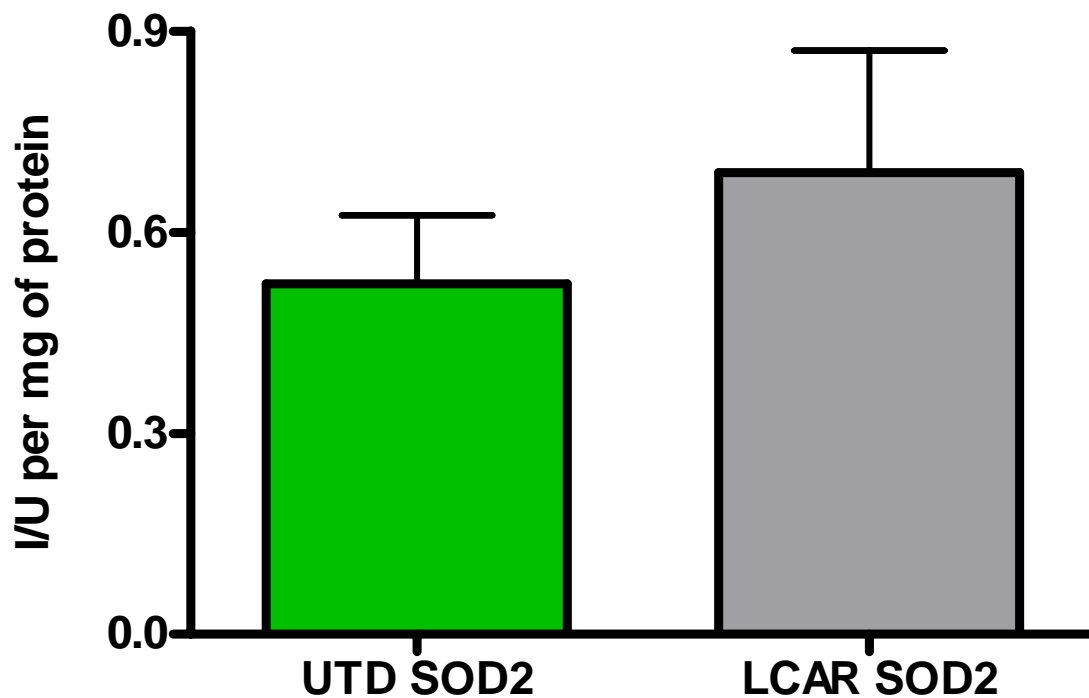
Fig. 18c Mitochondrial SOD (SOD2) activity in RHSC after 2 hours of carnitine treatment. Carnitine treatment did not significantly alter SOD2 activity. Unpaired, two tailed T-test. Each bar represents a minimum of 8 samples; each sample represents 4 pooled slices.
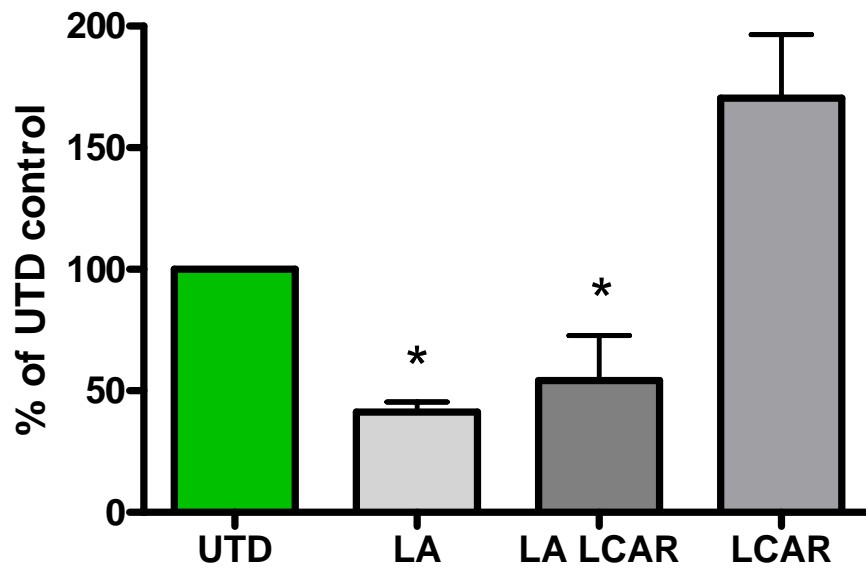
Fig. 19a Cytosolic superoxide in RHSC treated with carnitine in the presence of lipoic acid (LA). LA significantly reduced LCAR mediated increases in cytosolic superoxide levels. *=p<0.05, LCAR vs. groups One way ANOVA Tukey's post-hoc. Each bar represents a minimum of 4 samples.
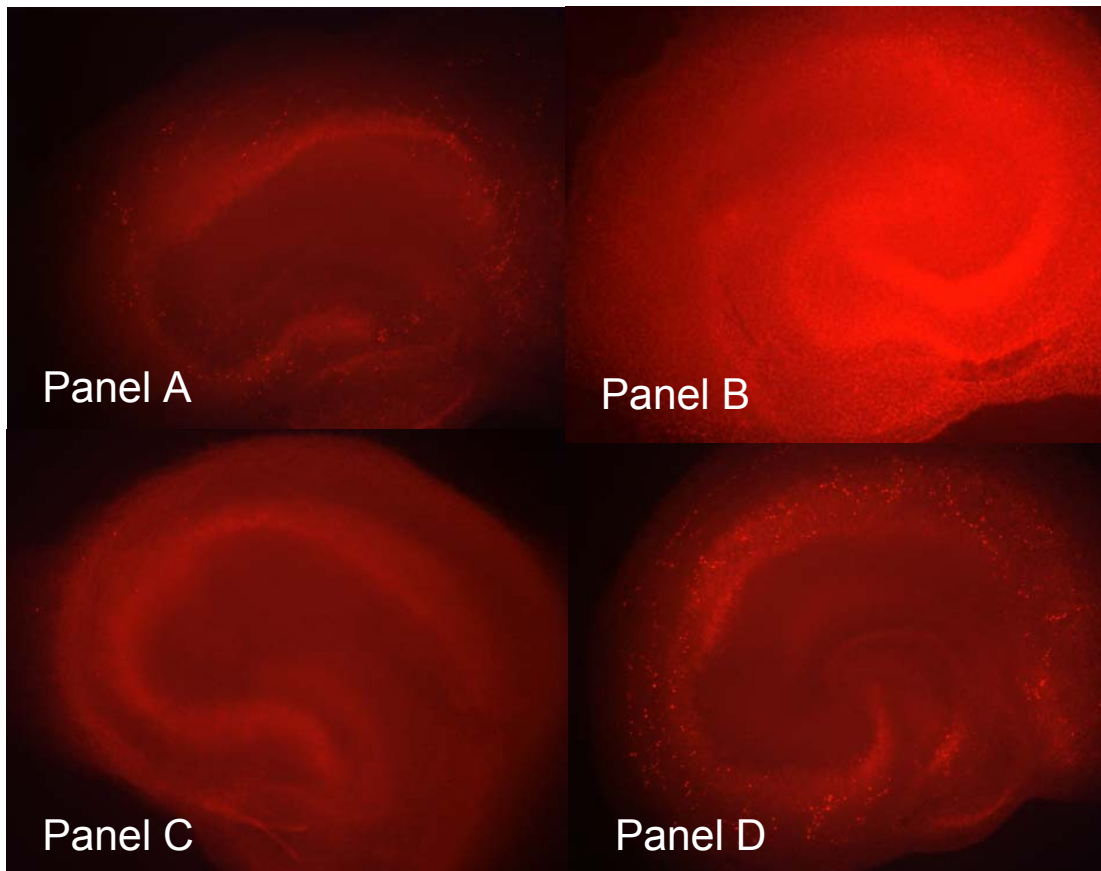
Fig. 19b Representative images of RHSC stained with DHE to measure cytosolic superoxide levels after 2h of LA and LCAR treatment. LA effectively reduces the LCAR mediated increase in superoxide. Panel A is LA+LCAR, panel B is LCAR, panel C is LA, panel D is untreated control. Image captured at 4x magnification.
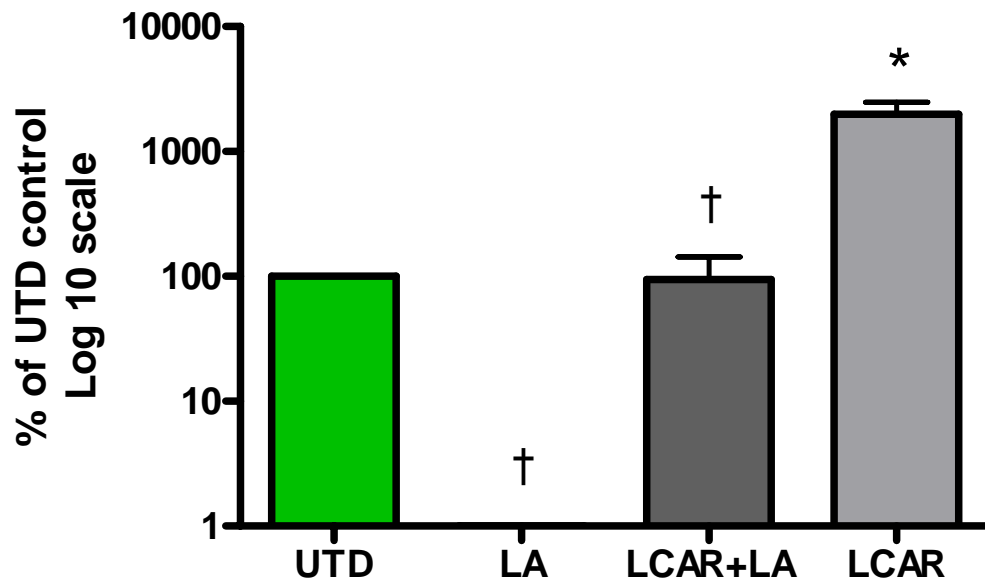
Fig. 20a Mitochondrial superoxide in RHSC treated with carnitine in the presence of lipoic acid (LA). LA significantly reduced LCAR mediated increases in mitochondrial superoxide levels. *=p<0.05 UTD vs. groups; †=p<0.05 LCAR vs. groups. One way ANOVA, Tukey's post-hoc. Each bar represents a minimum of 4 samples.
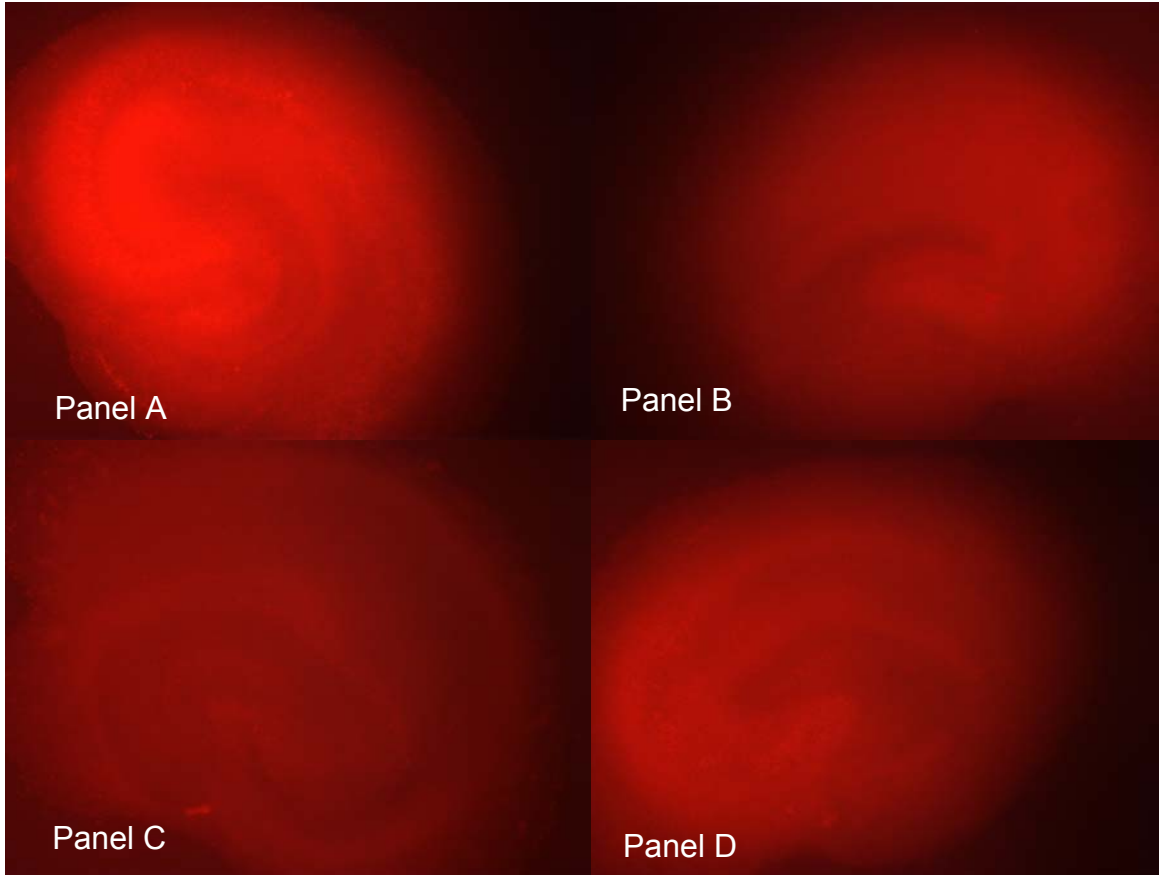
Fig.20b Representative images of RHSC stained with MITOSOX to measure mitochondrial superoxide levels after 2h of LA and LCAR treatment. LA effectively reduces the LCAR mediated increase in mitochondrial superoxide. Panel A is LCAR, panel B is untreated control, panel C is LA, panel D is LCAR+LA. Images captured at 4x magnification,
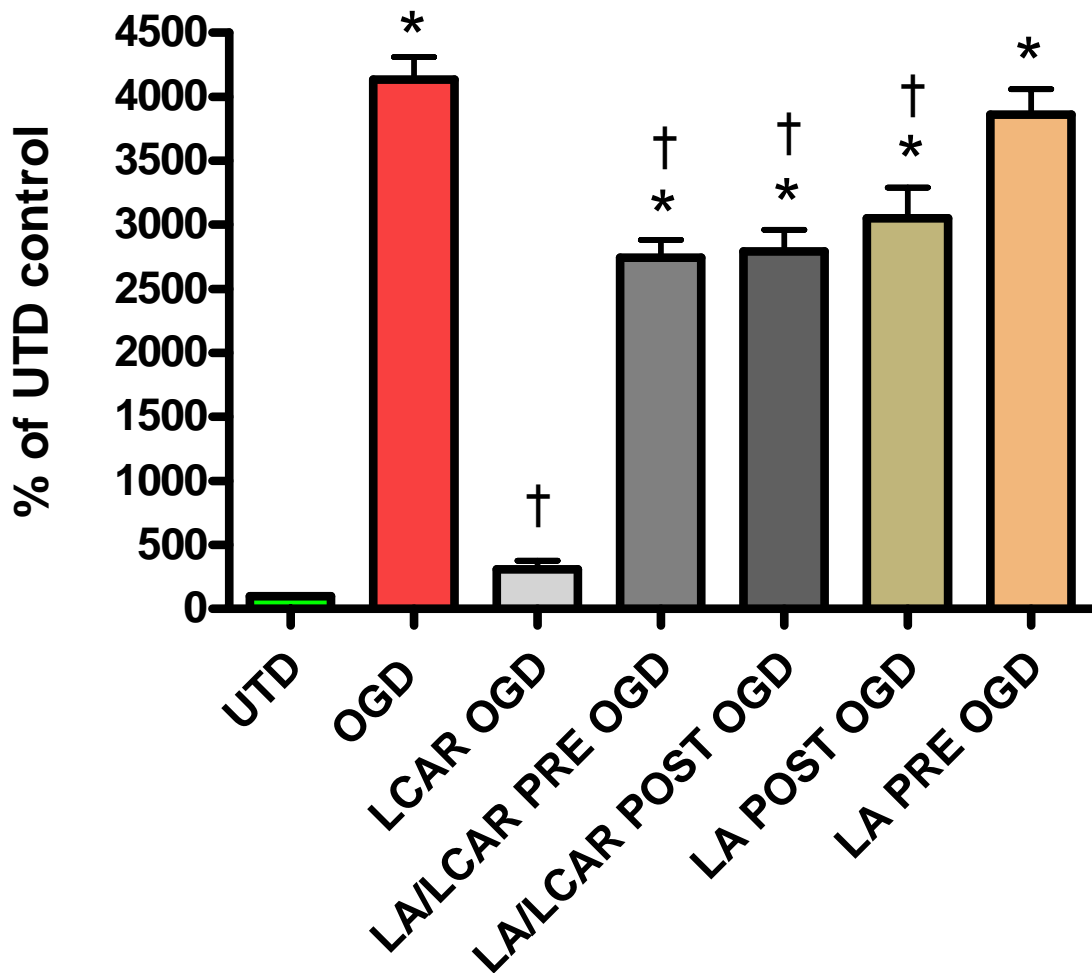
Fig. 21a Propidium iodide uptake 24 hours post-OGD in RHSC treated with carnitine and LA prior to and after OGD. Carnitine pre-treatment in the presence of LA resulted in a significant decrease in neuroprotection. The addition of both LA and carnitine after OGD significantly decreased neuronal death when compared to carnitine post-OGD treatment. Addition of LA prior to OGD failed to exert a neuroprotective effect while LA treatment post OGD decreased neuronal death. *=p<0.05 UTD vs. groups; †=p<0.05 OGD vs. groups. One way ANOVA, Tukey's post hoc. Each bar represents a minimum of 4 samples.
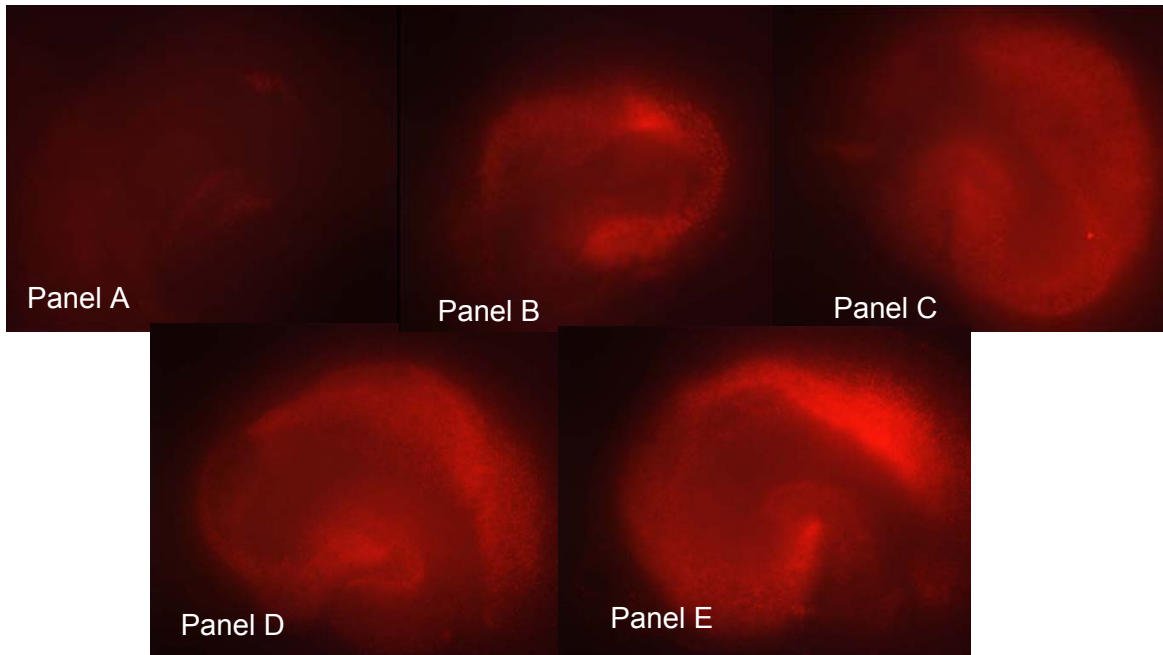
Fig. 21b Representative images of propidium iodide uptake in LA LCAR treated RHSC 24 hours after OGD. The addition of LA reduces the protective effect of LCAR. Panel A is untreated control, panel B is LA post-OGD, panel C is LCAR pre-OGD, panel D is LA LCAR pre OGD, panel E is untreated OGD. Images captured at 4x magnification.

carnitine-mediated neuroprotection is due, at least in part, to increases in ROS prior to OGD. This hypothesis is further supported by our finding that adding LA prior to OGD does not decrease neuronal death, but adding LA after OGD does confer significant neuroprotection. Based on these observations we hypothesized decreased ROS levels (due to LA-mediated ROS scavenging) prior to OGD resulted in decreased cellular antioxidant defenses and therefore made neurons vulnerable to ROS mediated damage. To test this hypothesis we added LA to RHSC's and measured the effect on SOD1 and SOD2 expression levels.

3.7 The Effect of an Anti-oxidant on LCAR Treatment

The addition of LA resulted in significant decreases in both SOD1 and SOD2 expression when compared to the untreated control group [fig. 23, 24] ($p < 0.05$). Carnitine treatment in the presence of LA nullified the increase in SOD1 expression suggesting SOD1 is modulated by carnitine-mediated increases in superoxide, and this observation may explain the increased neuronal death (propidium iodide uptake; fig. 22) observed in the experimental groups treated with LA (LA+LCAR, LA) prior to OGD.

Taken together, these observations suggest carnitine is conferring neuroprotection by modulating superoxide levels leading to an increase in SOD1 expression and activity prior to OGD. This finding, however, does not entirely explain the decreased ROS levels measured after OGD. Previous work by Zemlyak et al [25] indicates AAV-mediated overexpression of SOD1 does not protect neurons against OGD [56]. However, overexpression of SOD1 in conjunction with catalase prior to OGD results in significant levels of neuroprotection [56]. This finding suggests the increase in SOD1 activity and

Fig. 22a Western blot analysis of SOD1 expression after 2 hours of carnitine treatment in the presence or absence of LA. LA significantly decreased SOD1 expression in carnitine treated RHSC. *=$p<0.05$ UTD vs. groups; †=$p<0.05$ LCAR vs. groups. One way ANOVA, Tukey's post-hoc. Each bar represents a minimum of 3 samples; each sample is composed of 4 pooled slices.
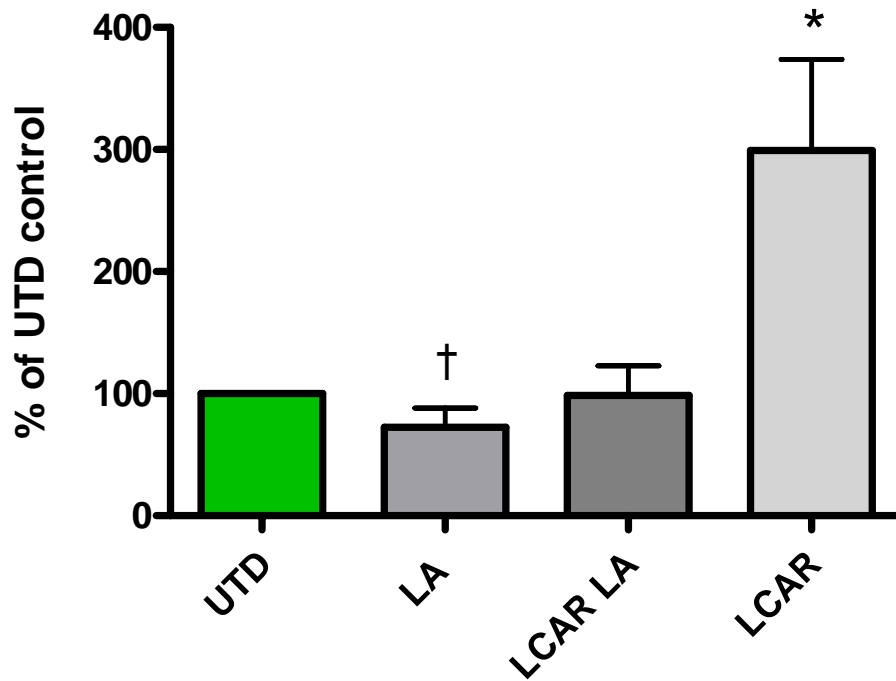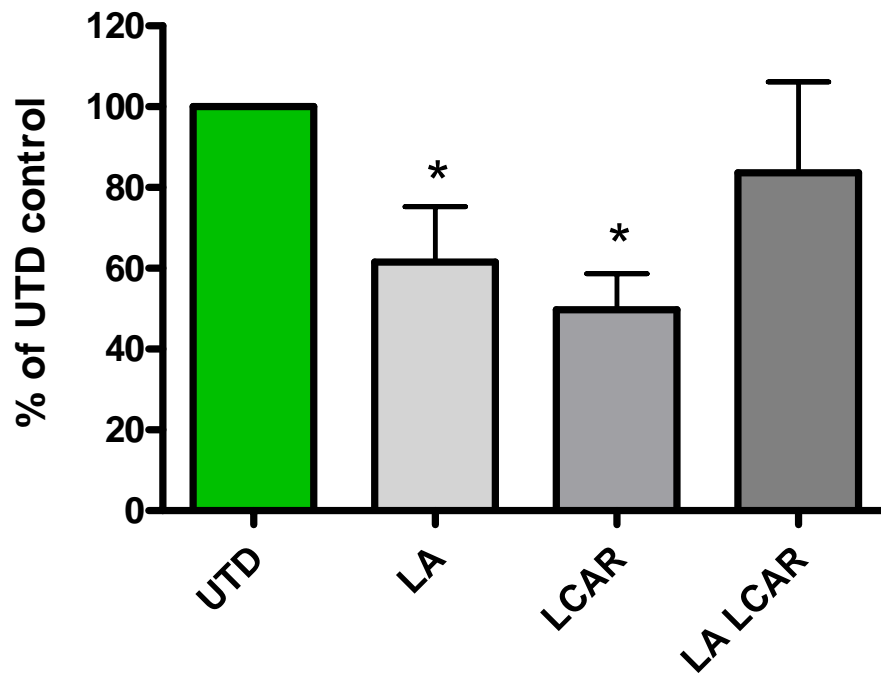
Fig. 23a Western blot analysis of SOD2 expression after 2 hours of carnitine treatment in the presence or absence of LA. LA significantly decreased SOD2 expression in untreated RHSC. LA treatment in the presence of carnitine blocked the carnitine mediated decrease in SOD2 expression. *=p<0.05 UTD vs. groups. One way ANOVA, Tukey's post-hoc. Each bar represents a minimum of 4 samples; each sample represents 4 pooled slices.

expression may be coupled to increases in catalase, glutathione peroxidase, or GSH reductase to convert H_2O_2 to water and avoid the formation of hydroxyl radical via the Fenton reaction. Based on Zemlyak's previous studies of SOD1 and OGD, we hypothesized carnitine mediated neuroprotection was due to increases in both SOD1 expression/activity and catalase expression/activity. To begin testing this hypothesis we measured H_2O_2 levels prior to and after OGD.

3.8 The Effect of LCAR on H_2O_2 levels and Catalase Expression after OGD

Utilizing a membrane permeable fluorescent dye specific for H_2O_2 (DCF-DA), we observed a significant increase in H_2O_2 in the carnitine treated RHSC's prior to OGD [fig.25]. At 2, 12, and 24 hours post-OGD H_2O_2 was significantly decreased in the carnitine treated OGD group, but remained elevated in the OGD group [fig. 26]. This observation, combined with our data showing superoxide remains elevated for at least 6 hours following OGD, suggests OGD results in a 'superoxide bottleneck' as SOD1 converts physiologically large amounts of superoxide to H_2O_2. As H_2O_2 is produced it is rapidly converted to water by carnitine-induced increases in catalase expression. To test this hypothesis we performed Western blot analysis to measure the effect of carnitine treatment on catalase expression prior to OGD.Western blot analysis showed carnitine treatment increases the expression of catalase prior to OGD [fig. 27]. This finding suggests catalase is playing a role in decreasing hydrogen peroxide levels after OGD.
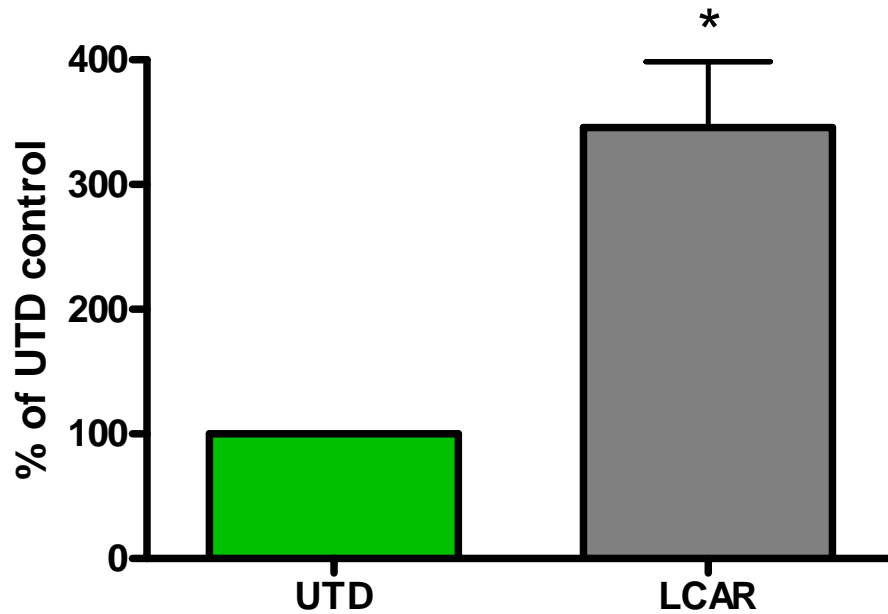
Fig. 24a Hydrogen peroxide levels in RHSC after 2 hours of carnitine treatment. Carnitine treatment significantly increased hydrogen peroxide. *=p<0.05 Unpaired two-tailed T-test. Each bar represents a minimum of 12 samples.
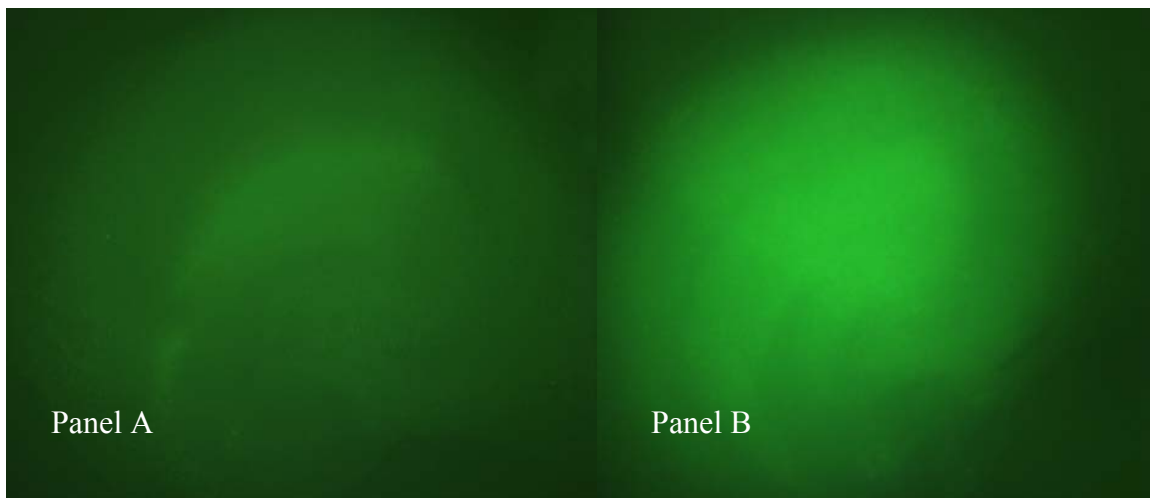
Fig 24b Representative images of DCF-DA staining in RHSC after 2h of LCAR treatment. LCAR increases H_2O_2 after 2 hour of treatment. Panel A is untreated control, panel B is LCAR treated. Images captured at 4x magnification,
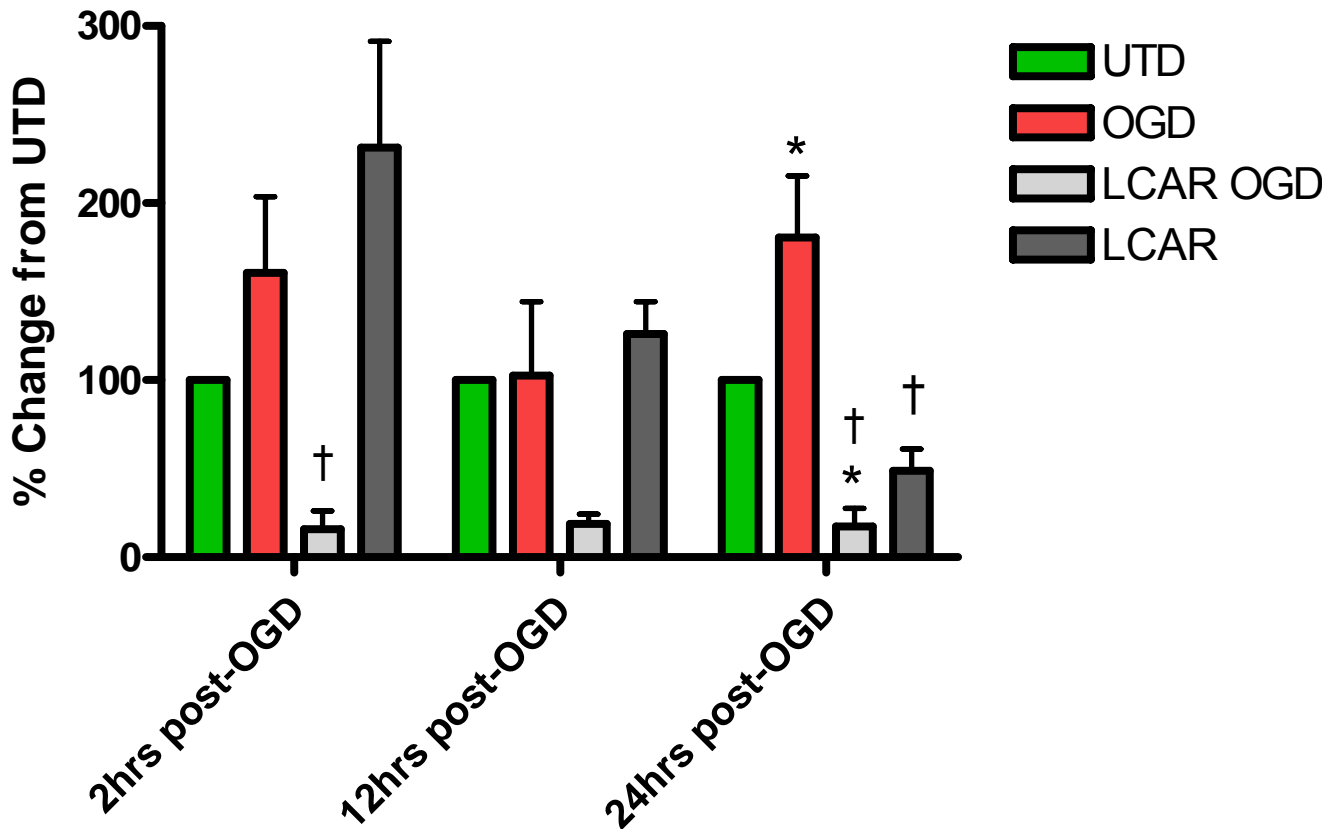
Fig. 25 H_2O_2 levels in RHSC treated with carnitine and exposed to OGD. Carnitine treated cultures exposed to OGD showed a significant decrease in H_2O_2 at 2, 12, and 24 hours post OGD. Carnitine treatment in non-OGD cultures showed a significant increase in H_2O_2 at 2 hours post-OGD that gradually declined at 12 and 24 hours post-OGD. *=p<0.05, One way ANOVA, Tukey's post-hoc. Each bar represents a minimum of 3 samples.
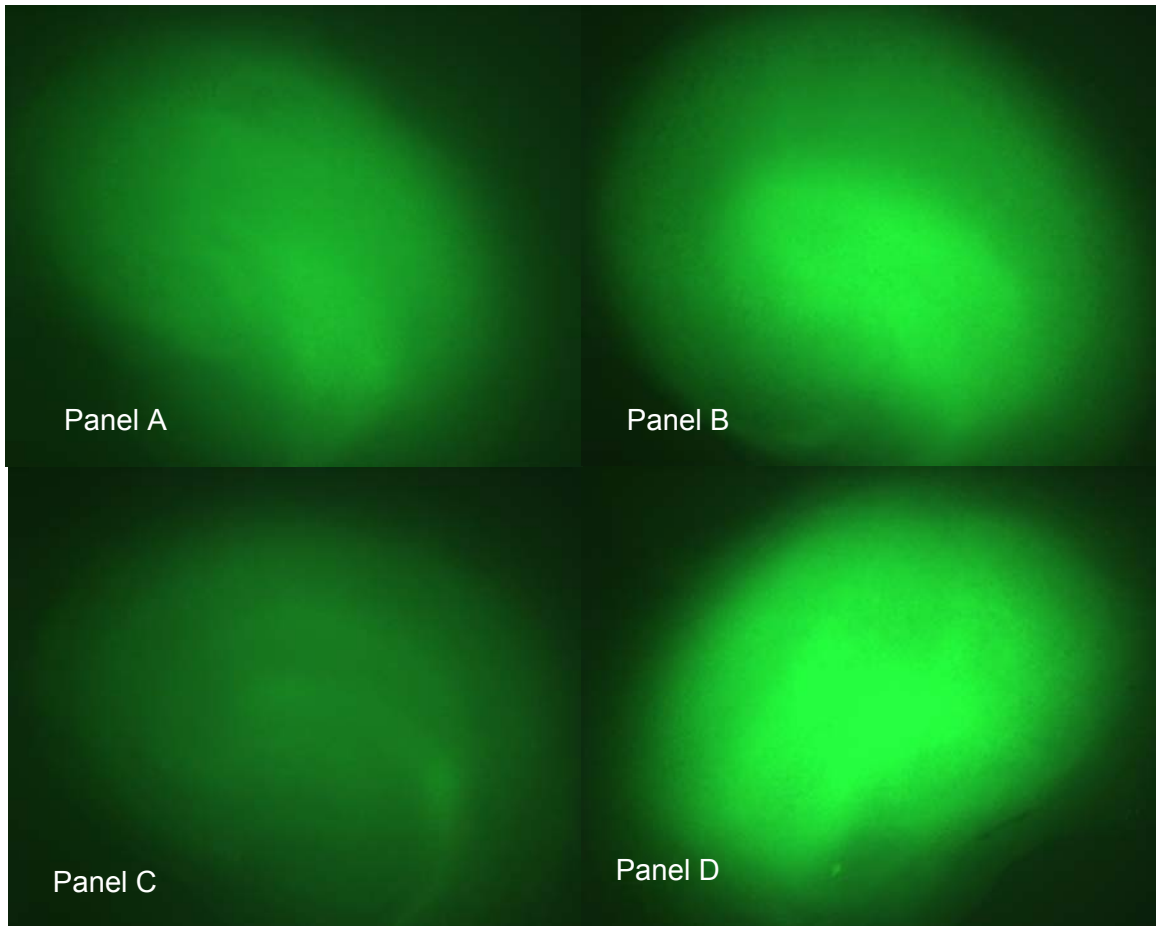
Fig. 25b Representative images of DCF-DA staining in RHSC after 2h of OGD. Panel A is untreated control, panel B is untreated OGD, panel C is LCAR pre-OGD, panel D is LCAR non-OGD. Images captured at 4x magnification.
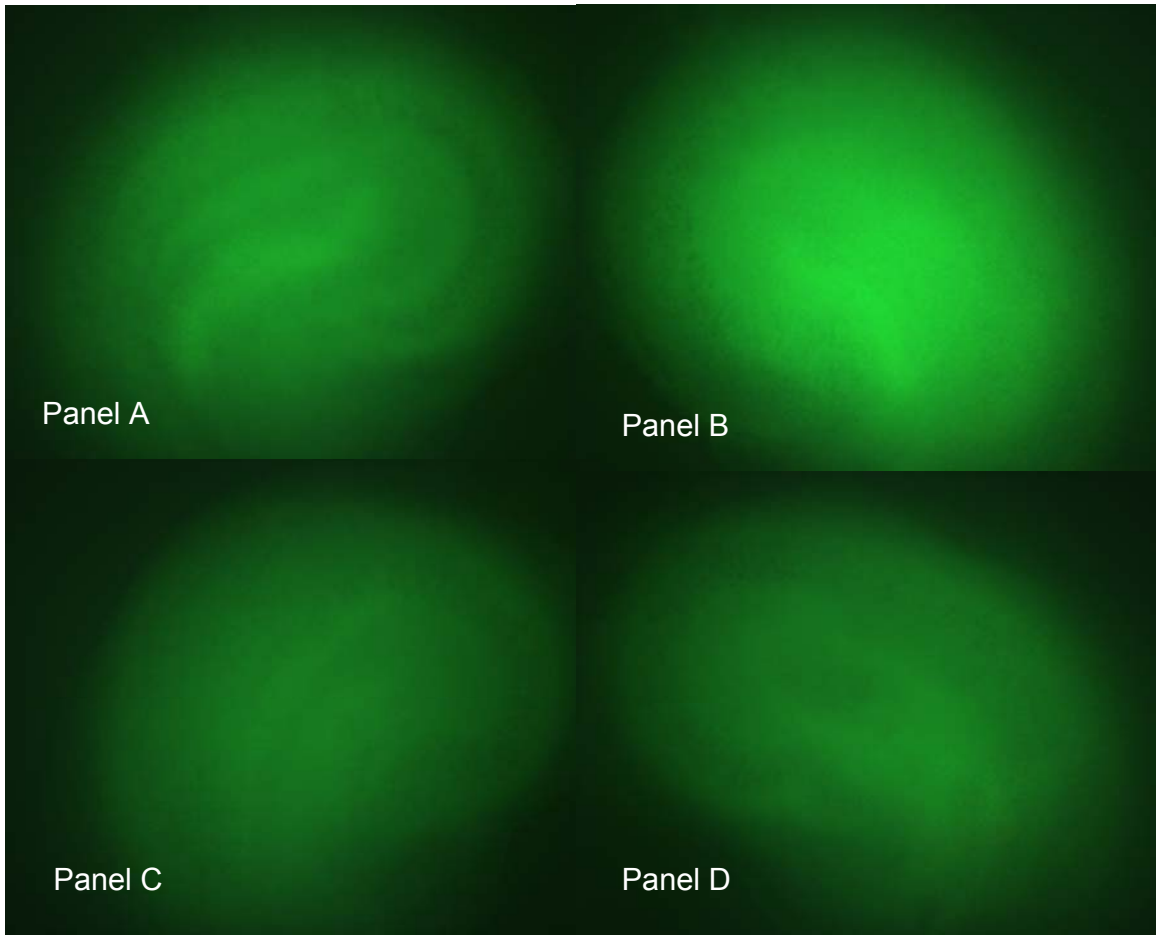
Fig. 25C Representative images of DCF-DA staining in RHSC after 24h of OGD. LCAR treatment decreases H_2O_2 after OGD. Panel A is untreated control, panel B is untreated OGD, panel C is LCAR pre-OGD, panel D LCAR non-OGD. Images captured at 4x magnification.
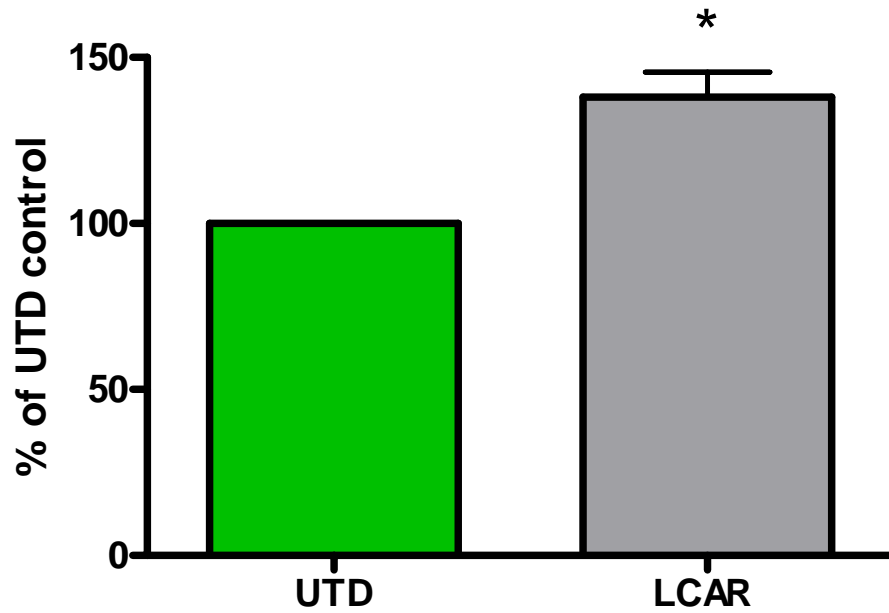
Fig. 26a Western blot analysis of catalase expression in RHSC after 2 hours of carnitine treatment. Carnitine treatment resulted in a significant increase in catalase expression. *=p<0.05, unpaired two tailed T-test. Each bar represents a minimum of 5 samples; each sample is composed of 4 pooled slices.
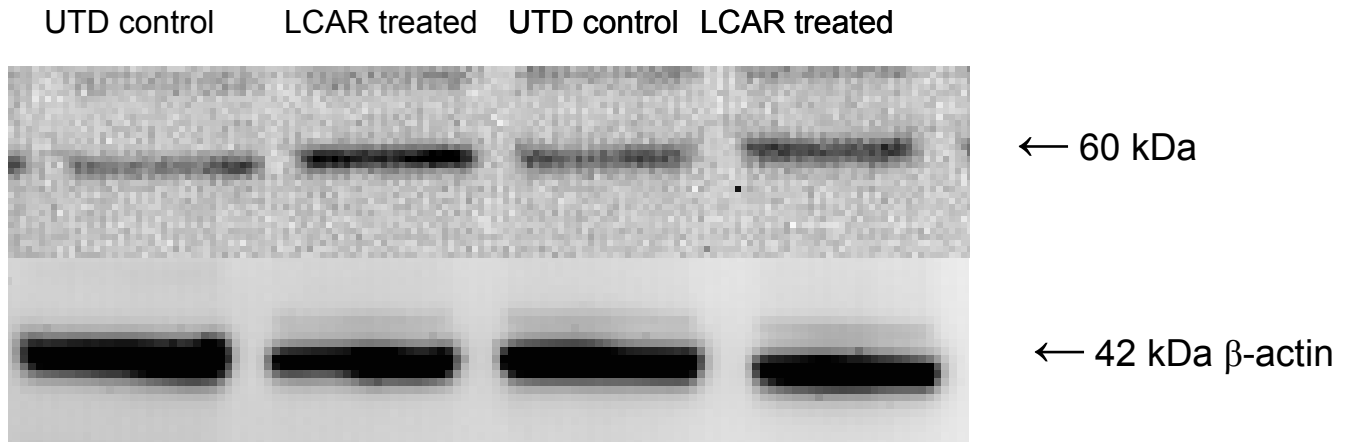
Fig. 26b Representative images of Western blot analysis showing catalase expression after two hours of LCAR treatment. LCAR increases expression of of catalase Also shown β-actin loading control.

To further define this effect we measured catalase activity in carnitine treated slices and observed an increase in enzymatic activity when compared to untreated slices [fig. 28]. To determine if this effect was due to carnitine mediated increases in ROS we treated hippocampal slices with carnitine in the presence of LA and measured catalase expression and activity.

Utilizing Western blot analysis and a catalase activity assay we observed a significant decrease in catalase expression and activity in the carnitine/LA treatment group [Fig. 28, 29] While it is not entirely possible to determine if this effect is due to LA scavenging superoxide, H_2O_2 or both, it does suggest carnitine treatment is modulating catalase by increasing ROS prior to OGD.

While these observations indicate carnitine is exerting a neuroprotective effect by inducing a ROS mediated increase in SOD1 expression/ activity and catalase expression/ activity prior to OGD, they fail to explain why the addition of LA does not completely abolish the neuroprotective effect. Furthermore, the addition of LA with carnitine after OGD significantly reduced the level of cell death normally observed when carnitine was added after OGD. Comparing this observation with superoxide data obtained at 24 hours post-OGD, we noted the decrease in cell death was disproportionate with the level of superoxide (DHE) present when carnitine was added post-OGD.

In light of these two observations, it is possible multiple mechanisms are being actively modulated by carnitine treatment. Based on our previous observation that carnitine prevents metabolic dysfunction we elected to study MMP as a measurement of mitochondrial health and viability. We hypothesized carnitine treatment was preventing
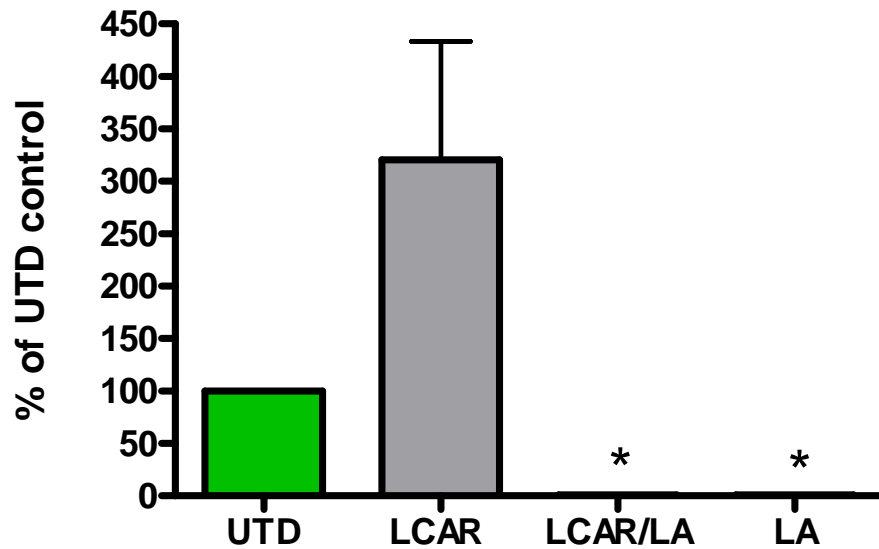
Fig. 27 Catalase activity assay in RHSC treated with carnitine in the presence or absence of LA. Carnitine treated cultures showed a significant increase in catalase activity when compared to untreated controls. The addition of LA significantly reduced the carnitine-mediated increase in catalase activity indicating carnitine mediated increases in ROS modulate catalase activity. One way ANOVA, Tukey's post-hoc. *=p<0.05 LCAR vs. groups. Each bar represents a minimum of 3 samples; each sample is composed of 4 pooled slices.
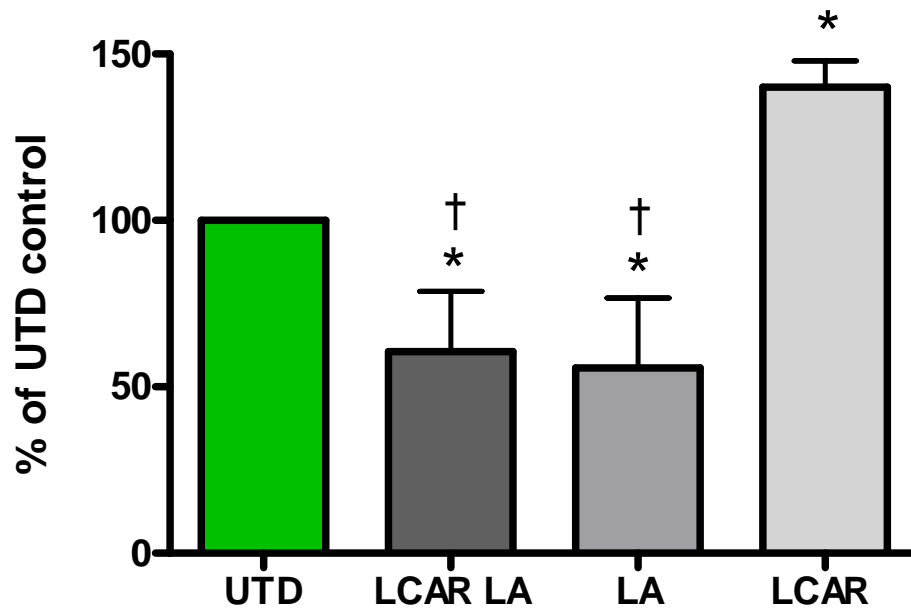
Fig. 28a Western blot analysis of catalase expression in RHSC after 2 hours of carnitine treatment in the presence or absence of LA. Carnitine treatment resulted in a significant increase in catalase expression. Treatment with LA in the presence of carnitine resulted in a significant decrease in catalase expression indicating carntine mediated increases in ROS modulate catalase expression. One way ANOVA, Tukey's post-hoc *=p<0.05 UTD vs. groups; †=p<0.05 LCAR vs. groups. Each column represents a minimum of 4 samples; each sample is composed of 4 pooled slices
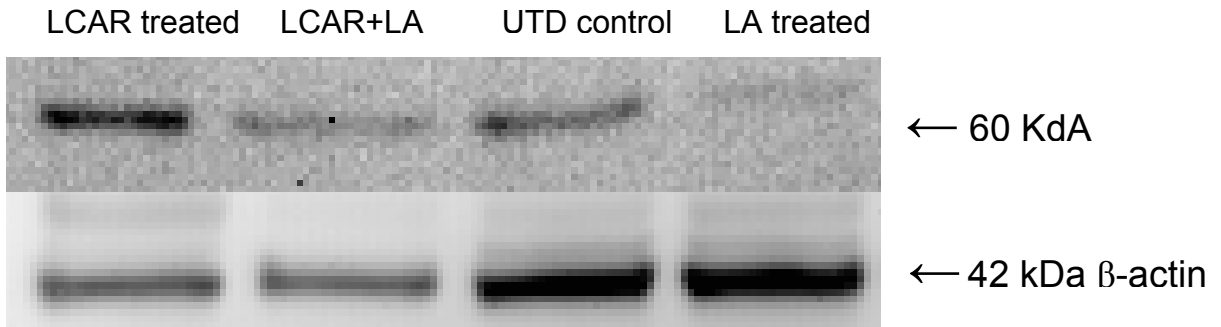
Fig. 28b Representative images of Western blot analysis showing catalase expression after two hours of LCAR LA treatment. LA decreases the LCAR mediated increase in catalase expression. Also shown β-actin loading control.

metabolic dysfunction by blocking the irreversible depolarization of MMP induced by OGD.

3.9 Measurement of MMP in LCAR treated RHSC exposed to OGD

Utilizing Rhodamine 123 fluorescent staining, we measured mitochondrial membrane potential at 2, 6, 12, 24, and 48 hours post-OGD. At 2 hours post-OGD there was no significant difference in any of the OGD exposed groups, but in the carnitine treated cultures a significant increase in rhodamine staining was observed suggesting carnitine treatment may result in a significant hyperpolarizing effect. At 6, 12 and 24 hours post-OGD we observed a significant MMP depolarization in untreated RHSC's exposed to OGD with the majority of neurons depolarized ($p<0.05$) at 48 hours post-OGD [fig. 31]. In contrast, carnitine treated slices exposed to OGD showed a significant MMP depolarization at 6 and 12 hours post-OGD, but showed a complete recovery (basal repolarization) of MMP at 48 hours post-OGD [fig. 31].

In previous studies of mitochondria exposed to OGD, depolarization of MMP is an irreversible phenomenon due to the calcium or ROS mediated opening of the mitochondrial permeability transition pore (MPTP) [27]. However, based on our observations of MMP repolarization in the carnitine OGD slices, it appears unlikely that MMP modulation was due to the formation and activation of the MPTP pore. Current
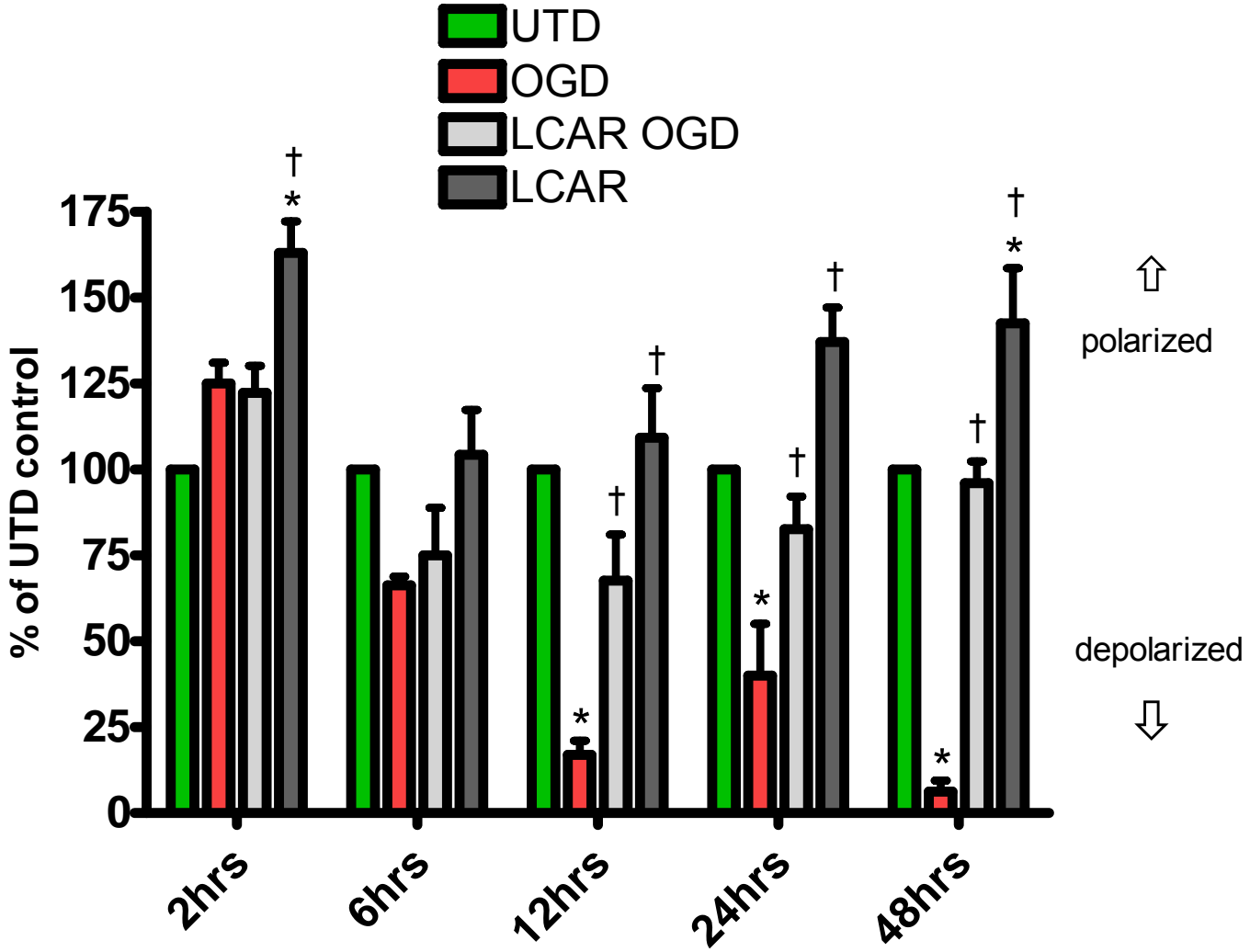
Fig. 29a Mitochondrial membrane potential (MMP) in RHSC treated with carnitine and exposed to OGD. Carnitine treatment in non-OGD cultures resulted in a significant hyperpolarization at 2, 24, and 48 hours post-OGD. Carnitine treated cultures exposed to OGD showed a significant depolarization at 12 hours post-OGD. At 24 and 48 hours post-OGD MMP did not significantly differ from untreated, non-OGD controls. Untreated RHSC exposed to OGD showed a mild hyperpolarization at 2 hours post-OGD, however at 6, 12, 24, and 48 hours a significant MMP depolarization was observed. *=p<0.05 UTD vs. groups; †=p<0.05 OGD vs. groups One way ANOVA,Tukey's post-hoc. Each bar represents a minumum of 4 samples.
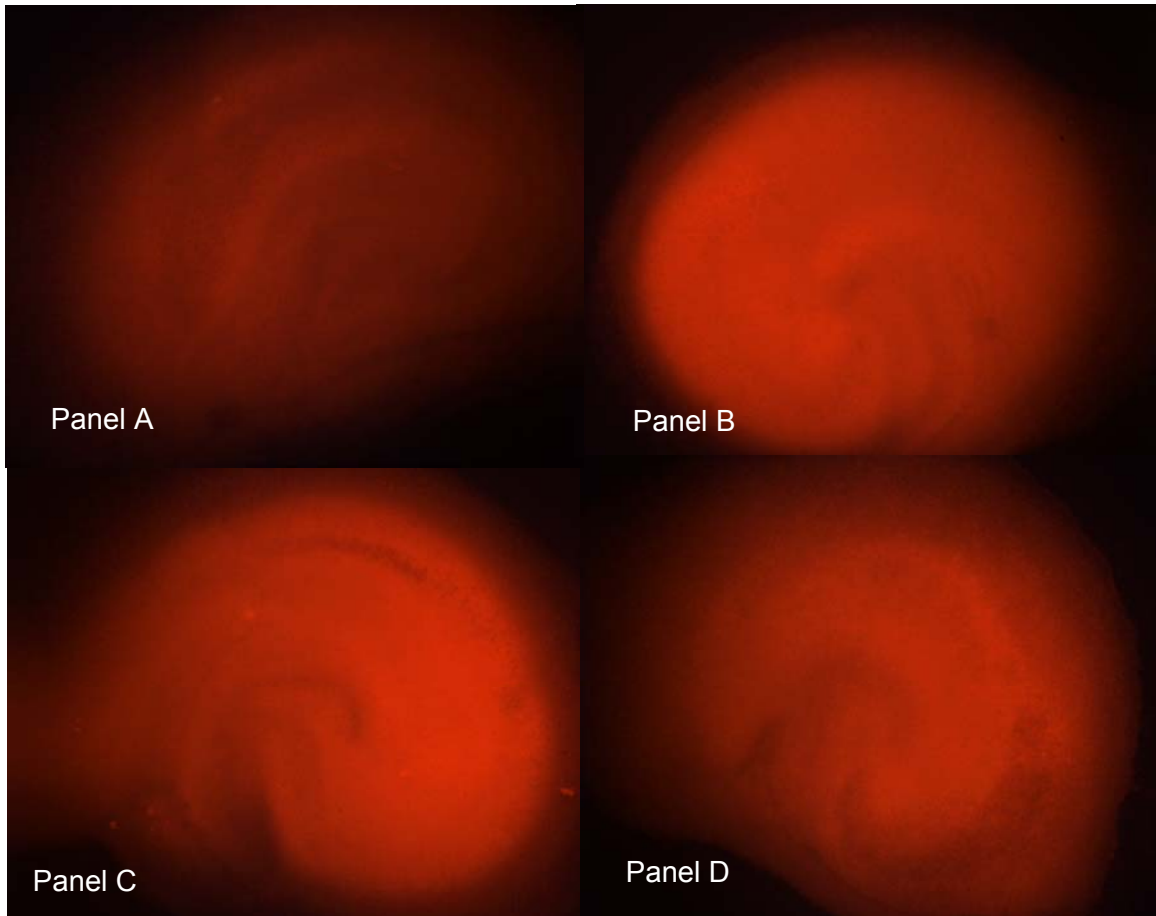
Fig. 29b Representative images of Rhodamine 123 staining in RHSC after 48h of OGD. LCAR prevents the loss of MMP at 48 hours post-OGD. Panel A is untreated OGD, panel B is untreated control, panel C is LCAR non-OGD, panel D LCAR pre-OGD. Images captured at 4x magnification.
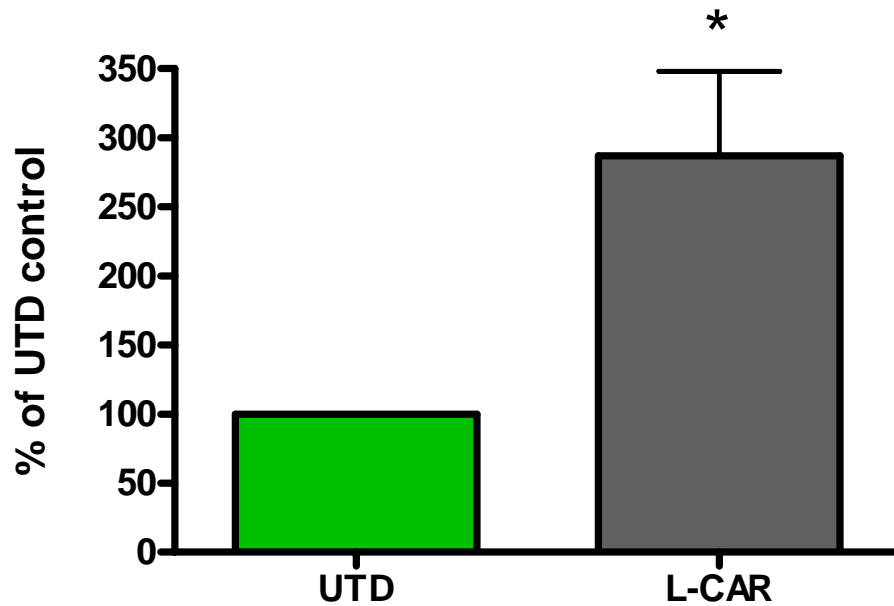
Fig. 30a Western blot analysis of UCP-2 expression in RHSC after 2 hours of carnitine treatment. Carnitine treatment resulted in a significant increase in UCP-2 expression. *=p<0.05, unpaired two tailed T-test. Each bar represents a minimum of 5 samples; each sample is composed of 4 pooled slices.
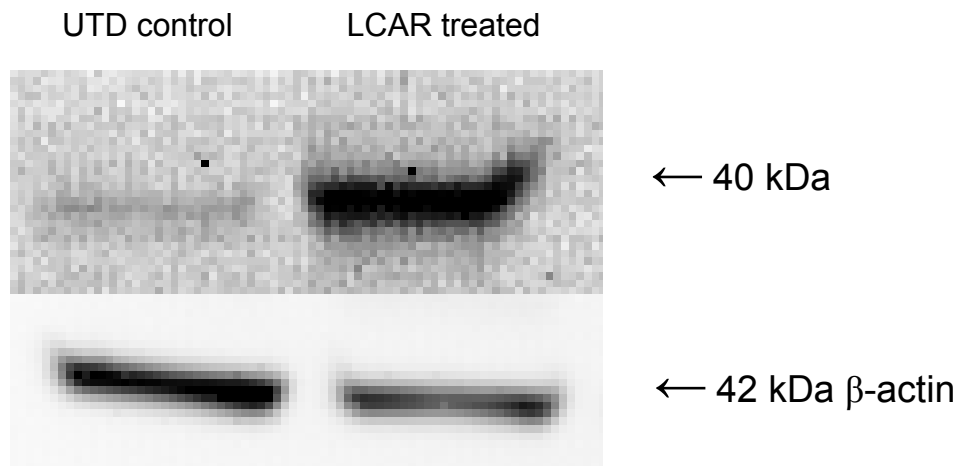

Fig. 30b Representative images of Western blot analysis showing

UCP-2 expression after two hours of LCAR treatment. LCAR treatment increases

UCP-2 protein levels. Also shown β-actin loading control.

research indicates depolarization of MMP does not necessarily result in ATP depletion leading to neuronal death. In previous work by Mattiasson et al [57] and Korde et al [58] application of a MMP uncoupler (2,4 DNP) showed mild depolarization prior to OGD (1hrs) resulted in significant decreases in ROS and neuronal death [57].

The induction of a mild, transient depolarization we observed in carnitine treated RHSC's may be the product of a cellular mechanism designed to decrease ROS production. Combining this effect with the increased ROS scavenging we have observed with carnitine treatment may account for the rapid decrease in superoxide and H_2O_2 observed after OGD. In an effort to determine the possible mechanism responsible for the transient depolarization, we focused our attention on mitochondrial uncoupling proteins (UCP's).

Uncoupling proteins are pores within the inner mitochondrial membrane activated by superoxide in the presence of fatty acids or hydroxynoneals, a byproduct of oxidized fatty acids [59-62]. Once activated they decrease mitochondrial proton motive force by allowing protons to pass from the intermembrane space into the mitochondrial matrix effectively bypassing proton return through complex V (ATPase). While this effect decreases ATP production it also decreases concurrent ROS production from cellular respiration and allows ROS already produced within the mitochondria to translocate into the cytosol [57, 59, 60, 62-65]. The temporary disruption of ATP production also prevents the formation of the MPTP (ATP dependent) and decreases the glutamate induced calcium influx into the mitochondria by modulating MMP. The net effect of this activity is a reduction in MPTP activation, ROS production, and mitochondrially-mediated apoptosis [25, 66].

Previous work by Mattison et al [57] showed over-expression of UCP-2 prior to hypoxia-ischemia exerted a neuroprotective effect [57]. Based on Mattison's findings and the effect of carnitine treatment on MMP polarization, we hypothesized part of carnitine's neuroprotective mechanism was an increase in UCP-2 expression prior to OGD. This effect would allow mitochondria greater control over MMP polarization and would also allow a significant amount of carnitine generated ROS to efflux from the mitochondria into the cytosol and thus protect mitochondrial membranes critical for metabolic viability. To begin testing this hypothesis we treated hippocampal slices with carnitine and measured UCP-2 expression levels.

3.10 Measurement of UCP-2 protein in LCAR treated RHSC exposed to OGD

After two hours of carnitine treatment, UCP-2 expression increased over 250% [fig. 32]. At 24 hours post-OGD the carnitine-mediated increase in UCP-2 expression was present in RHSC's exposed to OGD as well as non-OGD controls. Exposure to OGD in untreated slices also increased UCP-2 expression at 24 hours [fig. 33]. Based on these observations and MMP polarization data, we hypothesized the increase in UCP-2 expression in the untreated RHSC's exposed to OGD did not result in a significant neuroprotective effect because it occurred after OGD. Increasing UCP-2 expression after a hypoxic-ischemic insult may be an adaptive response to increased superoxide levels that further increases mitochondrial dysfunction. Addition of the uncoupling effect of UCP-2 to MPTP activation may explain the severe irreversible depolarization observed in untreated RHSC's exposed to OGD. In contrast, the increased expression of UCP-2 in
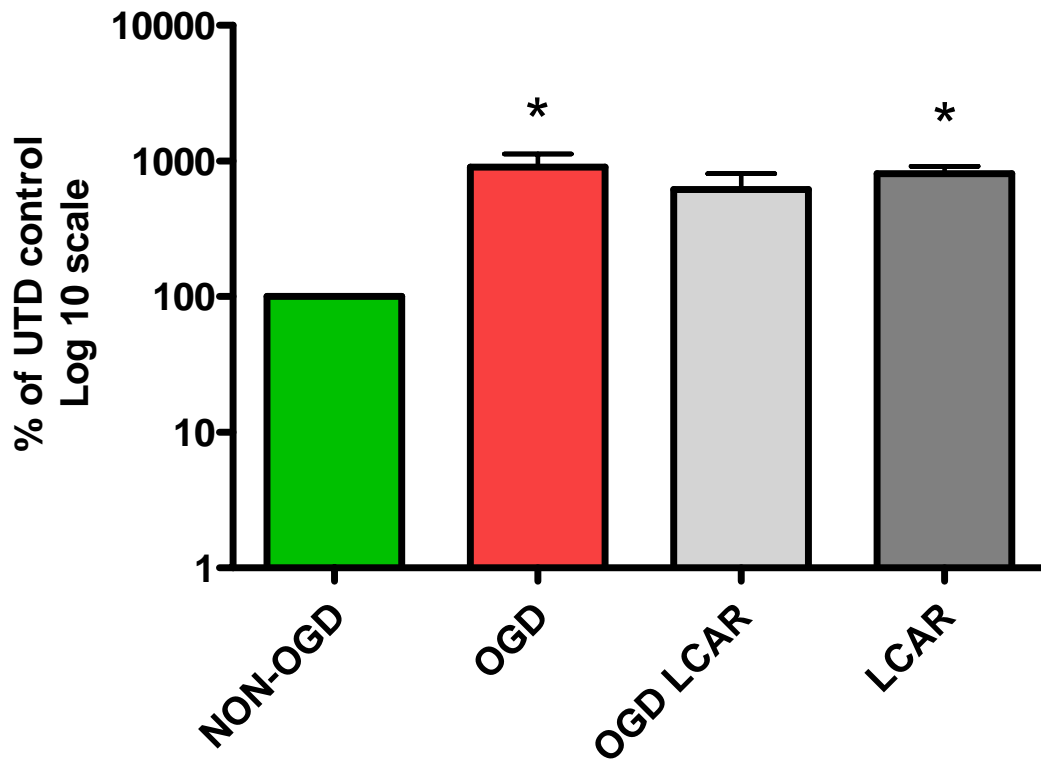
Fig. 31a Western blot analysis of UCP-2 expression in carnitine treated RHSC exposed to OGD. Untreated cultures exposed to OGD showed a significant increase in UCP-2 expression at 24 hours post-OGD. *=p<0.05 UTD vs. groups. One way ANOVA, Tukey's post-hoc. Each bar represents a minimum of 4 samples; each sample is composed of 4 pooled slices.
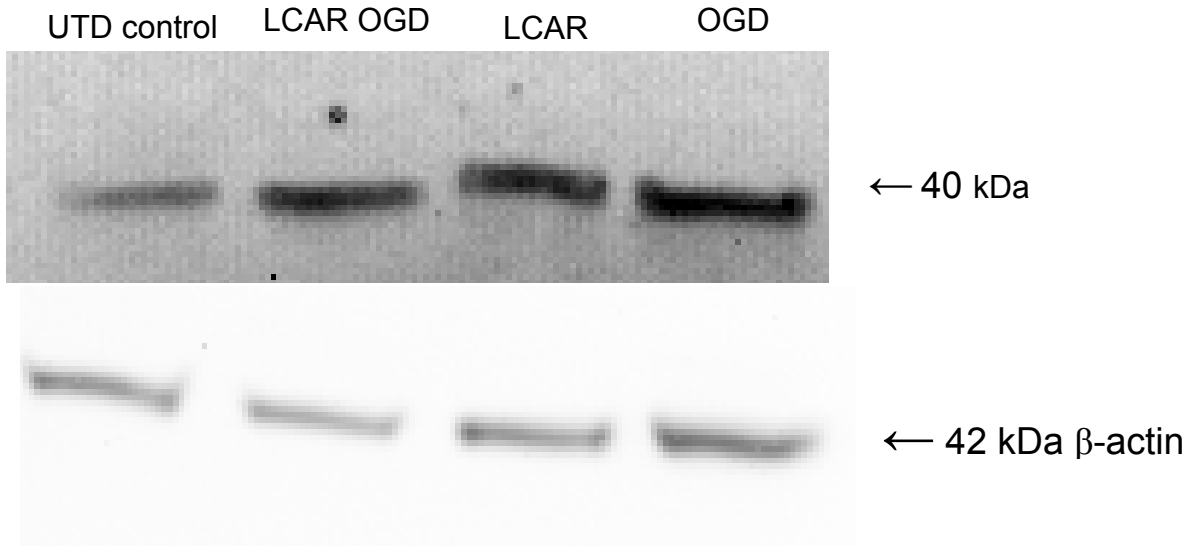
Fig. 31b Representative images of Western blot analysis showing UCP-2 expression 24h post OGD. OGD, LCAR treatment, and LCAR treatment prior to OGD all resulted in an increase in UCP-2 expression at 24 hours post OGD. Also shown β-actin loading control.

carnitine treated cultures prior to OGD would allow immediate activation to reversibly depolarize the MMP and avoid MPTP activation. To test this hypothesis we measured cell death (PI uptake) while pharmacologically blocking the activity of UCP-2 with guanosine diphosphate, (GDP) prior to and immediately after OGD and in the presence or absence of carnitine.

3.11 Cell Death Following OGD in the Presence of UCP-2 Inhibition

We observed a significant decrease in neuroprotection when carnitine was administered in the presence of UCP-2 inhibition ($p < 0.05$; fig. 34). To further elucidate this effect we inhibited UCP-2 in the presence of carnitine, exposed them to OGD and measured an decrease in cell death when compared to UCP-2 inhibited RHSC's exposed to OGD [fig. 34]. While these observations suggest carnitine is exerting a neuroprotective effect through UCP-2, they further suggest this effect is not solely responsible for the decreased cell death.

In further studies we added carnitine prior to OGD and inhibited UCP-2 after OGD. Under these conditions we observed a significant increase in neuronal death when compared to RHSC's treated with carnitine in the presence of UCP-2 inhibition. This finding suggests carnitine treatment reduces neuronal death by increasing UCP-2 prior to OGD and inhibition of increased UCP-2 expression after OGD results in greater cell death. This effect may be due to a loss of mitochondrial control over MMP uncoupling that result in increased superoxide production and MPTP activation. This hypothesis is further supported by our finding that inhibition of UCP-2 in the presence of carnitine prior to OGD resulted in decreased cell death. It is possible this effect is due to the
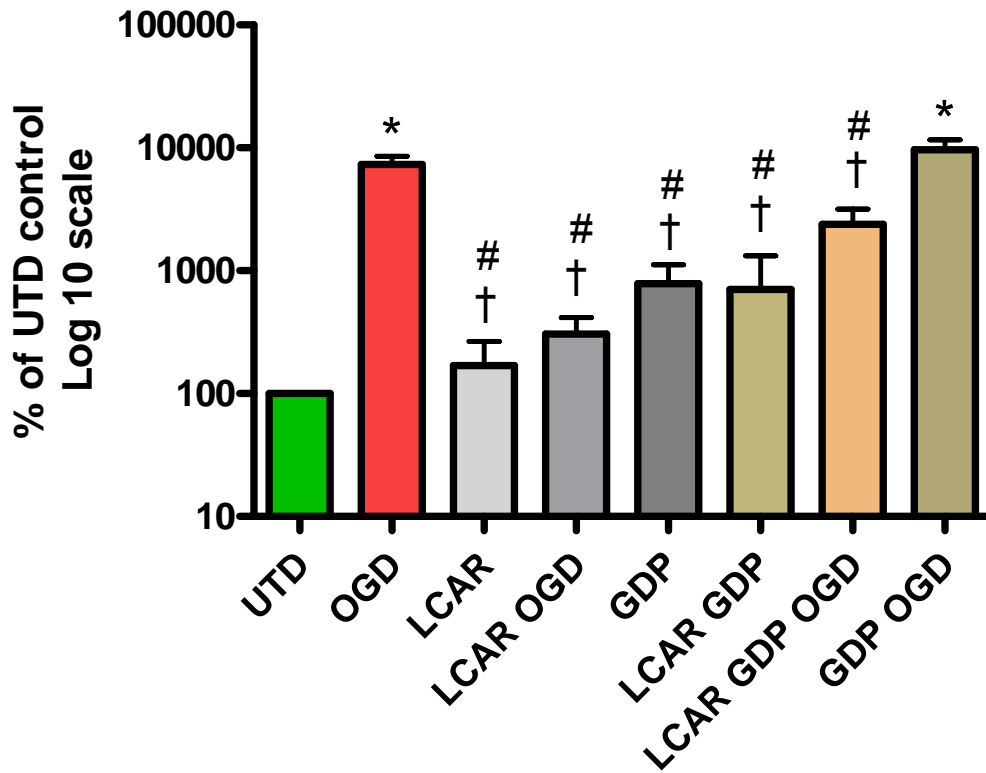
Fig. 32a Neuronal death in RHSC treated with carnitine in the presence or absence of UCP-2 inhibiton. Carnitine treatment in the presence of UCP-2 inhibition prior to OGD results in decreased neuroprotection when compared to carntine treatment alone. The addition of carnitine in the presence of UCP-2 inhibition significantly decreased neuronal death from OGD when compared to UCP-2 inhibited cultures exposed to OGD. *=$p<0.05$ UTD vs. groups, †=$p<0.05$ OGD vs. groups, #=$p<0.05$ GDP OGD vs groups. One way ANOVA, Tukey's post-hoc. Each bar represents a minimum of 3 samples.
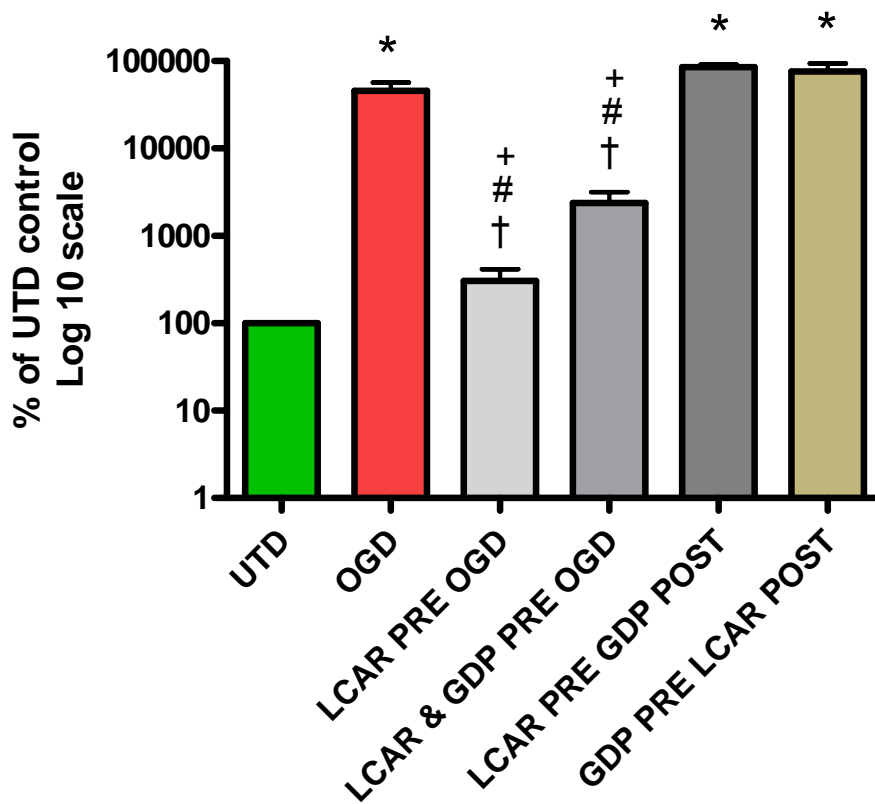
Fig. 32b Neuronal death in RHSC treated with carnitine in the presence or absence of UCP-2 inhibiton. Carnitine treatment prior to OGD and UCP-2 inhibition after OGD resulted in a significant increase in neuronal death when compared to UCP-2 inhibited cultures treated with carnitine prior to OGD. The addition of carnitine in the presence of UCP-2 inhibition prior to OGD significantly decreased neuronal death from OGD when compared to untreated cultures exposed to OGD. *=p<0.05 UTD vs. groups, †=p<0.05 OGD vs. groups, #=p<0.05 LCAR pre-OGD GDP post-OGD vs. groups, +=p<0.05 GDP pre-OGD LCAR post-OGD vs. groups. One way ANOVA, Tukey's post-hoc. Each bar represents a minimum of 4 samples.

modulation of alternative mechanisms to compensate for the loss of UCP-2 function prior to OGD.

Previous studies by Mattiasson et al [57] demonstrated activation of UCP-2 (by superoxide or hydroxynoneal) results in a mild, reversible depolarization of MMP that allows ROS to exit the mitochondria before damaging the inner mitochondrial membrane [57].Our observation that carnitine treatment increases UCP-2 expression may explain how mitochondria in carnitine treated cells rapidly shunt large amounts of superoxide into the cytosol. Based on previous data showing carnitine treatment increases cytosolic superoxide levels but decreases SOD2 expression, we hypothesized UCP-2 activation was reducing mitochondrial superoxide after OGD by shunting superoxide into the cytosol. To test this hypothesis we inhibited UCP-2, treated with carnitine and measured mitochondrial superoxide levels to determine if UCP-2 was allowing carnitine-generated superoxide to exit the mitochondria.

3.12 The Effect of UCP-2 Inhibition on ROS Levels

Utilizing Mitosox fluorescent assay, we observed a significant increase in mitochondrial superoxide after 2 hours of UCP-2 inhibition ($p < 0.05$) [fig. 35]. This effect was multiplied when carnitine was added in the presence of UCP-2 inhibition indicating UCP-2 is playing a significant role in decreasing carnitine-generated mitochondrial superoxide. This observation also suggests that under basal conditions UCP-2 may be playing a role in mild uncoupling to prevent excessive increases in superoxide as well as facilitating the efflux of superoxide into to the cytosol to protect lipid membranes and mtDNA.

Fig. 33a Mitochondrial superoxide in RHSC treated with carnitine for 2 hours in the presence or absence of UCP-2 inhibition. Carnitine treatment in the presence of UCP-2 inhibition resulted in a significant increase in mitochondrial superoxide. UCP-2 inhibition of RHSC resulted in a significant increase in mitochondrial superoxide when compared to untreated control cultures. *=p<0.05 UTD vs. groups, †=p<0.05 LCAR GDP vs. groups. One way ANOVA, Tukey's post-hoc. Each bar represents a minimum of 6 samples.
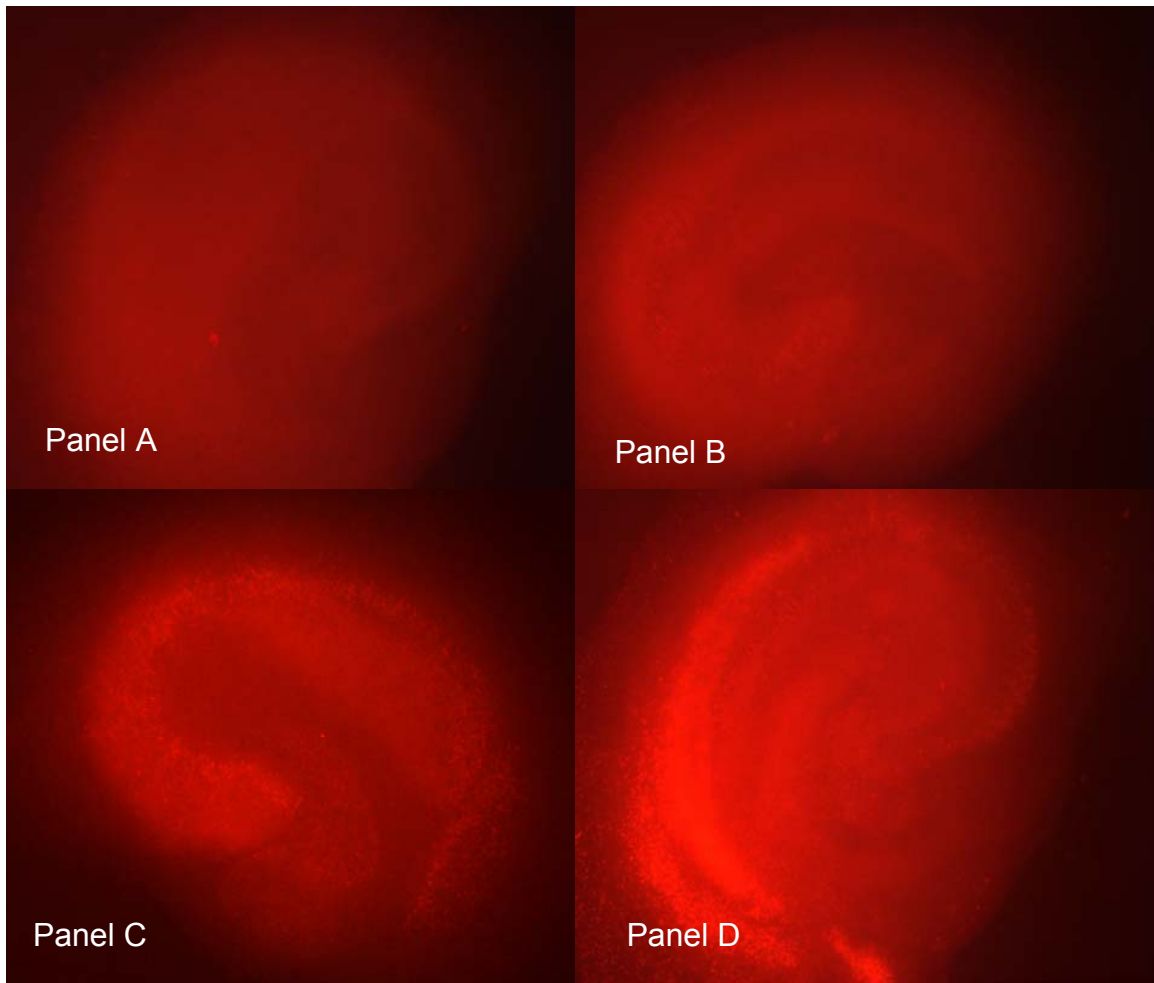
Fig. 33b Representative images of RHSC stained with MITOSOX after 2 hours of carnitine GDP treatment. Inhibition of UCP-2 in the presence of LCAR significantly increases mitochondrial superoxide. Panel A is untreated control, panel B is GDP, panel C is LCAR, panel D is GDP LCAR.

At 24 hours post-OGD we observed significantly lower levels of mitochondrial superoxide in carnitine-treated, OGD exposed RHSC's when compared to UCP-2 inhibited slices treated with carnitine and exposed to OGD ($p<0.05$) [fig. 36]. UCP-2 inhibition prior to OGD resulted in a significant increase in mitochondrial superoxide when compared to OGD alone. This observation suggests UCP-2 significantly decreases mitochondrial superoxide in untreated, OGD exposed cultures.

To further determine if UCP-2 was allowing the translocation of a significant amount of superoxide, we inhibited UCP-2 and then utilized DHE staining to measure cytosolic superoxide. Inhibition of UCP-2 resulted in a decrease in cytosolic superoxide 24 hours after OGD [fig 37], and this effect was present both with and without carnitine treatment. The observation that UCP-2 inhibition prior to OGD significantly increases mitochondrial superoxide and decreases the presence of cytosolic superoxide suggests UCP-2 is shuttling superoxide out of the mitochondria after OGD.

UCP-2 inhibition in the presence of carnitine resulted in levels of cytosolic superoxide that did not significantly differ from carnitine treatment alone. This observation suggests carnitine may be modulating extra-mitochondrial mechanisms that generate superoxide. NADPH oxidase, xanthine oxidase, phospholipase A2 (PLA2), and oxidative metabolism of arachadonic acid have all been shown to generate superoxide that increase neuronal damage after hypoxia-ischemia [67, 68]. While the effect of OGD and carnitine on these mechanisms remains undefined, it is possible the increased superoxide levels we observed are due to enzymatic or PLA2 activation by carnitine treatment.
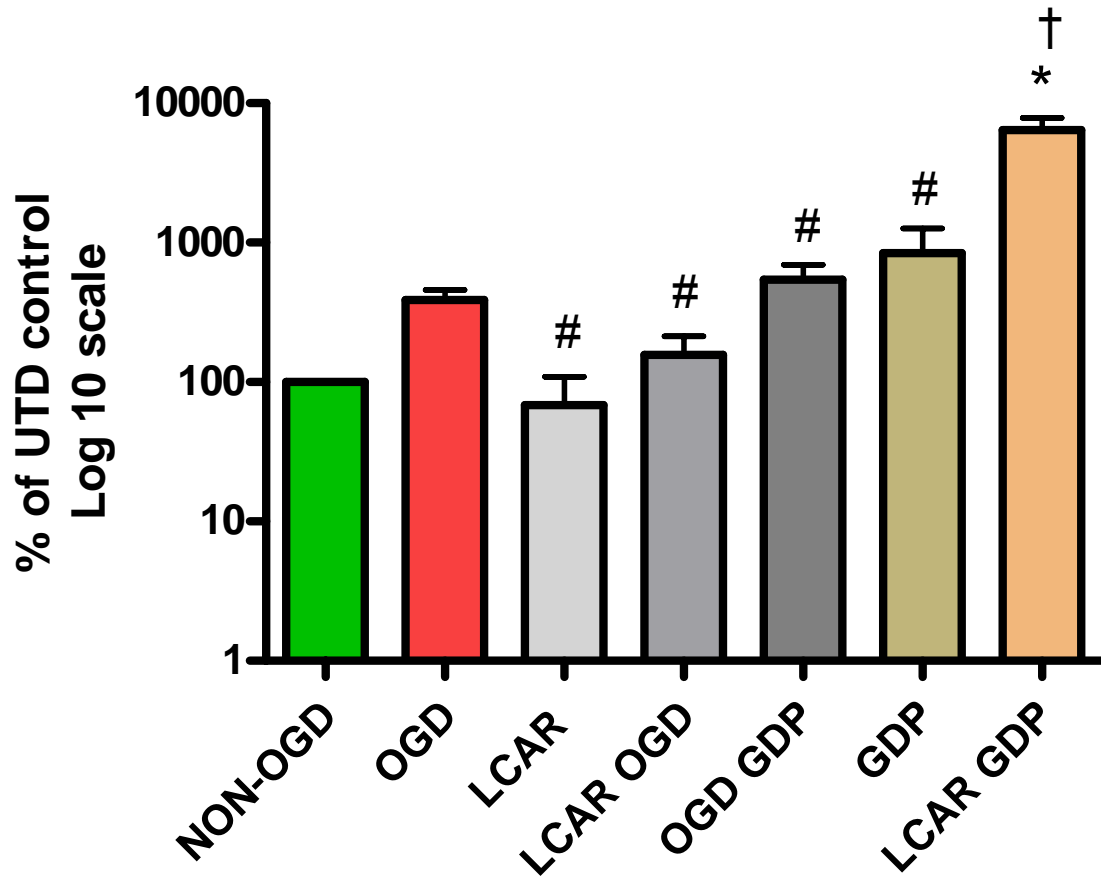
Fig. 34 Mitochondrial superoxide in RHSC treated with carnitine in the presence or absence of UCP-2 inhibition. At 24 hours post-OGD, inhibition of UCP-2 in the presence of carnitine resulted in a significant increase in mitochondrial superoxide. *=p<0.05 UTD vs groups, †=p<0.05 OGD vs. groups, #=p<0.05 LCAR GDP vs. groups. One way ANOVA, Tukey's post-hoc. Each bar represents a minimum of 5 samples.
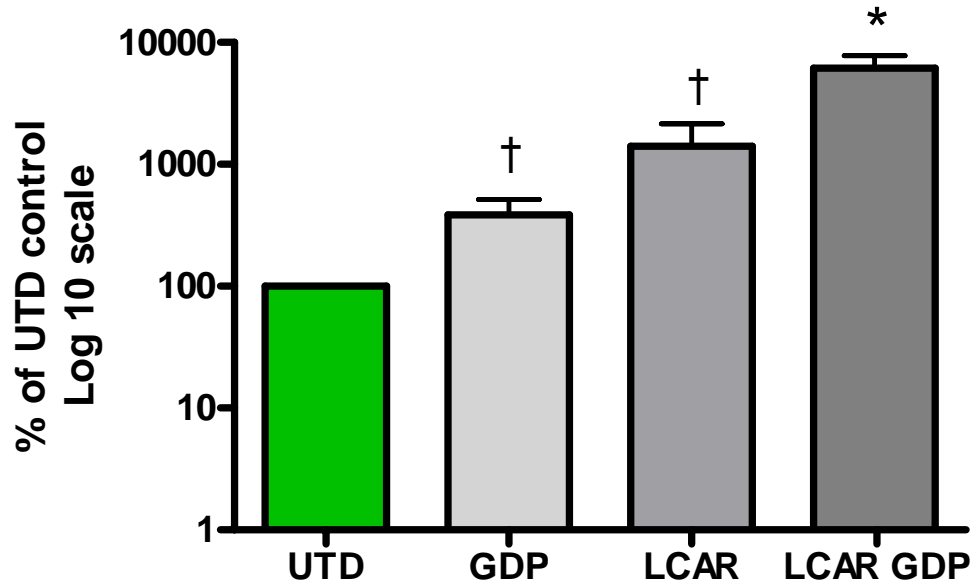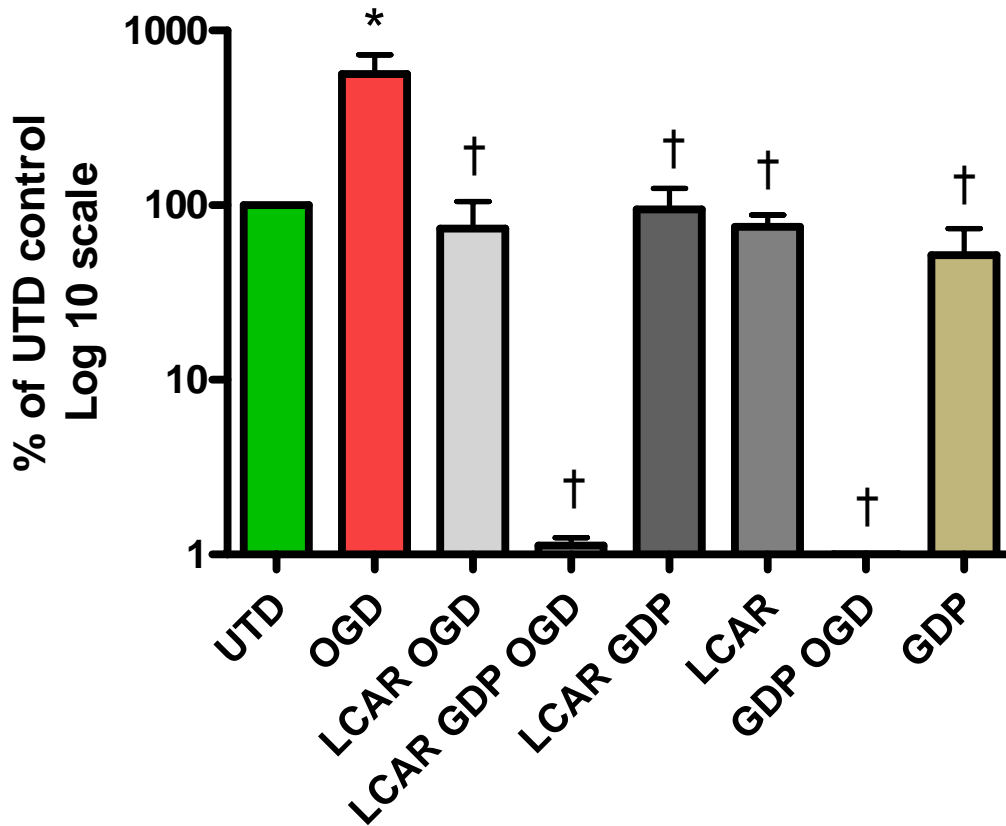
Fig. 35 Cytosolic superoxide in RHSC treated with carnitine in the presence or absence of GDP. At 24 hours post-OGD, GDP treated cultures (with and without carnitine) exposed to OGD showed a significant decrease in cytosolic superoxide. *=p<0.05 UTD vs. groups, †=p<0.05 OGD vs. groups. One way ANOVA, Tukey's post-hoc. Each bar represents a minimum of 4 samples.

The hypothesis that UCP-2 activation decreases mitochondrial superoxide by shunting it into the cytosol may elucidate several undefined points in our collected data. Previous Western blot data shows carnitine treatment induces three key alterations: increased UCP-2 expression, decreased mitochondrial SOD (SOD2) expression, and increased cytosolic SOD (SOD1) expression. Previous work by Echtay [59] showed UCP-2 is activated by superoxide in the presence of fatty acids and inhibited by SOD [59]. From these findings we hypothesized the activation of UCP-2 results in a translocation of superoxide into the cytosol that stimulates increased expression of SOD1.

3.13 UCP-2 Inhibition Alters SOD Expression in the Presence of LCAR

To begin testing this hypothesis we inhibited UCP-2, treated with carnitine and performed Western blot analysis for SOD1 and SOD2. We observed an increase in SOD2 expression while inhibiting UCP-2 in the presence of carnitine [fig. 38]. This finding suggests inhibition of UCP2 blocks ROS efflux and results in increased SOD2 expression as a compensatory mechanism. Further support for this hypothesis is the decreased neuronal death observed when GDP is administered with carnitine prior to OGD, possibly due to increased SOD2 levels prior to OGD. Treating with carnitine prior to OGD and inhibiting UCP-2 post-OGD resulted in a significant increase in neuronal death, possibly because SOD2 levels are decreased and mitochondrial ROS cannot efflux into the cytosl through UCP-2.
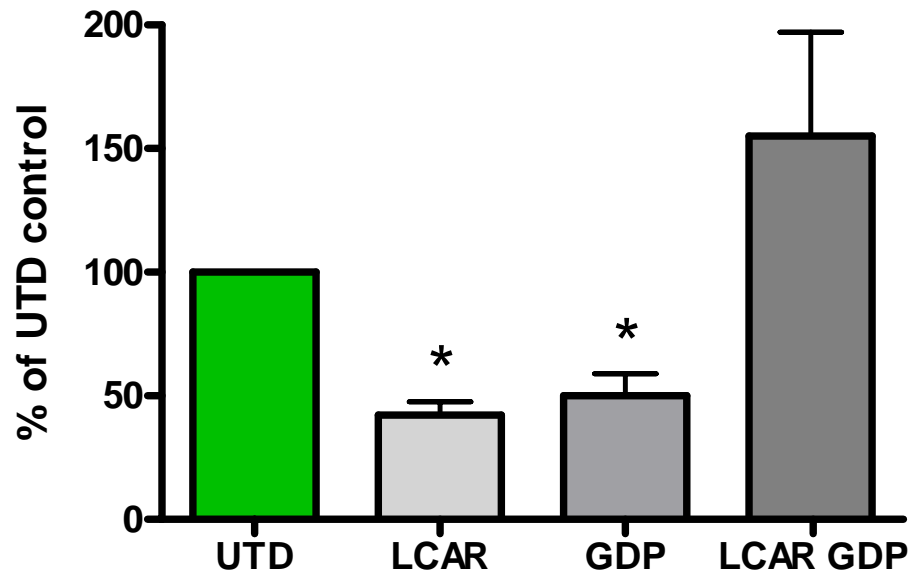
Fig. 36a Western blot analysis of SOD2 expression after 2 hours of carnitine treatment in the presence or absence of GDP. Inhibition of UCP-2 decreased SOD2 expression, however, UCP-2 inhibition in the presence of carnitine significantly increased SOD2 expression. *=p<0.05 LCAR GDP vs. groups One way ANOVA, Tukey's post-hoc. Each bar represents a minimum of 6 samples.
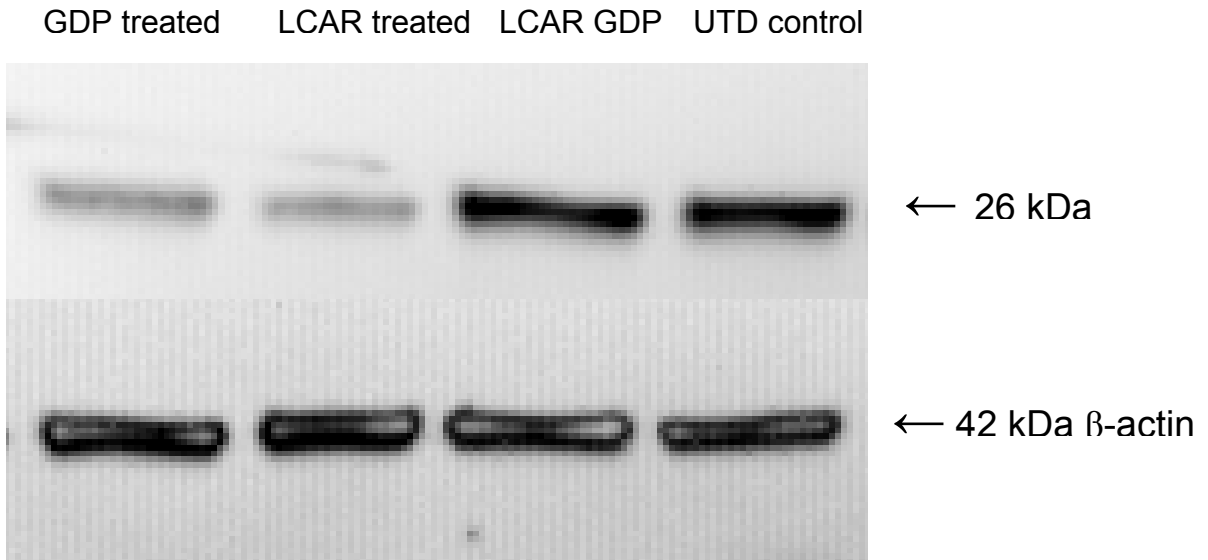
Fig. 36b Representative images of Western blot analysis showing SOD2 expression after two hours of LCAR GDP treatment. Also shown β-actin loading control.

Western blot analysis of SOD1 expression in carnitine treated, UCP-2 inhibited RHSC showed a significant increase in SOD1 expression [fig 39]. This finding suggests the possibility that UCP-2 is not solely responsible for shunting mitochondrial ROS into the cytosol. The inner mitochondrial membrane contains 35 anion carriers including adenine nucleotide translocase (ANT) which has been shown to exhibit molecular characteristics similar to UCP-2. In light of the carnitine/GDP-mediated increase in superoxide (~5500%) it is entirely possible that a unique (UCP-2 independent) anion carrier was activated allowing superoxide to efflux into the cytosol. To test this hypothesis we treated slices with carnitine, inhibited UCP-2 and measured cytosolic superoxide.

Utilizing DHE staining we observed an increase in cytosolic superoxide after 2 hours of UCP-2 inhibition ($p<0.05$) [fig 40]. The UCP-2 inhibition in carnitine treated RHSC resulted in a significant increase in cytosolic superoxide suggesting superoxide was shunted out of the mitochondria by UCP-2 independent mechanism(s). This observation is further supported by previous experimental data showing carnitine treatment in the presence of UCP-2 inhibition prior to OGD resulted in significantly decreased cell death when compared to RHSC that received carnitine prior to OGD and UCP-2 inhibition after OGD. Inhibition of UCP-2 function in the presence of carnitine
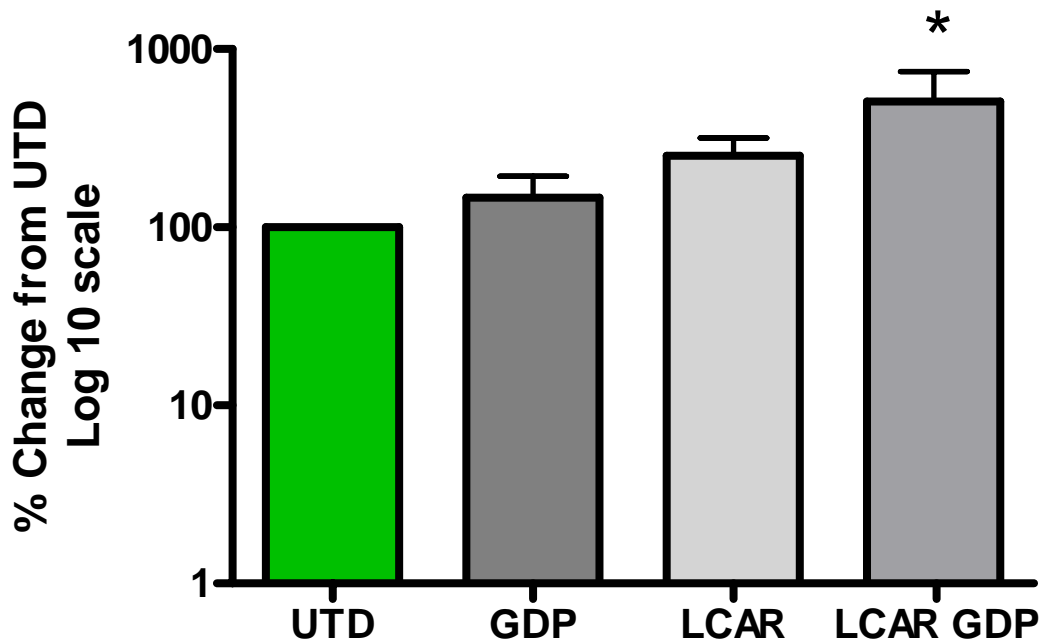
Fig. 37a Western blot analysis of SOD1 expression after 2 hours of carnitine treatment in the presence or absence of GDP. Carnitine treatment in the presence of UCP-2 inhibition significantly increased SOD1 expression. *=p<0.05 UTD vs. groups One way ANOVA, Tukey's post-hoc. Each bar represents a minimum of 4 samples; each sample is composed of 4 pooled slices.

UTD control   GDP treated   LCAR GDP   LCAR treated

← 23 kDa

← 42 kDa β-actin
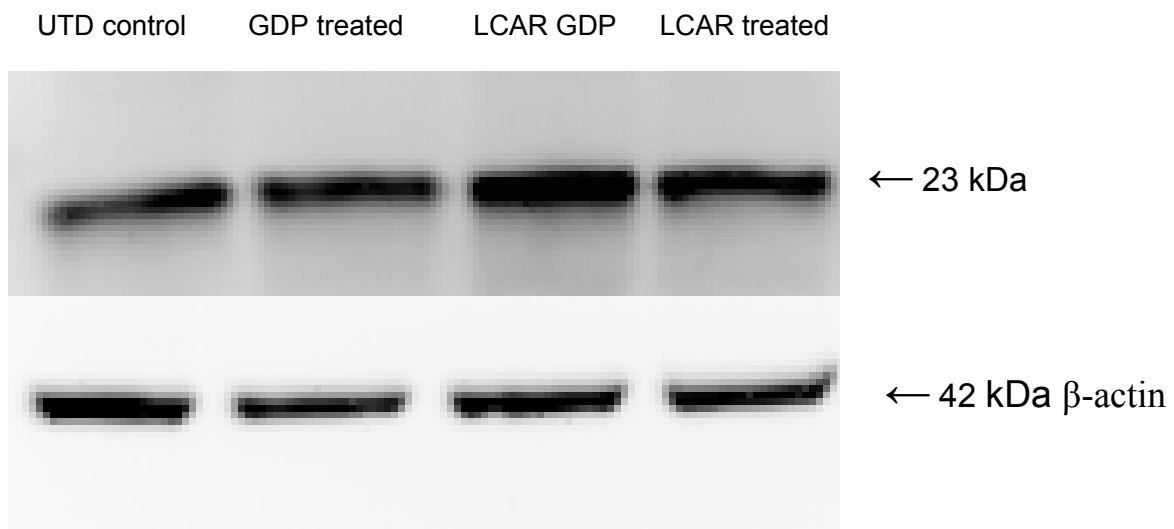
Fig. 37b Representative images of Western blot analysis showing SOD1 expression after two hours of LCAR GDP treatment. Also shown β-actin loading control.
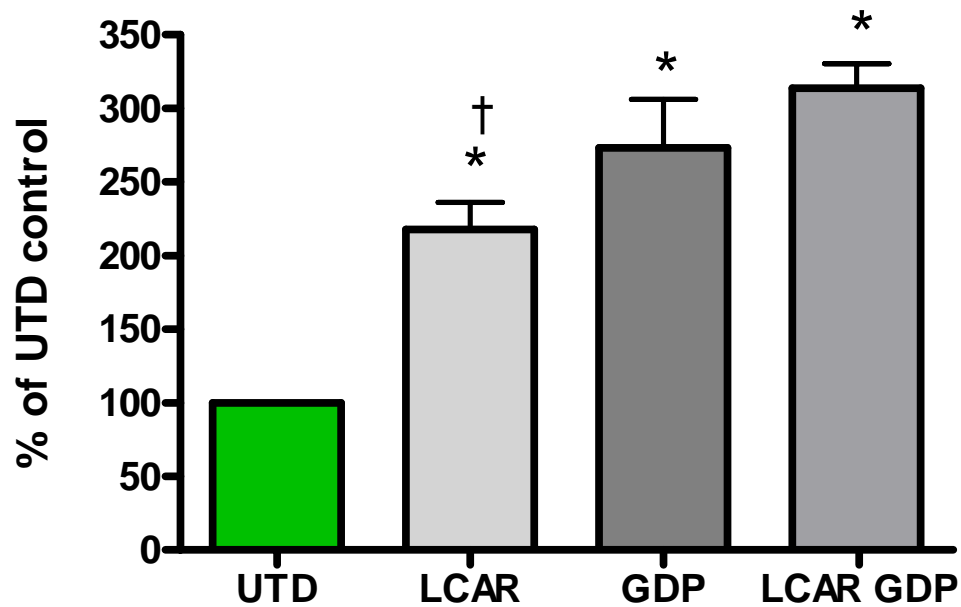
Fig. 38a Cytosolic superoxide in RHSC treated with carnitine in the presence or absence of GDP. Inhibition of UCP-2 in the presence of carnitine significantly increased cytosolic superoxide. *=p<0.05 UTD vs. groups; †=p<0.05 LCAR GDP vs. groups. One-way ANOVA, Tukeys post-hoc. Each bar represents a minimum of 7 samples.

prior to OGD may induce alterations in secondary (UCP-2 independent mechanisms) mitochondrial proteins that compensate for the loss of UCP-2 function. Treating RHSC with carnitine prior to OGD and inhibiting UCP-2 after OGD ensures the cell cannot compensate for the loss of function prior to OGD.

3.14 MMP in the Presence of UCP-2 Inhibition

To further test the hypothesis that UCP-2 independent mechanisms are activated when UCP-2 is inhibited prior to OGD we treated RHSC with carnitine, inhibited UCP-2, and measured MMP. Slices exposed to 2 hours of UCP-2 inhibition showed a significant MMP depolarization suggesting inhibition of basal levels of UCP-2 results in a spontaneous depolarization of MMP through an independent, unrelated mechanism(s). A significant hyperpolarizing effect was noted in RHSC treated with carnitine in the presence of UCP-2 inhibition [fig. 41]. This observation suggests UCP-2 activation modulates the hyperpolarizing effect of carnitine treatment and in turn this effect may further contribute to the increased UCP-2 expression we observed in carnitine treated RHSC.

Rhodamine data in RHSC shows UCP-2 plays a role in modulating carnitine induced hyperpolarization of MMP. While it is possible increased UCP-2 expression may be a mitochondrial adaptation to hyperpolarized membrane potential, activation of UCP-2 requires superoxide in the presence of fatty acids or hydroxynoneals (oxidized fatty acids). In previous studies we observed increases in superoxide, both prior to and after OGD, in carnitine treated RHSC. In light of this observation we hypothesized carnitine
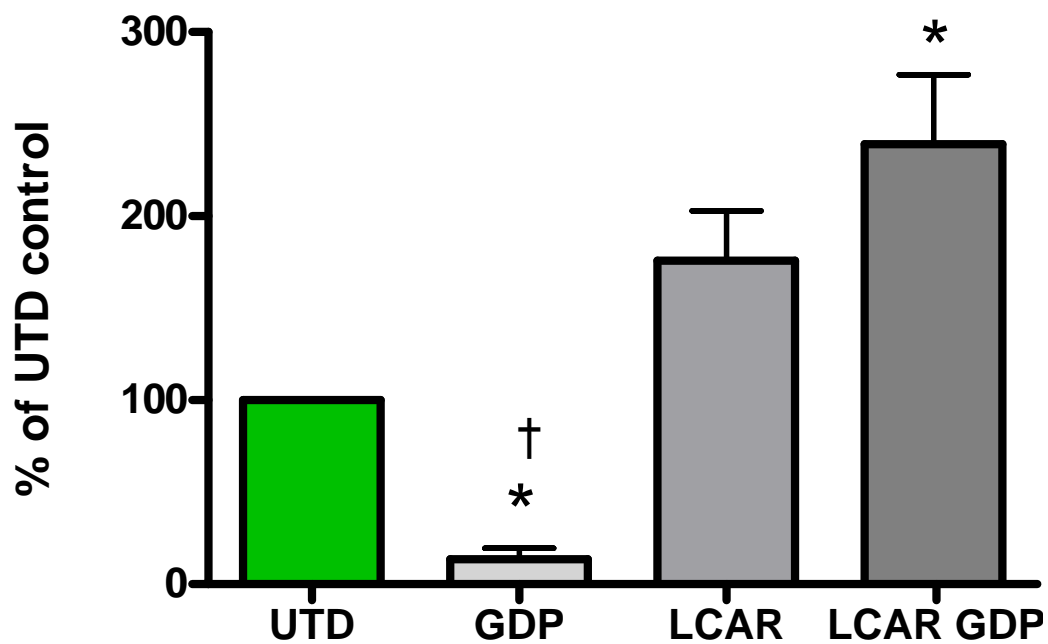
Fig. 39a Mitochondrial membrane potential (MMP) in RHSC treated with carnitine in the presence or absence of GDP. Inhibition of UCP-2 resulted in a significant MMP depolarization, however, inhibition of UCP-2 in the presence of carnitine resulted in a MMP hyperpolarizing effect. *=p<0.05 UTD vs. groups, †=p<0.05 LCAR vs. groups. One-way ANOVA, Tukey's post-hoc. Each bar represents a minimum of 5 samples.
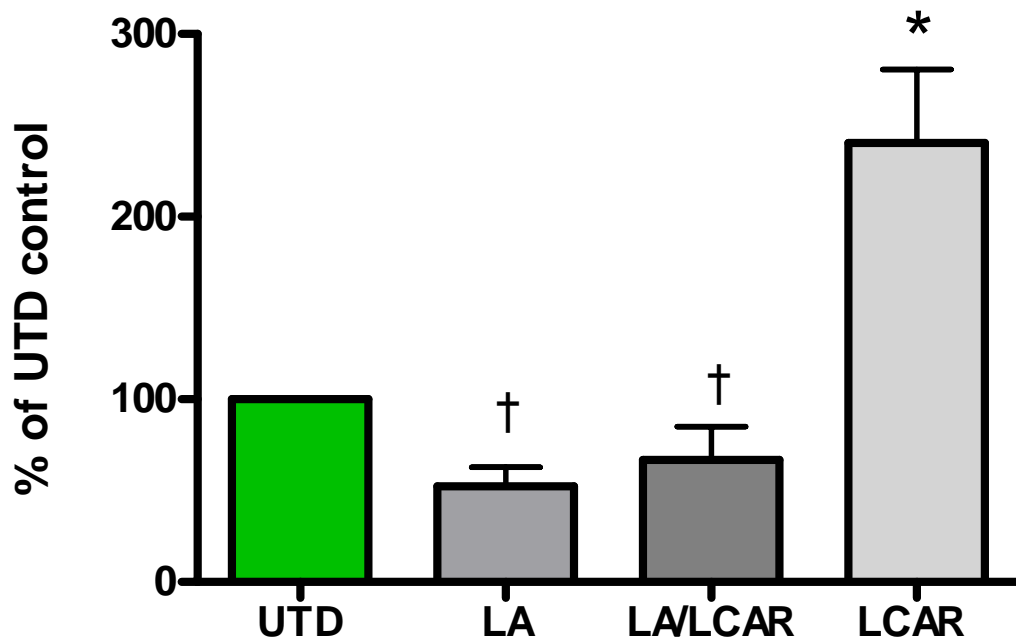
Fig 40a Western blot analysis of UCP-2 expression after 2 hours carnitine treatment in the presence or absence of lipoic acid (LA). Carnitine treatment in the presence of LA significantly decreased UCP-2 expression. *=p<0.05 UTD vs LCAR, †=p<0.05 LCAR vs. groups One way ANOVA, Tukey's post-hoc. Each bar represents a minimum of 4 samples; each sample is composed of 4 pooled specimens.

mediated superoxide was not only activating UCP-2, but also inducing increased expression levels prior to OGD.

3.15 UCP-2 Protein Levels in the Presence of LCAR and an Anti-oxidant

To test this hypothesis we treated slices with LCAR and an anti-oxidant (lipoic acid) and measured UCP-2 expression. Western blot analysis showed a LA-mediated decrease in UCP-2 expression. Carnitine treatment in the presence of LA resulted in a significant decrease in UCP-2 expression [fig. 42] indicating the carnitine mediated increase in UCP-2 is due, at least in part, to increased superoxide levels.

To further study this effect, we treated slices with carnitine and GDP to induce increases in mitochondrial superoxide. Based on our previous study with anti-oxidant treatment in which we observed a decrease in UCP-2 expression we hypothesized increasing mitochondrial superoxide would result in a corresponding increase in UCP-2 expression. To significantly increase mitochondrial superoxide in RHSC we treated with carnitine in the presence of UCP-2 inhibition.

Inhibition of UCP-2 in the presence of carnitine resulted in a significant increase in UCP-2 expression [fig. 43]. While this finding does not rule out the possibility of an alternative mechanism compensating as a result of UCP-2 inhibition, it does suggest mitochondrial superoxide plays a role in modulating UCP-2 expression.

Fig 41a Western blot analysis of UCP-2 expression after 2 hours carnitine treatment in the presence or absence of GDP. Carnitine treatment in the presence of UCP-2 inhibition significantly increased UCP-2 expression. *=$p<0.05$ UTD vs. groups, †=$p<0.05$ LCAR vs. groups. One way ANOVA, Tukey's post-hoc. Each bar represents a minimum of 3 samples; each sample represents 4 pooled slices.
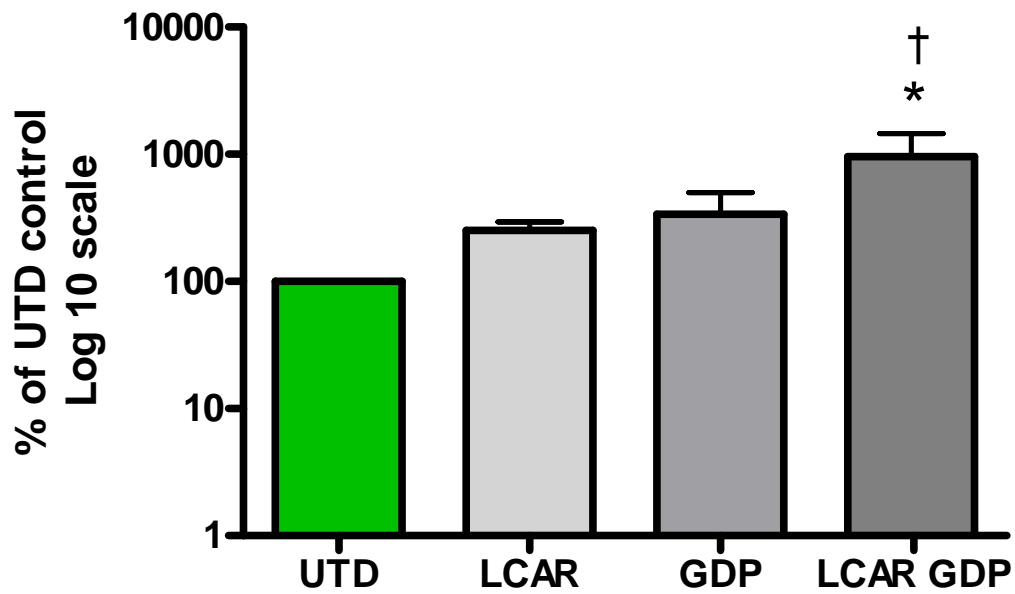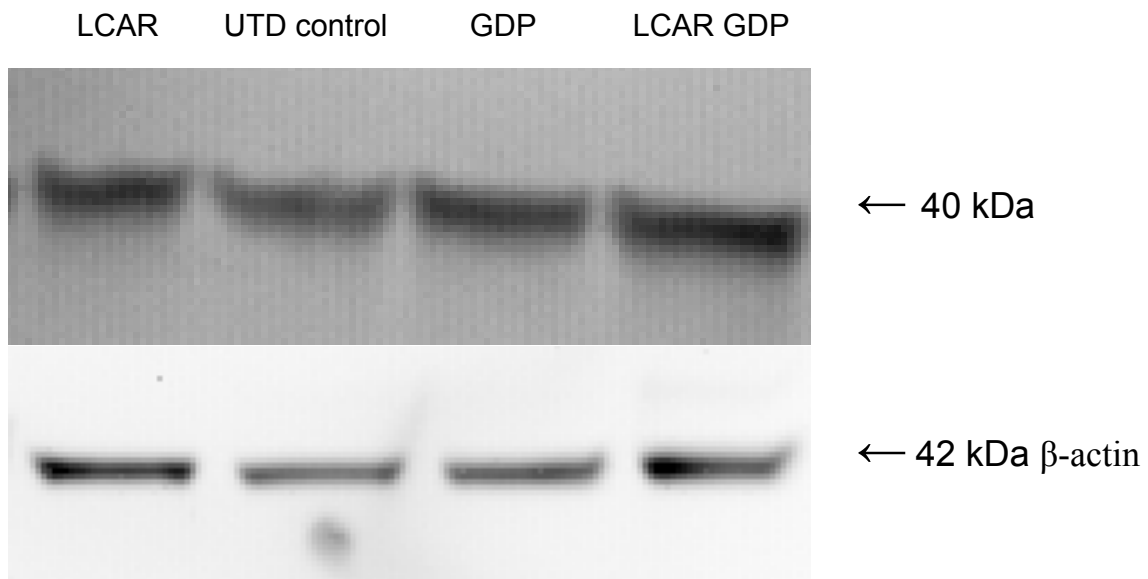
Fig. 41b Representative images of Western blot analysis showing UCP-2 expression after 2h of LCAR GDP treatment. Also shown β-actin loading control.

Chapter 4

DISCUSSION

4.1 LCAR as a Treatment for HIE

Hypoxic ischemic encephalopathy (HIE) is a neurological disease that lacks an effective, standardized medical treatment. Currently the only protocol approved for the prevention of HIE is mild hypothermia. The CoolCap is hypothermic tool that reduces brain temperature (3-4^0 C) and must be employed prior to the secondary phase of energy failure that occurs 6-24 hours after the initial insult. Efficacy with this treatment is considered marginal with possible side effects (metabolic acidosis, leukocyte malfunctions, pulmonary hypertension, abnormal cardiac rhythm) occurring as a result of the rewarming process [2, 69].

The utilization of emerging neuroprotective therapies for neonatal HI is hampered by two issues: potential toxicity/side effects and inefficacy when administered post HI. Carnitine treatment, when used as a standard protocol, may be a useful prophylactic treatment for neonatal stroke. Currrently, carnitine treatment is used in infants and children as a treatment for carnitine palmitoyl transferase II (CPTII) deficiencies and mitochondrial myopathies and encephalo-myopathies[40, 70, 71]. The compound can be administered easily, has no noted side effects, and can be given in high doses with extremely low toxicity [39, 47]. In light of these factors it would be possible to set up a dosing regimen several days prior to birth and, in cases of neonatal HI, for at least 72 hours after the event. In addition to the stroke prevention this protocol could also serve as an immediate treatment for babies born with CPTII or carnitine deficiencies. The low

cost of carnitine (~20 cents for 500mg) and widespread availability make it a plausible treatment for expecting mothers in developing countries that do not have access to costlier hypothermic treatment and adequate follow up care.

The purpose of this study was to elucidate the mechanism(s) of carntine mediated neuroprotection associated with acute hypoxia ischemia. Previous _in vivo_ studies indicated caritine treatment prior to acute HI prevents neuronal cell death in the hippocampus. This observation was recapitulated in RHSC in our laboratory showing the _in vivo_ effect correlated with our _in-vitro_ model. Conversely, the addition of carnitine after OGD consistently resulted in a significant increase in cell death. These observations indicate the neuroprotective effect is due, at least in part, to alterations introduced prior to HI.

Previous studies by Ames [39, 51, 75, 76] noted carnitine treatment increased ROS as an effect of increased cellular respiration and we observed this effect in our hippocampal slice culture model. Using DHE, Mitosox, and DCF-DA dyes, we observed a carnitine-mediated increase in ROS prior to OGD but a significant decrease in superoxide and hydrogen peroxide after OGD. The ability of carnitine-treated neurons to effectively decrease ROS after OGD indicates carnitine increases ROS scavenging ability. This finding, coupled with the observation that carnitine must be administered prior to HI, led us to hypothesize the possibility of a carnitine-induced ROS burst that alters neuronal scavenging capability prior to OGD.

Supporting this hypothesis is data showing carnitine mediated increases in superoxide results in two specific mitochondrial effects: 1) decreased SOD2 expression and 2) increased UCP-2 expression. While decreasing SOD2 expression may appear

counterintuitive, previous work by Echtay [59] showed SOD directly inhibits UCP-2 activity and this finding may explain our observation: decreasing SOD2 expression would allow an increase in UCP-2 activity. Based on our data showing anti-oxidant treatment significantly decreases UCP-2 expression, decreasing SOD2 would allow an increase superoxide leading to a corresponding increase in UCP-2 expression.

Furthermore, SOD activity assays showed RHSC treated with carnitine had SOD2 activity levels that did not differ from untreated controls even though the expression of SOD2 in carnitine treated cultures was significantly decreased. This effect may be a due to several factors including a neuronal adaptation to maintain a basal scavenging rate while decreasing overall SOD2 expression. It may also be due to a decrease in active SOD2 protein in the controls while a greater percentage of the LCAR treated group maintains active SOD2. This would allow SOD2 to effectively dismutate any superoxide that fails to efflux into the cytosol while keeping expression levels low enough to allow increased expression and activation of UCP-2.

In turn, the mild activation of UCP-2 prevents carnitine induced hyperpolarization of MMP and ensures mitochondrial polarization remains within the optimal (~150mV) range to produce ATP through F1F0-ATPase and complex V. If cellular respiration increases rapidly (carnitine treatment) the inner mitochondrial membrane becomes hyperpolarized (>180mV) resulting in decreased ATP synthesis, increased calcium influx and elevated ROS production [25, 35, 72]. Our experimental data showing carnitine treatment in the presence of UCP-2 inhibition results in a significant MMP hyperpolarization indicates UCP-2 is modulating MMP during carnitine treatment.

UCP-2 activation in the presence of carnitine facilitates superoxide efflux from the mitochondria into the cytosol and induces, at least in part, increased expression of SOD1. This finding was further confirmed by inhibition of UCP-2 in conjunction with carntine treatment that resulted in increased mitochondrial superoxide and decreased cytosolic superoxide indicating UCP-2 translocates a significant amount of superoxide into the cytosol. As superoxide exits the mitochondria through UCP-2, increased levels of SOD1 convert it to H_2O_2. Excess H_2O_2 is converted to water by catalase present in the cytosol. As carnitine induces increased H_2O_2 from superoxide, catalase expression and activity increase as an adaptive response.

Oxygen glucose deprivation (OGD) in untreated neurons results in a rapid decrease in available glucose and oxygen resulting in acute ATP depletion and the accumulation of lactate. Simultaneously, excitatory amino acids glutamate and aspartate are released inducing excessive calcium influx into the neuron. As these two events occur, the mitochondria attempts to restore ATP production and buffer calcium influx. As OGD continues, ATP levels continue to decline rapidly resulting in energetic failure of the Na/K pump and the Na/Ca exchanger. The loss of Na/K regulation results in an uncontrolled influx of Na and H_2O that induces cytoxic edema resulting in membrane damage [2, 26]. This effect is followed by a loss of Ca regulation that induces the formation and activation of the mitochondrial permeability transition pore resulting in a spontaneous, irreversible depolarization of MMP that cripples bioenergetic mechanisms and further depletes ATP[20].

In carnitine treated neurons, OGD results in increased mitochondrial superoxide. This effect, coupled with the possible increase of mitochondrial fatty acids (due to carnitine-mediated transport), could lead to increased activation of UCP-2. This effect, coupled with carnitine mediated increases in UCP-2, could result in a mild, reversible depolarization of MMP. The UCP-2 mediated depolarization would accomplish two tasks: 1) induce a decrease in protonmotive force thereby decreasing ROS production; and 2) prevent the formation and activation of the MPTP that results in irreversible depolarization of MMP. As ROS levels decrease over time UCP-2 activation ceases, MMP repolarizes to basal levels, and mitochondrial viability remains intact.

In untreated neurons, bioenergetic mechanisms begin to fail and energy from the electron transport chain and protonmotive force is shunted to produce ROS. As ROS levels increase they overwhelm cellular anti-oxidant defenses and scavenge lipid membranes resulting in toxic, oxidized fatty acids and a loss of mitochondrial structural integrity. As mitochondrial membranes disintegrate, oxidized cardiolipin releases cytochrome c from the inner membrane allowing it to translocate through the damaged mitochondria into the cytosol activating apaf-1 leading to caspase 3 activation and subsequent apoptosis. [12, 20, 31]

In contrast, carnitine treated neurons rapidly shuttle superoxide out of the mitochondria through increased UCP-2. Once in the cytosol, increased expression/activity of SOD1 converts large amounts of OGD generated superoxide to H_2O_2. Once in the cytosol H_2O_2 is rapidly converted to water by increased expression/activity of catalase.

Based on our observations carnitine treatment may play a role in treating long term neurodegenerative disorders that involve mitochondrial dysfunction and ROS production leading to cell death. Previous research by both Liu (2002) and Ames (2003) indicate carnitine may have clinical potential in delaying the cognitive decline associated with age or disease by improving mitochondrial efficiency [39, 50, 73-76].

4.2 LCAR Treatment in Neurodegenerative Disorders Involving Mitochondrial Dysfunction

Alzheimer's disease (AD) is a neurodegenerative disorder characterized by the formation of Aβ plaques, neurofibrillary tangles, and profound neuronal loss. Biochemical analysis of CNS tissue from Alzheimer's patients has shown abnormalities in cytochrome oxidase (COX) activity localized to the cerebral cortex and hippocampus. COX is the terminal enzyme in the electron transport chain responsible for catalyzing the transfer of electrons from ferrocytochrome c to molecular oxygen to form water. [77-80]. Studies in AD patients show mitochondrial expression of COX subunits II and IV are significantly lower due to increases in mutations (due to ROS damage) in mitochondrial DNA [81]. The end result of these mutations is reduced COX activity that results in decreased mitochondrial ATP production and increased in ROS [82, 83] [81, 84, 85].

Utilization of carnitine might serve to alleviate this issue by increasing UCP-2 expression and ROS scavenging ability, and could allow AD affected neurons to modulate MMP to quickly reduce damaging ROS levels. Carnitine treatment would also increase fatty acid transport into the mitochondria resulting in increased metabolic viability. In light of the increased cognition and ambulation Ames et al [39, 51, 75, 76,

111

86] noted when aged rats were treated with carnitine, it is not unrealistic to hypothesize the possible cognitive benefit of carnitine treatment in Alzheimers disease.

Another neurodegenerative disorder characterized by mitochondrial dysfunction is Parkinson's disease (PD). While the causative agents for PD remains unknown it has been linked to reduced activity of complex I in the mitochondrial membrane. Further research has developed a novel model of PD that involves the infusion of rotenone, a mitochondrial complex I inhibitor. This technique results in the selective death of dopaminergic nerve terminals and causes retrograde degeneration of the substantia nigra that mimics PD pathology [87]. At the molecular level complex I inhibition results in depleted ATP, decreased Na^+/K+ ATPase activity and depolarized neurons. This in turn allows the activation of NMDA receptors (Mg plug removal) which induces an influx of calcium that the dysfunctional mitochondria fail to adequately buffer. The end result is calcium mediated activation of apoptosis leading to neuronal death [88].

While it remains unknown if complex I dysfunction is an originating cause of PD or a symptom that contributes to disease progression, there is substantial research indicating PD dopaminergic neurons undergo mitochondrial dysfunction as a critical step in disease progression. Further studies have suggested complex I dysfunction is tied to ROS damage that occurs due to the age-related decrease in enymatic activity of ROS scavenging enzymes [89]. Currently, there is a growing body of research that directly links mitochondrially generated oxidative stress with the death of dopaminergic neurons within substantia nigra. In light of this finding, treatment of mitochondrial dysfunction may be a key target for therapeutic intervention.

Based on our finding that carnitine decreases ROS production through modulation of MMP, increases ROS scavenging ability, and preserves metabolic viability suggest it may have clinical relevance as a treatment for patients suffering from PD. Since the compound has no known interactions, it may be possible to administer carnitine in high doses in conjunction with other drug therapies such as Levodopa and Carbidopa.

Chapter 5

CONCLUSION

In this study we have evaluated the neuroprotective effect of carnitine on neonatal hippocampal slice cultures exposed to acute oxygen glucose deprivation (OGD). Working within this model system we have observed a significant decrease in cell death, both by mitochondrially-mediated apoptosis and necrosis, when carnitine is present prior to OGD. Carnitine treatment preserved synaptic and metabolic viability and prevented the OGD-induced irreversible loss of mitochondrial membrane potential by modulating uncoupling protein-2. In further studies we observed carnitine decreased reactive oxygen species by increasing the expression and activity of cytosolic superoxide dismutase and catalase.

As an endogenous compound with low toxicity, carnitine represents the possibility of a prophylactic treatment for neonatal stroke. In adult stroke patients, carnitine may have a role as a daily treatment for patients who are considered at-risk for secondary strokes. In light of the beneficial effect on mitochondrial health carnitine may have further applications in neurodegenerative diseases such as Alzheimers and Parkinson's that involve mitochondrial dysfunction as a key aspect of the pathological process.

Acknowledgments

Bibliography

1. Berger, R., *Perinatal Brain Injury.* Journal of Perinatal Medicine, 2000. **28**(4): p. 261-285.
2. Tonse, N.R., *Hypoxic-Ischemic Encephalopathy*, in *Emedicine Pediatrics Neonatology*, T. Rosenkrantz, Editor. 2006.
3. Sran, S.K. and R.J. Baumann, *Outcome of neonatal strokes.* Am J Dis Child, 1988. **142**(10): p. 1086-8.
4. *Study on propionyl-L-carnitine in chronic heart failure.* Eur Heart J, 1999. **20**(1): p. 70-6.
5. Hellstrom-Westas, L., et al., *Earlier Apgar score increase in severely depressed term infants cared for in Swedish level III units with 40% oxygen versus 100% oxygen resuscitation strategies: a population-based register study.* Pediatrics, 2006. **118**(6): p. e1798-804.
6. Groenendaal, F., M.J. Benders, and L.S. de Vries, *Pre-wallerian degeneration in the neonatal brain following perinatal cerebral hypoxia-ischemia demonstrated with MRI.* Semin Perinatol, 2006. **30**(3): p. 146-50.
7. Ambalavanan, N., et al., *Predicting outcomes of neonates diagnosed with hypoxemic-ischemic encephalopathy.* Pediatrics, 2006. **118**(5): p. 2084-93.
8. Chao, C.P., C.G. Zaleski, and A.C. Patton, *Neonatal hypoxic-ischemic encephalopathy: multimodality imaging findings.* Radiographics, 2006. **26 Suppl 1**: p. S159-72.
9. Fan, L.W., et al., *Minocycline attenuates hypoxia-ischemia-induced neurological dysfunction and brain injury in the juvenile rat.* Eur J Neurosci, 2006. **24**(2): p. 341-50.
10. Hunt, R., *Perinatal and neonatal ischaemic stroke: a review.* Thrombosis Research, 2004. **118**(1): p. 39-48.
11. Billiards, S.S., et al., *Is the late preterm infant more vulnerable to gray matter injury than the term infant?* Clin Perinatol, 2006. **33**(4): p. 915-33; abstract x-xi.
12. Nelson, K., *Stroke in newborn infants.* The Lancet, 2004. **3**(3): p. 150-158.
13. Nelson, K.B., *Perinatal ischemic stroke.* Stroke, 2007. **38**(2 Suppl): p. 742-5.
14. Pavlovic, J., et al., *Neuropsychological problems after paediatric stroke: two year follow-up of Swiss children.* Neuropediatrics, 2006. **37**(1): p. 13-9.
15. Miller, S.P., et al., *Patterns of brain injury in term neonatal encephalopathy.* J Pediatr, 2005. **146**(4): p. 453-60.
16. Wu, Y.W., et al., *Cerebral palsy in a term population: risk factors and neuroimaging findings.* Pediatrics, 2006. **118**(2): p. 690-7.
17. McQuillen, P.S., et al., *Temporal and anatomic risk profile of brain injury with neonatal repair of congenital heart defects.* Stroke, 2007. **38**(2 Suppl): p. 736-41.
18. Liu, J.B., et al., *[Role of cerebral computed tomography in the evaluation of brain injury following hypoxia in neonates].* Zhongguo Dang Dai Er Ke Za Zhi, 2006. **8**(3): p. 195-7.
19. Hemmen, T.M. and P.D. Lyden, *Induced hypothermia for acute stroke.* Stroke, 2007. **38**(2): p. 794-9.

20. McLean, C., *Mechanisms of hypoxic-ischemic injury in the term infant.* Seminars in Perinatology, 2004. **28**(6): p. 425-432.

21. Bassan, H., et al., *Periventricular hemorrhagic infarction: risk factors and neonatal outcome.* Pediatr Neurol, 2006. **35**(2): p. 85-92.

22. Berger, R.P., et al., *Serum biomarkers after traumatic and hypoxemic brain injuries: insight into the biochemical response of the pediatric brain to inflicted brain injury.* Dev Neurosci, 2006. **28**(4-5): p. 327-35.

23. Northington, F., *Apoptosis in perinatal hypoxic-ischemic brain injury-how important is it and should it be inhibited?* Brain Research Reviews, 2005. **50**(2): p. 244-257.

24. George, S., et al., *Induced cerebral hypothermia reduces post-hypoxic loss of phenotypic striatal neurons in preterm fetal sheep.* Exp Neurol, 2007. **203**(1): p. 137-47.

25. Budd, S., *Mechanisms of Neuronal Damage in Brain Hypoxia/ischemia: Focus on the role of mitochondrial calcium accumulation.* Pharmacology and Therapeutics, 1998. **80**(2): p. 203-229.

26. Vexler, Z., *Inflammation in adult and neonatal stroke.* Clinical Neuroscience Research, 2006. **6**(5): p. 293-313.

27. Vallee, L., et al., *Stroke, hemiparesis and deficient mitochondrial beta-oxidation.* Eur J Pediatr, 1994. **153**(8): p. 598-603.

28. Chen, S.J., M.E. Bradley, and T.C. Lee, *Chemical hypoxia triggers apoptosis of cultured neonatal rat cardiac myocytes: modulation by calcium-regulated proteases and protein kinases.* Mol Cell Biochem, 1998. **178**(1-2): p. 141-9.

29. Nadtochiy, S.M., A.J. Tompkins, and P.S. Brookes, *Different mechanisms of mitochondrial proton leak in ischaemia/reperfusion injury and preconditioning: implications for pathology and cardioprotection.* Biochem J, 2006. **395**(3): p. 611-8.

30. de la Monte, S.M. and J.R. Wands, *Molecular indices of oxidative stress and mitochondrial dysfunction occur early and often progress with severity of Alzheimer's disease.* J Alzheimers Dis, 2006. **9**(2): p. 167-81.

31. Puka-Sundvall, M., et al., *Impairment of mitochondrial respiration after cerebral hypoxia-ischemia in immature rats: relationship to activation of caspase-3 and neuronal injury.* Brain Res Dev Brain Res, 2000. **125**(1-2): p. 43-50.

32. Hilton, G.D., et al., *Glutamate-mediated excitotoxicity in neonatal hippocampal neurons is mediated by mGluR-induced release of Ca++ from intracellular stores and is prevented by estradiol.* Eur J Neurosci, 2006. **24**(11): p. 3008-16.

33. Sumi, K., et al., *[A case of MELAS (mitochondrial myopathy, encephalopathy, lactic acidosis and stroke-like episodes) with progressive cytochrome c oxidase deficiency].* Rinsho Shinkeigaku, 1989. **29**(7): p. 901-8.

34. Kim, J.H., et al., *Depletion of ATP and release of presynaptic inhibition in the CA1 region of hippocampal slices during hypoglycemic hypoxia.* Neurosci Lett, 2007. **411**(1): p. 56-60.

35. Kirkland, R., *Bax affects production of reactive oxygen by the mitochondria of non-apoptotic neurons.* Experimental neurology, 2006. **Article in press corrected proof**.

36. Zhu, C., et al., *Different apoptotic mechanisms are activated in male and female brains after neonatal hypoxia-ischaemia.* J Neurochem, 2006. **96**(4): p. 1016-27.

37. Uemura, O., et al., *Secondary carnitine palmitoyltransferase deficiency in chronic renal failure and secondary hyperparathyroidism.* Tohoku J Exp Med, 1996. **178**(3): p. 307-14.

38. Hagen, T.M., et al., *Acetyl-L-carnitine fed to old rats partially restores mitochondrial function and ambulatory activity.* Proc Natl Acad Sci U S A, 1998. **95**(16): p. 9562-6.

39. Ames, B.N., *Delaying the mitochondrial decay of aging in the brain.* Clinical Neuroscience Research, 2003. **2**(5-6): p. 331-338.

40. Ramsay, R.R. and V.A. Zammit, *Carnitine acyltransferases and their influence on CoA pools in health and disease.* Mol Aspects Med, 2004. **25**(5-6): p. 475-93.

41. Wainwright, M.S., et al., *L-carnitine reduces brain injury after hypoxia-ischemia in newborn rats.* Pediatr Res, 2003. **54**(5): p. 688-95.

42. Hudson, S. and N. Tabet, *Acetyl-L-carnitine for dementia.* Cochrane Database Syst Rev, 2003(2): p. CD003158.

43. Hino, K., et al., *L-carnitine inhibits hypoglycemia-induced brain damage in the rat.* Brain Res, 2005. **1053**(1-2): p. 77-87.

44. Zanelli, S.A., et al., *Mechanisms of ischemic neuroprotection by acetyl-L-carnitine.* Ann N Y Acad Sci, 2005. **1053**: p. 153-61.

45. Dugan, L.L. and J.S. Kim-Han, *Astrocyte mitochondria in in vitro models of ischemia.* J Bioenerg Biomembr, 2004. **36**(4): p. 317-21.

46. Garcia, C.L., et al., *The protective effect of L-carnitine in peripheral blood human lymphocytes exposed to oxidative agents.* Mutagenesis, 2005.

47. Hagen, T.M., et al., *Feeding acetyl-L-carnitine and lipoic acid to old rats significantly improves metabolic function while decreasing oxidative stress.* Proc Natl Acad Sci U S A, 2002. **99**(4): p. 1870-5.

48. Hagen, T.M., C.M. Wehr, and B.N. Ames, *Mitochondrial decay in aging. Reversal through supplementation of acetyl-L-carnitine and N-tert-butyl-alpha-phenyl-nitrone.* Ann N Y Acad Sci, 1998. **854**: p. 214-23.

49. Ilias, I., et al., *L-Carnitine and acetyl-L-carnitine in the treatment of complications associated with HIV infection and antiretroviral therapy.* Mitochondrion, 2004. **4**(2-3): p. 163-8.

50. Liu, J., et al., *Memory loss in old rats is associated with brain mitochondrial decay and RNA/DNA oxidation: partial reversal by feeding acetyl-L-carnitine and/or R-alpha -lipoic acid.* Proc Natl Acad Sci U S A, 2002. **99**(4): p. 2356-61.

51. Ames, B.N., *The metabolic tune-up: metabolic harmony and disease prevention.* J Nutr, 2003. **133**(5 Suppl 1): p. 1544S-8S.

52. Al-Majed, A., *Carnitine esters prevent oxidative stress damage and energy depletion following transient forebrain ischemia in the rat hippocampus.* Clinical Exp. Pharmacol Physiol, 2006. **33**(8): p. 725-733.

53. Abdul, H.M., et al., *Acetyl-L-carnitine-induced up-regulation of heat shock proteins protects cortical neurons against amyloid-beta peptide 1-42-mediated oxidative stress and neurotoxicity: implications for Alzheimer's disease.* J Neurosci Res, 2006. **84**(2): p. 398-408.

54. Dhitavat, S., et al., *Folate, vitamin E, and acetyl-L-carnitine provide synergistic protection against oxidative stress resulting from exposure of human neuroblastoma cells to amyloid-beta.* Brain Res, 2005. **1061**(2): p. 114-7.

55. Kim, J.H., et al., *Transient recovery of synaptic transmission is related to rapid energy depletion during hypoxia.* Neurosci Lett, 2006. **400**(1-2): p. 1-6.

56. Zemlyak, I., et al., *Gene therapy in the nervous system with superoxide dismutase.* Brain Res, 2006. **1088**(1): p. 12-8.

57. Mattiasson, G., et al., *Uncoupling protein-2 prevents neuronal death and diminishes brain dysfunction after stroke and brain trauma.* Nat Med, 2003. **9**(8): p. 1062-8.

58. Korde, A.S., et al., *The mitochondrial uncoupler 2,4-dinitrophenol attenuates tissue damage and improves mitochondrial homeostasis following transient focal cerebral ischemia.* J Neurochem, 2005. **94**(6): p. 1676-84.

59. Echtay, K., *Superoxide activates mitochondrial uncoupling proteins.* Nature, 2002. **415**: p. 96-99.

60. Brand, M.D., et al., *Mitochondrial superoxide and aging: uncoupling-protein activity and superoxide production.* Biochem Soc Symp, 2004(71): p. 203-13.

61. Chan, C.B., et al., *Uncoupling protein 2 and islet function.* Diabetes, 2004. **53 Suppl 1**: p. S136-42.

62. Echtay, K.S. and M.D. Brand, *Coenzyme Q induces GDP-sensitive proton conductance in kidney mitochondria.* Biochem Soc Trans, 2001. **29**(Pt 6): p. 763-8.

63. Fink, B.D., et al., *UCP2-dependent proton leak in isolated mammalian mitochondria.* J Biol Chem, 2002. **277**(6): p. 3918-25.

64. Guo, P., et al., *Association of uncoupling protein-2 expression with increased reactive oxygen species in residual myocardium of the enlarged left ventricle after myocardial infarction.* Heart Vessels, 2005. **20**(2): p. 61-5.

65. Maragos, W.F. and A.S. Korde, *Mitochondrial uncoupling as a potential therapeutic target in acute central nervous system injury.* J Neurochem, 2004. **91**(2): p. 257-62.

66. Bigini, P., et al., *Acetyl-L-carnitine shows neuroprotective and neurotrophic activity in primary culture of rat embryo motoneurons.* Neurosci Lett, 2002. **329**(3): p. 334-8.

67. Walder, C.E., *Ischemic stroke injury is reduced in mice lacking a functional NADPH oxidase.* Stroke, 1997. **28**(11): p. 2252-2258.

68. Muralikrishna, A., *Phospholipase A2, reactive oxygen species, and lipid peroxidation in cerebral ischemia.* Free Radical Biol Med., 2006. **40**(3): p. 376-87.

69. Gluckman, P., *Selective head cooling with mild systemic hypothermia after neonatal encephalopathy.* Lancet, 2005. **365**: p. 663-670.

70. Thompson, J.E., et al., *MR in children with L-carnitine deficiency.* AJNR Am J Neuroradiol, 1996. **17**(8): p. 1585-8.

71. De Vivo, D.C., *The expanding clinical spectrum of mitochondrial diseases.* Brain Dev, 1993. **15**(1): p. 1-22.

72. Foster, K., *Optical and pharmacological tools to investigate the role of mitochondria during oxidative stress and neurodegeneration.* Progress in Neurobiology, 2006. **79**(3): p. 136-171.

73. Liu, J., et al., *Delaying brain mitochondrial decay and aging with mitochondrial antioxidants and metabolites.* Ann N Y Acad Sci, 2002. **959**: p. 133-66.

74. Liu, J., et al., *Comparison of the effects of L-carnitine and acetyl-L-carnitine on carnitine levels, ambulatory activity, and oxidative stress biomarkers in the brain of old rats.* Ann N Y Acad Sci, 2004. **1033**: p. 117-31.

75. Ames, B.N., *Micronutrients prevent cancer and delay aging.* Toxicol Lett, 1998. **102-103**: p. 5-18.

76. Ames, B.N. and J. Liu, *Delaying the mitochondrial decay of aging with acetylcarnitine.* Ann N Y Acad Sci, 2004. **1033**: p. 108-16.

77. Atamna, H., *Heme binding to Amyloid-beta peptide: mechanistic role in Alzheimer's disease.* J Alzheimers Dis, 2006. **10**(2-3): p. 255-66.

78. Kins, S., et al., *Subcellular trafficking of the amyloid precursor protein gene family and its pathogenic role in Alzheimer's disease.* Neurodegener Dis, 2006. **3**(4-5): p. 218-26.

79. Misiti, F., et al., *Protective effect of rhubarb derivatives on amyloid beta (1-42) peptide-induced apoptosis in IMR-32 cells: a case of nutrigenomic.* Brain Res Bull, 2006. **71**(1-3): p. 29-36.

80. Nilsen, J., et al., *Estrogen protects neuronal cells from amyloid beta-induced apoptosis via regulation of mitochondrial proteins and function.* BMC Neurosci, 2006. **7**: p. 74.

81. Ekert, A., *Mitochondrial dysfunction, apoptotic cell death, and Alzheimer's disease.* Biochemical Pharmacology, 2003. **66**(8): p. 1627-1634.

82. Pallas, M. and A. Camins, *Molecular and biochemical features in Alzheimer's disease.* Curr Pharm Des, 2006. **12**(33): p. 4389-408.

83. Reichert, S.A., J.S. Kim-Han, and L.L. Dugan, *The mitochondrial permeability transition pore and nitric oxide synthase mediate early mitochondrial depolarization in astrocytes during oxygen-glucose deprivation.* J Neurosci, 2001. **21**(17): p. 6608-16.

84. Virmani, M.A., et al., *The action of acetyl-L-carnitine on the neurotoxicity evoked by amyloid fragments and peroxide on primary rat cortical neurones.* Ann N Y Acad Sci, 2001. **939**: p. 162-78.

85. Steen, C., et al., *Metabolic stroke in isolated 3-methylcrotonyl-CoA carboxylase deficiency.* Eur J Pediatr, 1999. **158**(9): p. 730-3.

86. Ames, B.N., *A role for supplements in optimizing health: the metabolic tune-up.* Arch Biochem Biophys, 2004. **423**(1): p. 227-34.

87. Sherer, T., *Mechanism of Toxicity in Rotenone Models of Parkinson's Disease.* Journal of Neuroscience, 2003. **23**(34): p. 10756-10764.

88. Jenner, P., *Oxidative stress as a cause of nigral cell death in Parkinson's disease and incidental Lewy body disease.* Ann Neurology, 1992. **32**(Suppl:S82-7).

89. Greenamyre, J., *Mitochondrial dysfunction in Parkinson's disease.* Biochem Soc Symp, 1999. **66**: p. 85-97.